

Republic of Iraq
Ministry of Higher Education
and Scientific Research
Al-Nahrain University
College of Science
Department of Chemistry



Experimental and Computational Studies of Some Drugs as Corrosion Inhibitors for Aluminium and Some Its Alloys in Saline solution

A Thesis

Submitted to the College of Science/Al-Nahrain University as a partial
fulfillment of the requirements for the Degree of Master of Science
in Chemistry

By

Samar Thamer Hameed

B.Sc. Chemistry / College Science / Al-Nahrain University

Supervised by

Dr. Taghried Ali Salman
(Asst. Prof.)

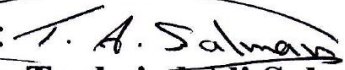
Dr. Shatha Fadil AL-Saidi
(Asst. Prof.)


Apr. 2015

Jumada II 1436

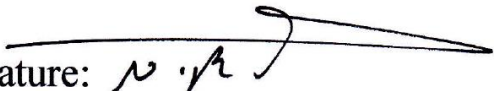
Supervisors Certification

We, certify that this thesis entitled “**Experimental and Computational Studies of Some Drugs as Corrosion Inhibitors for Aluminium and Some Its Alloys in Saline solution**” was prepared by “**Samar Thamer Hameed**” under our supervision at the College of Science / Al-Nahrain University as a partial fulfillment of the requirements for the Degree of Master of Science in Chemistry (Physical Chemistry).

Signature: 
Name: **Dr. Taghried Ali Salman**
Scientific Degree: Assistant Professor
Date: 24 \ 6 \ 2015

Signature: 
Name: **Dr. Shatha Fadil AL-Saidi**
Scientific Degree: Assistant Professor
Date: 24 \ 6 \ 2015

In view of the available recommendations, I forward this Thesis for debate by Examining Committee.

Signature: 
Name: **Dr. Nasreen R. Jber**
Title: Head of the Department of Chemistry
Date: 24 \ 6 \ 2015

Scientific Evaluation Report

This is to certify that I have read the thesis entitled, “**Experimental and Computational Studies of Some Drugs as Corrosion Inhibitors for Aluminium and Some Its Alloys in Saline solution**”, and corrected the scientific mistakes I found. The thesis is, therefore, qualified for debate.

Signature:

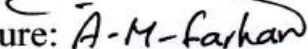


Name: **Asst. Prof. Dr. Anwar Thib M. AL-Thib**

Date: 24/ 6 /2015

Committee Certification

We, the examining committee, certify that we have read this thesis entitled “**Experimental and Computational Studies of Some Drugs as Corrosion Inhibitors for Aluminium and Some Its Alloys in Saline solution**” and examined the student “**Samar Thamer Hameed**” in its contents and that in our opinion, it is accepted for the Degree of Master of Science, in Physical Chemistry, with (Excellent) standing.

Signature: 

Name: **Dr. Ahlam M. Farhan**

Scientific Degree: Professor

Date: 24 \ 6 \ 2015

(Chairman)


Signature: 

Name: **Dr. Elham Majeed AL-Rufaie**

Scientific Degree: Assistant Professor

Date: 24 \ 6 \ 2015

(Member)

Signature: 

Name: **Dr. Mehdi S. Shihab**

Scientific Degree: Assistant Professor

Date: 24 \ 6 \ 2015

(Member)


Signature: 

Name: **Dr. Taghried Ali Salman**

Scientific Degree: Assistant Professor

Date: 24 \ 6 \ 2015

(Member/ Supervised)

Signature: 

Name: **Dr. Shatha Fadil AL-Saidi**

Scientific Degree: Assistant Professor

Date: 24 \ 6 \ 2015

(Member/ Supervised)

I, hereby certify upon the decision of the examining committee.

Signature:

Name: **Dr. Hadi M. A. Abood**

Scientific Degree: Assistant Professor

Title: Dean of College of Science

Date: \ \

Dedication

To

My Parents,

My Brother,

My Sisters

And My Close Friend.

Samar

Acknowledgement:-

*First of all, I am a sincerely grateful to **Allah** for enabling and helping me to perform and finish this work.*

*I wish to express my thanks and gratitude to my supervisors **Dr. Taghried Ali Salman** and **Dr. Shatha Fadil AL-Saidi** for their help, guidance and advises during my M.Sc study.*

*I address many thanks to **Dr. Abdulkareem AL-Samarraie** for their help with the experimental work, guidance, interesting and motivating discussions.*

*I am particularly thankful to my colleague and friend **Rana Gamall** who helped me in my work.*

Many thanks go to anyone who gave me help and was cooperative to this research appeared in the present form.

Samar

Summary:-

This thesis involves the investigation of the corrosion behaviour of pure aluminium as well as of two of aluminium – base alloys (5052Al and 2024Al) in sodium chloride solution over a temperature range (283 – 323 K) with and without ampicillin (AMP.), cephalixin (CEX.) and amoxicillin (AMOX.) as inhibitors.

The results of electrochemical experimental study revealed that:

1. The current density increases with increasing temperature in the range of (283-323) K.
2. The inhibition efficiency increases with increasing the concentration of inhibitors (AMP., CEX., and AMOX.), this means that these inhibitors act as an adsorption inhibitors on the surface for the corrosion of pure Al, 5052 Al, and 2024 Al in 3.5% NaCl.
3. The inhibition efficiency of AMP., CEX., and AMOX. decreases with increasing temperature from 283 to 323 K.
4. According to the corrosion potential, AMP., CEX., and AMOX. act as mixed type inhibitors since corrosion potential does not change approximately in NaCl solution.
5. The thermodynamic parameters of corrosion ΔH , ΔG , and ΔS have been calculated at different inhibitors concentrations and temperatures. The values of ΔG and ΔH indicate the spontaneous and exothermic corrosion processes respectively.

6. The general behaviour for the kinetic studies depend on the Arrhenius equation. Kinetic data show that the adsorption of AMP., CEX., and AMOX. on the surface of in 3.5% NaCl is physisorption type.
7. The negative values of thermodynamic functions of adsorption, ΔG_{ads} and ΔH_{ads} obtained from Langmuir isotherm, indicate the spontaneous and exothermic adsorption processes respectively.

This thesis also includes theoretical calculation of ampicillin, cephalixin and amoxicillin molecules using the density functional theory (DFT) (B3LYP) with 6–31G basis set, which indicate that AMOX. is best inhibitor. The comparison of theoretical and experimental data exhibit good relation.

The surface study by using Scanning Electron Microscopy (SEM) has been accomplished and the images show a smoother surface for pure aluminium sample in the presence (7.5×10^{-4} M) of ampicillin due to the formation of a protective barrier film through adsorption process.

List of contents

<i>Item No.</i>	<i>Subject</i>	<i>Page No.</i>
List of Content		I
List of Abbreviations and Symbols		IV
List of Figures		VI
List of Tables		IX
Chapter One - Introduction		1
1.1	General Introduction to Corrosion	2
1.2	Mixed Potential Theory	4
1.3	Aluminium and Aluminium Alloys	9
1.4	Corrosion Susceptibility of Aluminium Alloys	12
1.5	Types of Corrosion for Aluminium	15
1.5.1	Uniform Corrosion	16
1.5.2	Galvanic Corrosion	17
1.5.3	Crevice Corrosion	19
1.5.4	Pitting Corrosion	20
1.5.5	Intergranular Corrosion	23
1.5.6	Stress Corrosion Cracking	24
1.5.7	Corrosion Fatigue	25
1.5.8	Erosion – Corrosion	26
1.5.9	Exfoliation Corrosion	26
1.5.10	Filiform Corrosion	27
1.5.11	Stray – Current Corrosion	29
1.5.12	Deposition Corrosion	29
1.5.13	Hydrogen Embrittlement	30
1.6	Corrosion Inhibitors	31
1.6.1	Definition of Inhibitors	31
1.6.2	Classification of Inhibitors	32
1.6.2.1	Environmental Conditioners (Scavengers)	32
1.6.2.2	Interface Inhibitors	33
1.6.2.2.1	Liquid-Phase Inhibitors	34
1.6.2.2.1.1	Anodic Inhibitors (Passivator)	34

1.6.2.2.1.2	Cathodic Inhibitors	35
1.6.2.2.1.3	Mixed Inhibitors	37
1.6.2.2.2	Vapor-Phase Inhibitors	40
1.7	Green Corrosion Inhibitors	41
1.8	Quantum Chemistry and Corrosion Inhibitor Studies	43
1.9	The Literature Survey	45
1.10	The Aim of the Research	48
Chapter Two-Experimental		49
2.1	Materials and Chemicals	50
2.1.1	Aluminium Alloys	50
2.1.2	Chemicals	50
2.1.3	Inhibitors	51
2.1.3.1	Ampicillin	51
2.1.3.2	Amoxicillin	52
2.1.3.3	Cephalexin	53
2.2	Sample Preparation	54
2.3	Preparation of Solutions	54
2.4	The Experimental Equipment and Procedures	54
2.4.1	Electrochemical System	54
2.4.1.1	Potentiostat/Galvanostat	54
2.4.1.2	Host Computer	55
2.4.1.3	Corrosion Cell	56
2.4.1.4	Three-Electrode System	56
2.4.1.4.1	Working Electrode	57
2.4.1.4.2	Reference Electrodes	58
2.4.1.4.3	Auxiliary Electrode	60
2.4.1.5	The Thermostat	60
2.4.1.6	Magnetic Stirrer	60
2.4.2	Corrosion Measurement Procedures	61
2.4.2.1	Open Circuit Potential	61
2.4.2.2	Tafel Extrapolation	62
2.5	Quantum Chemical Calculation	62
2.6	Scanning Electron Microscopy (SEM) Analysis	63

Chapter Three - Results and Discussion	64
3.1 Potentiodynamic Polarization Measurements	65
3.1.1 Corrosion Current Density and Corrosion Potential	78
3.1.2 Corrosion Rate and Penetration Rate	79
3.1.3 Surface Coverage and Inhibition Efficiency	80
3.1.4 The Tafel Slopes and Transfer Coefficients	86
3.1.5 The Exchange Current Densities and Polarization Resistances	87
3.1.6 Activation Parameters of Corrosion	98
3.1.7 Thermodynamic Quantities of Corrosion	110
3.1.8 Adsorption Isotherm	124
3.2 Theoretical Calculations	132
3.3 Scanning Electron Microscopy	140
Chapter Four - Conclusions and Further Suggestions	141
4.1 Conclusions	142
4.2 Suggestions for Further Research	144
References	146
Appendix	160
Appendix 1. Electromotive Force Series For Metals	161

List of Abbreviations and Symbols

<i>Abbreviation</i>	<i>Meaning</i>
A	Pre-exponential factor
a	Atomic weight
AMOX.	Amoxicillin
AMP.	Ampicillin
b_a	Anodic Tafel slope
b_c	Cathodic Tafel slope
C	The concentration
CEX.	Cephalexin
C_R	Corrosion rate
E	Electrode potential
E_a	Activation energy
E_{corr}	Corrosion Potential
E_{HOMO}	The energy of the highest occupied molecular orbital
E_{LUMO}	The energy of the lowest unoccupied molecular orbital
F	Faraday constant
I	Current
i	Current density
i_{corr}	Corrosion current density
IGC	Intergranular corrosion
Inh.	Inhibitor molecule
i_o	Equilibrium exchange current density
K_{ads}	The equilibrium constant of the adsorption
M	Metal
m	Mass
P_R	Penetration rate
R	Gas constant
R²	Regression coefficient
R_p	Polarization resistance

SA	Surface area
SCC	Stress corrosion cracking
SCE	Saturated calomel electrode
SEM	Scanning Electron Microscopy
SHE	Standard Hydrogen Electrode
T	Absolute temperature
t	Time
TE	Total energy of molecule
WE	Working electrode
z	Metal valence
%IE	The inhibition efficiency
ρ	Density of metal
η	Over potential
α_a	Anodic transfer coefficients
α_c	Cathodic transfer coefficients
ΔE_{gap}	The energy gap between E_{LUMO} - E_{HOMO}
ΔG	Gibbs free energy change
ΔH	Enthalpy change
ΔN	The number of electrons transferred from the molecule to the surface
ΔS	Entropy change
θ	The metal surface covered
μ	Dipole moment

List of Figures

<i>Figure No.</i>	<i>Name of Figure</i>	<i>Page No.</i>
1.1.	Corrosion cell showing conditions that must exist for electrochemical corrosion.	4
1.2.	Plot of the Butler–Volmer equation	6
1.3.	Potential - pH equilibrium diagram for the system aluminium – water at 25°C	13
1.4.	Schematic representation of uniform corrosion	16
1.5.	Schematic representation of galvanic corrosion	17
1.6.	Schematic representation of crevice corrosion	20
1.7.	Schematic representation of pitting corrosion	21
1.8.	Schematic representation of the pitting activity of aluminium alloy in chloride solution	21
1.9.	Schematic representation of intergranular corrosion	23
1.10.	Schematic representation of stress corrosion cracking	24
1.11.	Schematic representation of corrosion fatigue	25
1.12.	Schematic representation of erosion – corrosion	26
1.13.	Schematic representation of exfoliation corrosion	27
1.14.	Schematic representation of the filiform corrosion mechanism	28
1.15.	Corrosion by hydrogen embrittlement	30
1.16.	Classification of inhibitors	33
1.17.	Effect of adding an anodic inhibitor	34
1.18.	The mechanism of actuation of the anodic inhibitors	35
1.19.	The mechanism of actuation of the cathodic inhibitors	36
1.20.	Effect of adding a cathodic inhibitor.	36
1.21.	The mechanism of actuation of the mixed inhibitors: acting through adsorption of the inhibitor on the metal surface	38
1.22.	Adding a mixed inhibitor.	38
2.1.	The chemical structure of ampicillin.	51
2.2.	The chemical structure of amoxicillin.	52
2.3.	The chemical structure of cephalexin	53
2.4.	The front panel of M Lab 200 potentiostat/galvanostat.	55

2.5.	Set-up the corrosion cell and three electrodes	56
2.6.	Working electrode	57
2.7.	(a) Schematic diagram of reference electrode (b) Reference electrode in Luggin capillary	59
2.8.	Complete system set up for polarization measurements	61
2.9.	Schematic polarization curve showing Tafel extrapolation	63
3.1.	Polarization plots for the corrosion of Pure Aluminium in 3.5% NaCl in the absence and presence of (7.5×10^{-4} M) Ampicillin, Cephalexin and Amoxicillin, at different temperature 283-323K	66
3.2.	Polarization plots for the corrosion of 5052 Aluminium in 3.5% NaCl in the absence and presence (7.5×10^{-4} M) Ampicillin, Cephalexin, Amoxicillin, at different temperature 283-323K	67
3.3.	Polarization plots for the corrosion of 2024 Aluminium in 3.5% NaCl in the absence and presence 7.5×10^{-4} M Ampicillin, Cephalexin, Amoxicillin, at different temperature 283-323K	68
3.4.	Inhibition efficiency of Amoxicillin for (a) Pure Al (b) 5052 Al (c) 2024 Al, in 3.5% NaCl at different temperatures and concentrations of Amoxicillin	85
3.5.	Arrhenius Plot of $\log i_{\text{corr}}$ versus $1/T$ for the corrosion of Pure Aluminium in 3.5% NaCl containing various concentrations of (a) Ampicillin (b) Cephalexin (c) Amoxicillin	101
3.6.	Arrhenius Plot of $\log i_{\text{corr}}$ versus $1/T$ for the corrosion of 5052 Aluminium in 3.5% NaCl containing various concentrations of (a) Ampicillin (b) Cephalexin (c) Amoxicillin	102
3.7.	Arrhenius Plot of $\log i_{\text{corr}}$ versus $1/T$ for the corrosion of 5052 Aluminium in 3.5% NaCl containing various concentrations of (a) Ampicillin (b) Cephalexin (c) Amoxicillin	103
3.8.	Plot of $\log C_R/T$ versus $1/T$ for the corrosion of Pure aluminium in 3.5% NaCl containing various concentrations of (a) Ampicillin (b) Cephalexin (c) Amoxicillin	104
3.9.	Plot of $\log C_R/T$ versus $1/T$ for the corrosion of 5052 aluminium in 3.5% NaCl containing various concentrations of (a) Ampicillin (b) Cephalexin (c) Amoxicillin	105
3.10.	Plot of $\log C_R/T$ versus $1/T$ for the corrosion of 2024 Aluminium in 3.5% NaCl containing various concentrations of	106

	(a) Ampicillin (b) Cephalexin (c) Amoxicillin	
3.11.	The variation of Gibbs free energies (ΔG) with temperature for the corrosion of Pure aluminium in 3.5% NaCl at absence and presence different concentrations of (a) Ampicillin (b) Cephalexin (c) Amoxicillin	112
3.12.	The variation of Gibbs free energies (ΔG) with temperature for the corrosion of 5052 Aluminium in 3.5% NaCl at absence and presence different concentrations of (a) Ampicillin (b) Cephalexin (c) Amoxicillin	113
3.13.	The variation of Gibbs free energies (ΔG) with temperature for the corrosion of 2024 Aluminium in 3.5% NaCl at absence and presence different concentrations of (a) Ampicillin (b) Cephalexin (c) Amoxicillin	114
3.14.	Langmuir isotherm plots for the adsorption of (a) Ampicillin (b) Cephalexin (c) Amoxicillin on Pure Aluminium in 3.5% NaCl.	126
3.15.	Langmuir isotherm plots for the adsorption of (a) Ampicillin (b) Cephalexin (c) Amoxicillin on 5052 Aluminium in 3.5% NaCl	127
3.16.	Langmuir isotherm plots for the adsorption of (a) Ampicillin (b) Cephalexin (c) Amoxicillin on 2024 Aluminium in 3.5% NaCl.	128
3.17.	The variation of Gibbs free energies (ΔG_{ads}) with temperature for the corrosion of (a) Pure Aluminium (b) 5052 Aluminium (c) 2024 Aluminium in 3.5% NaCl at absence and presence different Ampicillin, Cephalexin, and Amoxicillin concentrations	129
3.18.	The frontier molecular orbital density distributions as calculated by DFT method for (a) Ampicillin (b) Cephalexin (c) Amoxicillin	134
3.19.	The structure of ampicillin	137
3.20.	The structure of cephalexin.	138
3.21.	The structure of amoxicillin	139
3.22.	Scanning electron micrographs of (a) Polished Aluminium specimen, (b) In 3.5% NaCl, (c) In the presence of 7.5×10^{-4} M Ampicillin.	140

List of Tables

<i>Table NO.</i>	<i>Name of Table</i>	<i>Page No.</i>
1.1.	Aluminium alloys designation	10
1.2.	Selected applications for many aluminium alloys.	10
1.3.	Electrode potentials of some representative aluminium alloys and other metals.	19
2.1.	Composition of aluminium alloys, wt. %.	50
2.2.	List of reagents used.	50
3.1.	Potentiodynamic polarization parameters for Pure Aluminium without and with various concentrations of Ampicillin in 3.5% of NaCl aqueous solution at different temperatures	69
3.2.	Potentiodynamic polarization parameters for Pure Aluminium without and with various concentrations of Cephalexin in 3.5% of NaCl aqueous solution at different temperatures	70
3.3.	Potentiodynamic polarization parameters for Pure Aluminium without and with various concentrations of Amoxicillin in 3.5% of NaCl aqueous solution at different temperatures.	71
3.4.	Potentiodynamic polarization parameters for 5052 Aluminium without and with various concentrations of Ampicillin in 3.5% of NaCl aqueous solution at different temperatures	72
3.5.	Potentiodynamic polarization parameters for 5052 Aluminium without and with various concentrations of Cephalexin in 3.5% of NaCl aqueous solution at different temperatures.	73
3.6.	Potentiodynamic polarization parameters for 5052 Aluminium without and with various concentrations of Amoxicillin in 3.5% of NaCl aqueous solution at different temperatures	74
3.7.	Potentiodynamic polarization parameters for 2024 Aluminium without and with various concentrations of Ampicillin in 3.5% of NaCl aqueous solution at different temperatures.	75
3.8.	Potentiodynamic polarization parameters for 2024 Aluminium without and with various concentrations of Cephalexin in 3.5% of NaCl aqueous solution at different temperatures.	76

3.9.	Potentiodynamic polarization parameters for 2024 Aluminium without and with various concentrations of Amoxicillin in 3.5% of NaCl aqueous solution at different temperatures.	77
3.10.	Values of surface coverages and protection efficiencies for various concentrations of Ampicillin, Amoxicillin and Cephalexin in 3.5% of NaCl aqueous solution at five different temperatures on Pure Aluminium surface.	81
3.11.	Values of surface coverages and protection efficiencies for various concentrations of Ampicillin, Amoxicillin and Cephalexin in 3.5% of NaCl aqueous solution at five different temperatures on 5052 Aluminium surface.	82
3.12.	Values of surface coverages and protection efficiencies for various concentrations of Ampicillin, Amoxicillin and Cephalexin in 3.5% of NaCl aqueous solution at five different temperatures on 2024 Aluminium surface.	83
3.13.	Values of transfer coefficients (α_c , α_a), the polarization resistance (R_p) and equilibrium exchange current density (i_o) for corrosion of Pure aluminium in 3.5%NaCl solution without and with Ampicillin at temperature range 283 - 323K.	89
3.14.	Values of transfer coefficients (α_c , α_a), the polarization resistance (R_p) and equilibrium exchange current density (i_o) for corrosion of Pure Aluminium in 3.5%NaCl solution without and with Cephalexin at temperature range 283 - 323K.	90
3.15.	Values of transfer coefficients (α_c , α_a), the polarization resistance (R_p) and equilibrium exchange current density (i_o) for corrosion of Pure Aluminium in 3.5%NaCl solution without and with Amoxicillin at temperature range 283 - 323K	91
3.16.	Values of transfer coefficients (α_c , α_a), the polarization resistance (R_p) and equilibrium exchange current density (i_o) for corrosion of 5052 Aluminium in 3.5%NaCl solution without and with Ampicillin at temperature range 283 - 323K.	92
3.17.	Values of transfer coefficients (α_c , α_a), the polarization resistance (R_p) and equilibrium exchange current density (i_o) for corrosion of 5052 Aluminium in 3.5%NaCl solution without and with Cephalexin at temperature range 283 - 323K.	93

3.18.	Values of transfer coefficients (α_c , α_a), the polarization resistance (R_p) and equilibrium exchange current density (i_o) for corrosion of 5052 Aluminium in 3.5%NaCl solution without and with Amoxicillin at temperature range 283 - 323K.	94
3.19.	Values of transfer coefficients (α_c , α_a), the polarization resistance (R_p) and equilibrium exchange current density (i_o) for corrosion of 2024 Aluminium in 3.5%NaCl solution without and with Ampicillin at temperature range 283 - 323K	95
3.20.	Values of transfer coefficients (α_c , α_a), the polarization resistance (R_p) and equilibrium exchange current density (i_o) for corrosion of 2024 Aluminium in 3.5%NaCl solution without and with Cephalexin at temperature range 283 - 323K.	96
3.21.	Values of transfer coefficients (α_c , α_a), the polarization resistance (R_p) and equilibrium exchange current density (i_o) for corrosion of 2024 Aluminium in 3.5%NaCl solution without and with Amoxicillin at temperature range 283 - 323K.	97
3.22.	Activation parameters of the corrosion of Pure Aluminium in 3.5%NaCl in the absence and presence of different concentrations of Ampicillin, Cephalexin, Amoxicillin inhibitors	107
3.23.	Activation parameters of the corrosion of 5052 Aluminium in 3.5%NaCl in the absence and presence of different concentrations of Ampicillin, Cephalexin, Amoxicillin inhibitors.	108
3.24.	Activation parameters of the corrosion of 2024 Aluminium in 3.5%NaCl in the absence and presence of different concentrations of Ampicillin, Cephalexin, Amoxicillin inhibitors.	109
3.25.	The thermodynamic functions for corrosion of Pure Aluminium in 3.5% NaCl at different concentration of Ampicillin over the temperature range 283 - 323 K.	115
3.26.	The thermodynamic functions for corrosion of Pure Aluminium in 3.5% NaCl at different concentration of Cephalexin over the temperature range 283 - 323 K.	116
3.27.	The thermodynamic functions for corrosion of Pure Aluminium	117

	in 3.5% NaCl at different concentration of Amoxicillin over the temperature range 283 - 323 K.	
3.28.	The thermodynamic functions for corrosion of 5052 Aluminium in 3.5% NaCl at different concentration of Ampicillin over the temperature range 283 - 323 K.	118
3.29.	The thermodynamic functions for corrosion of 5052 Aluminium in 3.5% NaCl at different concentration of Cephalexin over the temperature range 283 - 323 K	119
3.30.	The thermodynamic functions for corrosion of 5052 Aluminium in 3.5% NaCl at different concentration of Amoxicillin over the temperature range 283 -323 K.	120
3.31.	The thermodynamic functions for corrosion of 2024 Aluminium in 3.5% NaCl at different concentration of Ampicillin over the temperature range 283 - 323 K.	121
3.32.	The thermodynamic functions for corrosion of 2024 Aluminium in 3.5% NaCl at different concentration of Cephalexin over the temperature range 283 - 323 K.	122
3.33.	The thermodynamic functions for corrosion of 2024 Aluminium in 3.5% NaCl at different concentration of Amoxicillin over the temperature range 283 - 323 K	123
3.34.	Thermodynamic parameters for adsorption of the inhibitors on the surface of Pure Aluminium in 3.5% NaCl.	130
3.35.	Thermodynamic parameters for adsorption of the inhibitors on the surface of 5052 Aluminium in 3.5% NaCl	130
3.36.	Thermodynamic parameters for adsorption of the inhibitors on the surface of 2024 Aluminium in 3.5% NaCl	131
3.37.	The calculated quantum chemical parameters of the studied compound.	133
3.38.	Mulliken atomic charges results of Ampicillin molecule:	137
3.39.	Mulliken atomic charges results of Cephalexin molecule:	138
3.40.	Mulliken atomic charges results of Amoxicillin molecule	139



CHAPTER ONE
INTRODUCTION



1.1 General Introduction to Corrosion

The word corrosion comes from the Latin word 'corrodere', which means 'gnaw away' [1]. According to American Society for Testing and Materials' corrosion glossary, corrosion is defined as "the chemical or electrochemical reaction between a material, usually a metal, and its environment that produces a deterioration of the material and its properties" [2]. In nature, most metals are found in a chemically combined state known as an ore. All of the metals (except noble metals such as gold, platinum, and silver) exist in nature in the form of their oxides, hydroxides, carbonates, silicates, sulfides, sulfates, etc., which are thermodynamically more stable at low-energy states. The metals are extracted from these ores after supplying a large amount of energy, gives pure metals in their elemental forms. Thermodynamically, as a result of this metallurgical process, metals attain higher energy levels, their entropies are reduced, and they become relatively more unstable, which is the driving force behind corrosion. It is a natural tendency to go back to their oxidized states of lower energies, to their combined states, by recombining with the elements present in the environment, resulting in a net decrease in free energy [3].

Corrosion of metallic structures is associated with the loss of material under the action of environment and is a huge problem for many activities. It links a lot of fields like aerospace, naval, automotive, constructional, and others. Material degradation due to corrosion calls for the replacement of damaged metallic parts, failure of equipment and engineering systems which can lead to fatal catastrophes. Corrosion of pipelines or tanks can lead even to

ecological disasters. Therefore problems associated with corrosion cause a significant economic impact and can lead to irretrievable human losses [4].

The basic process of metallic corrosion in aqueous solution consists of the anodic dissolution of metals and the cathodic reduction of oxidants present in the solution [5] (**Figure 1.1.**):

- Anodic oxidation:

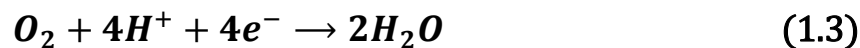


While, the cathodic reaction in metallic corrosion can be written in several different forms [6]:

- Hydrogen evolution:



- Oxygen reduction (Acid solution):



- Oxygen reduction (neutral or basic solution):



- Metal ion reduction:



- Metal Deposition:



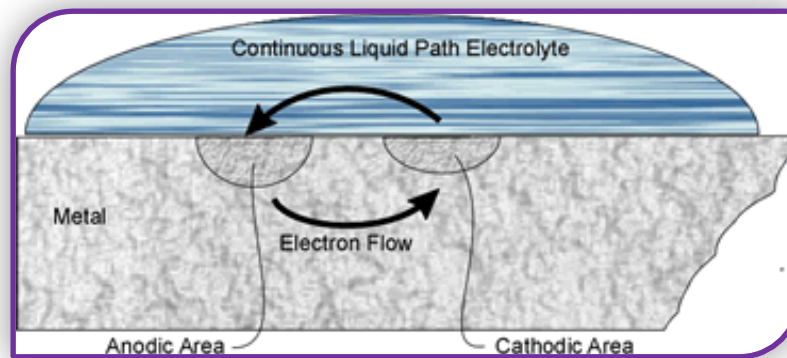


Figure1.1. Corrosion cell showing conditions that must exist for electrochemical corrosion [7].

1.2 Mixed Potential Theory

The theoretical basis for electrochemical corrosion testing is derived from the mixed potential theory. The basic assumptions of the theory are quite simple [8]:

- a) The kinetics of the various partial reactions can be treated separately.
- b) No net current flows from an electrode which is in equilibrium or at steady state.

The condition of no net current flow means that the total rate of reduction must equal the total rate of oxidation on the electrode surface.

When a reaction is forced away from equilibrium the current must flow in electrode, this caused electrochemical polarization (usually referred to simply as “polarization”), there are three types of polarization [9]:

1. *Activation polarization* is polarization caused by a slow electrode reaction.

2. *Concentration polarization* is polarization caused by concentration changes in reactants or products near an electrode surface.
3. *Ohmic polarization* is polarization caused by an ionic potential drop (IR drops) in solution or across surface films, such as oxides (or salts).

The degree of polarization is defined as the overvoltage (or overpotential) η given by the following equation [9]:

$$\eta = E - E_o \quad (1.7)$$

where E is the electrode potential for some condition of current flow (equilibrium potential) and E_o is the electrode potential for zero current flow (also called the open-circuit potential, corrosion potential, or rest potential).

The current applied to cause the departure from equilibrium is the net rate of reaction, thus [10],

$$i_{app} = \sum \tilde{i} - \sum \vec{i} \quad (1.8)$$

where \tilde{i} is the anodic current density, \vec{i} is the cathodic current density and i_{app} is the applied current density.

The basic law of charge – transfer reactions has been expressed through the (Butler – Volmer) for multisteps reaction equation as[11] :

$$i = i_o \left[\exp\left(\frac{\alpha_a n F \eta}{RT}\right) - \exp\left(\frac{-\alpha_c n F \eta}{RT}\right) \right] \quad (1.9)$$

where (i) is the measured current density, i_o is the equilibrium exchange current density, (α) is the transfer coefficient.

Figure1.2. shows a plot of the Butler–Volmer equation and Tafel slopes of $dE / d\log|i|$. The logarithm of the absolute value of the current density is plotted vs. the overvoltage $(E - E_o)$, or vs. the potential E . As seen in **Figure1.2.**, at sufficiently high overvoltages, both the cathodic and the anodic polarization curves display linear regions in the plot of $\log|i|$ vs. E [9].

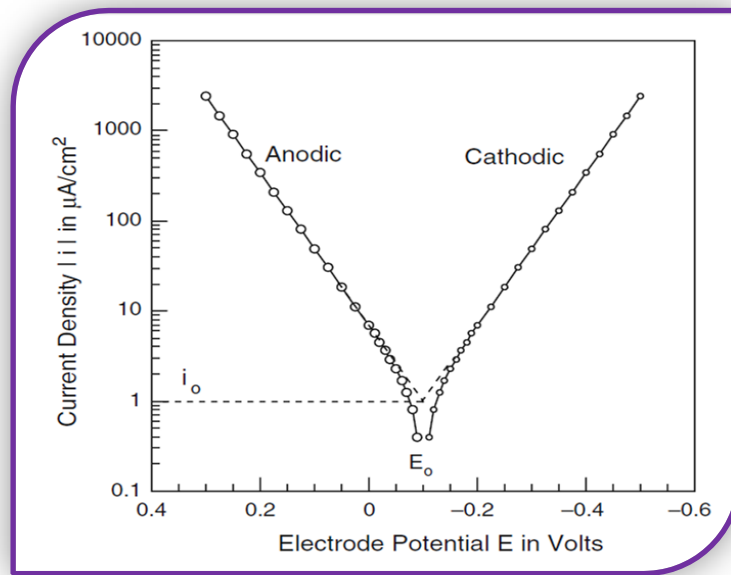


Figure 1.2. Plot of the Butler–Volmer equation[18].

The well-known Tafel equation follows from the Butler–Volmer equation as follows. At sufficiently high overvoltages, the rate of the reverse reaction becomes negligible, so for anodic reaction equation (1.9) can be written as [9]:

$$\hat{i} = i_o \exp \left[\frac{\alpha_a n F (E - E_o)}{RT} \right] \tag{1.10}$$

Taking logarithms of equation (1.10) gives:

$$\log \hat{i} = \log i_o + \frac{\alpha_a n F}{2.303 RT} (E - E_o) \tag{1.11}$$

Thus, a plot of $\log|i|$ vs. the overvoltage ($E - E_o$) (or of $\log|i|$ vs. the electrode potential E) gives a straight line, as shown in **Figure 1.2.** according to equation (1.11), when $E = E_o$, $i = i_o$, thus, the Tafel region can be extrapolated back to $E = E_o$ to give the exchange current density i_o , as shown in **Figure 1.2** [9].

Equation (1.11) can be rewritten as [9]:

$$\eta_a = b_a \log \frac{i}{i_o} \quad (1.12)$$

which is one form of the Tafel equation, where η_a is the anodic overvoltage and b_a is the anodic Tafel slope given by

$$b_a = \frac{dE}{d \log i} = \frac{2.303 RT}{\alpha_a n F} \quad (1.13)$$

A similar considerations also hold for the cathodic branch of the polarization curve

$$\eta_c = b_c \log \frac{i}{i_o} \quad (1.14)$$

where η_c is the cathodic overvoltage and b_c is the cathodic Tafel slope

$$b_c = \frac{dE}{d \log|i|} = - \frac{2.303 RT}{\alpha_c n F} \quad (1.15)$$

Figure 1.2., indicated that cathodic Tafel slopes have negative signs and anodic Tafel slopes have positive signs. Tafel slopes have the units of volts or millivolts per decade of current density [9].

For small overvoltages, the exponential terms in the Butler–Volmer equation for a corroding metal can be expanded using a MacLaurin series [9].

For any small variable x

$$e^x = 1 + x + \frac{x^2}{2!} + \dots \quad \text{and} \quad e^{-x} = 1 - x + \frac{x^2}{2!} + \dots \quad (1.16)$$

The use of equations (1.16) in equation (1.9) and dropping the second-order terms gives

$$\tilde{i} = i_{corr} \left\{ 1 + \frac{\alpha_a n F}{2.303 RT} \eta - \left[1 - \frac{(\alpha_c n F)}{2.303 RT} \eta \right] \right\} \quad (1.17)$$

or

$$\tilde{i} = i_{corr} \left[\frac{\alpha_a n F}{2.303 RT} + \frac{\alpha_c n F}{2.303 RT} \right] \eta \quad (1.18)$$

so that

$$\tilde{i} = 2.303 i_{corr} \left[\frac{1}{b_a} + \frac{1}{-b_c} \right] \eta \quad (1.19)$$

The derivative of $\frac{d\eta}{di}$ gives

$$\left(\frac{d\eta}{di} \right)_{\eta \rightarrow 0} = \frac{1}{2.303 i_{corr} \left(\frac{1}{b_a} + \frac{1}{|b_c|} \right)} = R_p \quad (1.20)$$

The differential in equation (1.20) is called the polarization resistance R_p , because it has the units of resistance. Solving for i_{corr} gives [9]:

$$i_{corr} = \frac{1}{2.303 \left(\frac{d\eta}{di} \right)_{\eta \rightarrow 0} \left(\frac{1}{b_a} + \frac{1}{|b_c|} \right)} \quad (1.21)$$

so that equation (1.21) can be written as

$$i_{corr} = \frac{1}{2.303 R_p \left(\frac{1}{b_a} + \frac{1}{|b_c|} \right)} \quad (1.22)$$

which is the *Stern–Geary equation* [9].

1.3 Aluminium and Aluminium Alloys

Aluminium is the third most common element after oxygen and silicon on earth [12]. Aluminium alloys are also the second in use only to steels as structural metals [13]. The development of applications for aluminium and its alloys, as well as the sustained rise in consumption can be attributed to several of its properties which are decisive criteria in users' choice of metals; these advantageous properties are [14].

- Lightness,
- Thermal conductivity,
- Electrical conductivity,
- Suitability of surface treatments,
- Corrosion resistance,
- Diversity of aluminium alloys,
- Diversity of semi-products,
- Ease with which aluminium can be formed (high ductility),
- Ease of recycling

The mechanical, physical, and chemical properties of aluminium alloys depend upon composition and microstructure. The addition of selected elements to pure aluminium greatly enhances its properties and usefulness. Because of this, most applications for aluminium utilize alloys having one or more elemental additions. The major alloying additions used with aluminium are copper, manganese, silicon, magnesium, and zinc. The total amount of these elements can constitute up to 10% of the alloy composition. Impurity elements are also present, but their total percentage is usually less than 0.15% in aluminium alloys [13]. **Table 1.1** shows the aluminium alloy groups [15].

Table 1.1. Aluminium alloys designation.

Alloy series	Main alloying element
1xxx	Aluminium greater than 99%
2xxx	Copper
3xxx	Manganese
4xxx	Silicon
5xxx	Magnesium
6xxx	Magnesium and silicon
7xxx	Zinc and magnesium
8xxx	Silicon and iron

Aluminium alloys are economical in many applications. They are used in the automotive industry, aerospace industry, in construction of machines, appliances, and structures, as cooking utensils, covers for housings of electronic equipment, as pressure vessels for cryogenic applications, and in innumerable other areas. **Tables 1.2** list typical applications for some of the more commonly used alloys [13].

Table 1.2. Selected applications for many aluminium alloys.

Alloy	Description and selected applications
1100	Commercially pure aluminium highly resistant to chemical attack and weathering. Low cost, ductile for deep drawing, and easy to weld. Used for high-purity applications such as chemical processing equipment. Also for nameplates, fan blades, flue lining, sheet metal work, spun holloware, and fin stock.

Table 1.2. (cont.)

Alloy	Description and selected applications
2024	This alloy used for high-strength structural applications. Fair workability and fair corrosion resistance. This alloy can used for truck wheels, many structural aircraft applications, gears for machinery, screw machine products, automotive parts, cylinders and pistons, fasteners, machine parts, ordnance, recreation equipment, screws and rivets.
3003	Most popular general-purpose alloy. Stronger than 1100 with same good formability and weldability. For general use, including sheet metal work, fuel tanks, chemical equipment, containers, cabinets, freezer liners, cooking utensils, pressure vessels, builder's hardware, storage tanks, agricultural applications, appliance parts, architectural applications, electronics, fan equipment, recreation vehicles, trucks and trailers.
5052	Stronger than 3003 yet readily formable. Good weldability and resistance to corrosion. Uses include pressure vessels, fan blades, tanks, electronic panels, electronic chassis, medium-strength sheet metal parts, hydraulic tube, appliances, agricultural applications, architectural uses, automotive parts, building products, chemical equipment, containers, cooking utensils, fasteners, hardware, highway signs, hospital and medical equipment, kitchen equipment, marine applications, railroad cars, recreation vehicles, trucks and trailers.
6061	Good formability, weldability, and corrosion resistance. Good general-purpose alloy used for a broad range of structural applications and welded assemblies including truck components, railroad cars, pipelines, marine applications, furniture, agricultural applications, aircrafts, architectural applications, automotive parts, building products, chemical equipment, electrical and electronic applications, fence wire, fan blades, general sheet metal, highway signs, hospital and medical equipment, kitchen equipment, machine parts, ordnance, recreation equipment, recreation vehicles, and storage tanks.

1.4 Corrosion Susceptibility of Aluminium Alloys

Aluminium, as indicated by its position in the electromotive force (emf) table (**Appendix 1**), is a thermodynamically reactive metal [16]. Because of its high electronegative potential (-1.66V), aluminium is one of the easiest metals to oxidise [14]. As mentioned, aluminium has excellent corrosion resistance and used as one of the primary metals of commerce. This resistance to corrosion is the result of the presence of a very thin, compact, and adherent film of aluminium oxide on the metal surface. Whenever a fresh surface is created by cutting or abrasion and is exposed to either air or water, a new film forms rapidly, growing to a stable thickness. The film formed in air at ambient temperature ≈ 5 nm (50 Å) thick. The thickness increases with temperature, and in the presence of water [13]. The uniform natural oxide layer formed in oxidising media; according to the following reaction



The free energy of this oxidation reaction, 21675 kJ, is one of the highest, this explains the very high affinity of aluminium towards oxygen [14].

As a general rule, the presence of acids or alkalis can change aluminium corrosion behaviour, according to Pourbaix diagram [17] [a diagram of potential versus pH] (**Figure 1.3**). The figure reflects the theoretical conditions at which aluminium becomes active or passive. From the diagram it can be seen that aluminium is stable in pH range from 4 to approximately 9 due to the presence of aluminium oxide film, which makes possible to use it in many applications where corrosion resistance is required. However, in acidic and alkali environments aluminium corrodes with the formation of Al^{3+}

and AlO_2^- ionic species respectively. It should also be noted that passivity of aluminium in neutral solutions can be overruled, when the solution contain species like chlorides that can cause breakdown of the oxide film and assist the corrosion of metal [18].

Alloy composition is considered to be one of the most important variables, which affect the corrosion behaviour of the metal. However, due to the presence of additional alloying metals the corrosion susceptibility of alloys increases [19].

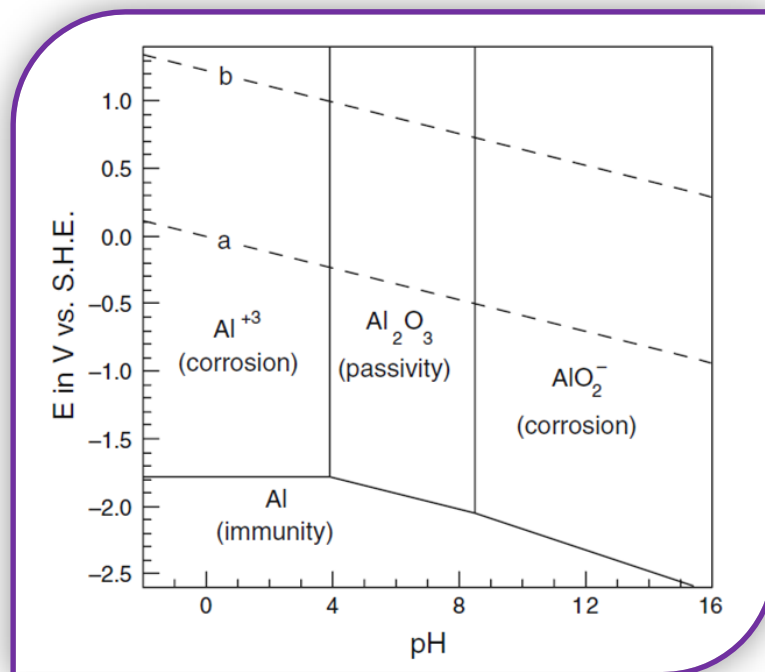


Figure 1.3. Potential - pH equilibrium diagram for the system aluminium – water at 25°C [9].

The fundamental reactions of the corrosion of aluminium in aqueous medium have been the subject of many studies. In simplified terms, the oxidation of aluminium in water proceeds according to the equation (1.24) [14]:



Metallic aluminium, in oxidation state 0, goes in solution as trivalent cation Al^{3+} when losing three electrons. This reaction is balanced by a simultaneous reduction in ions present in the solution, which capture the released electrons. In common aqueous media with a pH close to neutral such as fresh water, seawater, and moisture it can be shown by thermodynamic considerations that only two reduction reactions can occur:

- Reduction of H^{+} protons:



H^{+} protons result from the dissociation of water molecules:

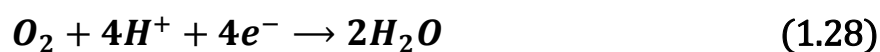


- Reduction of oxygen dissolved in water:

- In alkaline or neutral media:

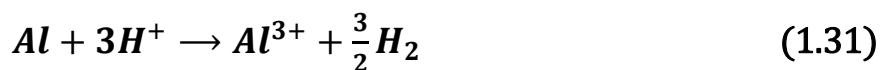


- In acidic media:

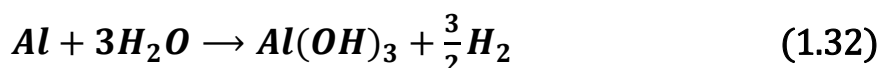


At 20 °C and under atmospheric pressure, the solubility of oxygen in water is 43.4 mg·kg⁻¹. It decreases with increasing temperature and is no more than 30.8 mg·kg⁻¹ at 40 °C, and 13.8 mg·kg⁻¹ at 80 °C [14].

Globally, the corrosion of aluminium in aqueous media is the sum of two electrochemical reactions, oxidation and reduction [14]:



or



This reaction is accompanied by a change in the oxidation state of aluminium, from 0 (in the metal), to +3, since aluminium loses three electrons that are picked up by 3H⁺. Aluminium corrosion results in the formation of alumina Al(OH)₃, which is insoluble in water and precipitates as a white gel.

1.5 Types of Corrosion for Aluminium

Different types of corrosion, more or less visible to the naked eye, can occur on aluminium, such as uniform (generalised) corrosion, pitting corrosion, stress corrosion, etc. The predominant type of corrosion depend on a certain number of factors that are intrinsic to the metal, the medium and the conditions of use. There is no form of corrosion that is specific to aluminium and its alloys [14].

1.5.1 Uniform Corrosion

Uniform corrosion is the most common form of corrosion in which all areas of the metal corrode at the same (or similar) rate [18] (**Figure 1.4**).

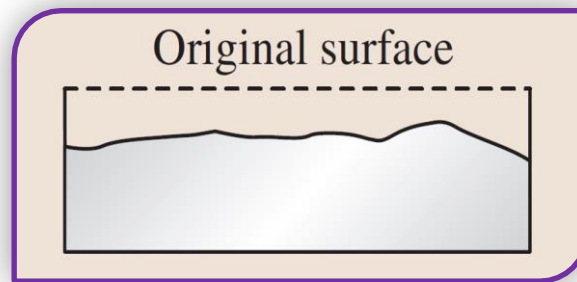


Figure 1.4. Schematic representation of uniform corrosion [20].

Uniform or general corrosion of aluminium is rare, except in special, highly acidic or alkaline corrodents. However, if the surface oxide film is soluble in the environment, as in phosphoric acid or sodium hydroxide, aluminium dissolves uniformly at a steady rate [16]. The dissolution rate of the film is greater than its rate of formation; however, the ratio of both rates can change over time [14]. If heat is involved, as with dissolution in sodium hydroxide, the temperature of the solution and the rate of attack increases. Depending on the specific ions present, their concentration, and their temperature, the attack can range from superficial etching to rapid dissolution. Dissolution is most uniform in pure aluminium and then next most uniform in dilute alloys and the non heat- treatable alloys [16].

1.5.2 Galvanic Corrosion

Galvanic corrosion (also called “dissimilar metal corrosion” or wrongly “electrolysis”) refers to corrosion damage induced when two dissimilar materials are coupled in a corrosive electrolyte [21] (**Figure 1.5.**).

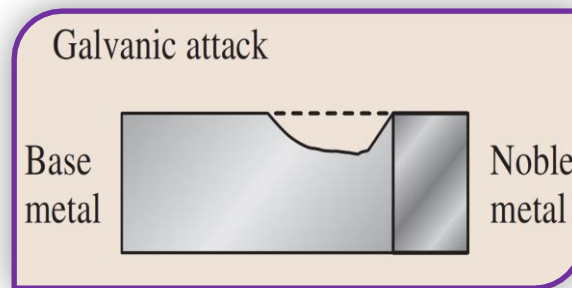


Figure 1.5. Schematic representation of galvanic corrosion [20].

The most common examples occur when aluminium alloys are joined to steel or copper and exposed to wet saline environments. In such situations the aluminium is more rapidly corroded than it would be in the absence of the dissimilar metal [13].

For each environment, metals can be arranged in a galvanic series from most to least active. **Table 1.3.** present the potentials based on measured in sodium chloride solution. It is important to remember that various aluminium alloys have sufficiently different corrosion potentials (as much as 0.4 V in some cases) to cause strong galvanic cells when in contact with each other [13].

The rate of corrosive attack when two metals are coupled depends on several factors [16]:

- a) The potential difference,
- b) The electrical resistance between the metals,
- c) The conductivity of the electrolyte,
- d) The cathode/anode area ratio,
- e) The polarization characteristics of the metals.

Although the corrosion potential can be used to predict which metal will be attacked galvanically, but the extent of attack cannot be predicted because of polarization. For example, the potential difference between aluminium and stainless steel exceeds that between aluminium and copper; however, the galvanic effect of stainless steel on aluminium, due to polarization [16].

In natural environments, including saline solutions, zinc is anodic to aluminium and corrodes preferentially, giving protection to the aluminium. Magnesium is also protective, although in severe marine environments, it can cause corrosion of aluminium because of the alkaline reaction. Cadmium is neutral to aluminium and can be used safely in contact with it. Copper and copper alloys, brass, bronze, and monel are the most harmful, followed closely by carbon steel in saline environments. Nickel is less aggressive than copper, approaching stainless steel in effect, as does chromium electroplate. Lead can be used with aluminium, except in marine environments [16].

Table 1.3. Electrode potentials of some representative aluminium alloys and other metals.

Al alloy or other metal	Potential* (V)	Al alloy or other metal	Potential* (V)	Al alloy or other metal	Potential* (V)
Chromium	+0.18 to -0.4	Tin	-0.49	Cadmium	-0.82
Nickel	-0.07	Lead	-0.55	1100 Al	-0.83
Silver	-0.08	Mild carbon steel	-0.58	5052 Al, 5086 Al	-0.85
Stainless steel (300 series)	-0.09	2219 Al	-0.64	Zinc	-1.10
Copper	-0.20	2024 Al	-0.69	Magnesium	-1.73

* measured in an aqueous solution of 53g of sodium chloride and 3g of H_2O_2 per liter at 25°C; 0.1N calomel reference electrode [21].

1.5.3 Crevice Corrosion

Crevice corrosion is a form of localized corrosion that occurs in zones of restricted flow where a metallic material surface is in contact with a small volume of confined, stagnant liquid whereas most of the material surface is exposed to the bulk environment (**Figure 1.6**) [22].

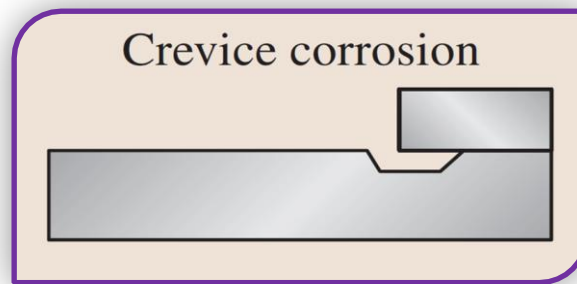


Figure 1.6. Schematic representation of crevice corrosion [20].

Crevice zones may result from the design of the component or from the formation of deposits during service, shutdown, or even fabrication. It occurs when there is a crevice that is created when two materials are in contact. The chemistry of crevice corrosion is very similar to pitting corrosion. Diffusion limitation of oxygen in a crevice can cause differential aeration that creates favorable conditions for metal dissolution and eventually a localized corrosion. Accumulation of chlorides in a crevice can accelerate the development of corrosion [22].

1.5.4 Pitting Corrosion

Pitting corrosion refers to highly localised attack at specific areas resulting in small pits that penetrate into the metal and may lead to perforation [18] (**Figure 1.7**).

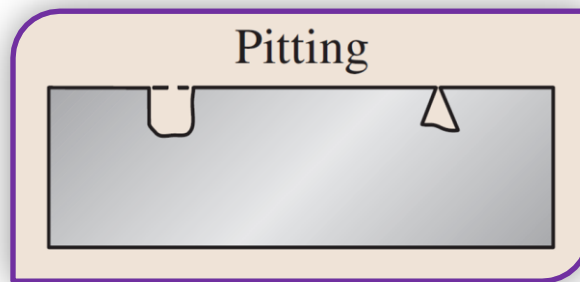


Figure 1.7. Schematic representation of pitting corrosion [20].

Pit shape can vary from shallow depressions to cylindrical or roughly hemispherical cavities [13]. Pitting formation is very common for different passive materials like stainless steels and nickel alloys with chromium, aluminium alloys in the presence of chlorides. It occurs when there is a breakdown of passive oxide film due to external factors [22]. The schematic picture of the mechanism of pitting propagation for aluminium alloys is shown in **Figure 1.8.**

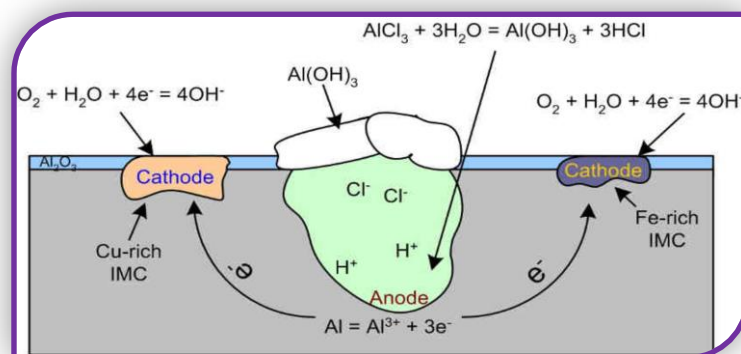


Figure 1.8. Schematic representation of the pitting activity of aluminium alloy in chloride solution [23].

In anodic part of the pit (**Figure 1.8**), the oxidation reaction occurs. The electrochemically active metal (aluminium) is removed from the alloy as aluminium ions and electrons are injected in the metal [14]:



At the same time the cathodic process occurs at noble electrochemical places like copper or iron containing as intermetallics, and involves the reduction process of dissolved oxygen in water and hydroxyl ions formation:



Though the reaction of hydrogen evolution is possible in an acidic environment:



Electron transfer between cathodic and anodic parts is provided by bulk alloy. In case of localized corrosion if the cathode area is much bigger than the anodic one. Then the anodic current density is significantly higher than the cathodic one, so the dissolution of metal from the anodic part becomes very rapid. Aluminium in a cationic form attracts chloride ions from the solution, therefore hydrochloric acid is produced as a consequence of water hydrolysis of aluminium cations. This leading to a significant acidification of the solution near the anode, according to following equation [19]:



Such decrease of pH promotes further dissolution of aluminium and the total process becomes autocatalytic. An insoluble cap of aluminium hydroxide is formed in contact with neutral bulk solution at the pit mouth (**Figure 1.8**). The cap is porous enough for the transport of chloride ions to the pit [24].

Propagation of pitting further into the metal surface may result in mechanical failure of a constructional part during the service application, which can be a serious problem causing significant damage [23].

1.5.5 Intergranular Corrosion

Intergranular (transgranular or intercrystalline) corrosion (IGC) is a form of localized attack in which a narrow path is corroded out preferentially along the grain boundaries of a metal [21] (**Figure 1.9**).

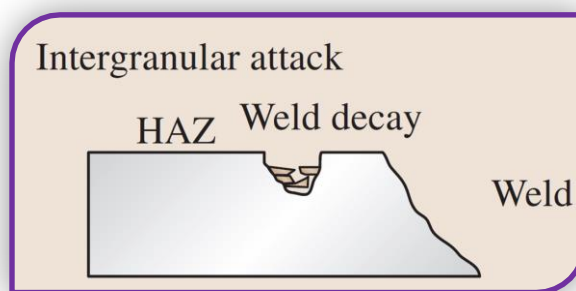


Figure 1.9. Schematic representation of intergranular corrosion [20].

Intercrystalline corrosion is caused by a difference in the electrochemical potentials between the bulk of the grain and the grain boundaries where intermetallic phases precipitate [14].

Intergranular corrosion occurs to some extent in most heat treatable. High-strength products (2xxx and 7xxx alloys), it is often related to copper depleted regions or to anodic precipitates at the grain boundary region. Because corrosion is limited to the immediate grain boundary region, IGC is difficult to detect without the aid of a microscope. This localization penetrates more quickly than pitting corrosion. But it reaches a self-limiting depth due to limited transport of oxygen and corroding species down the narrow corrosion path. When the depth of penetration ceases, IGC spreads laterally over the entire surface [16].

1.5.6 Stress Corrosion Cracking

Stress corrosion cracking (SCC) can be defined as crack formation due to simultaneous effects of static tensile stresses and corrosion [25] (**Figure 1.10**).

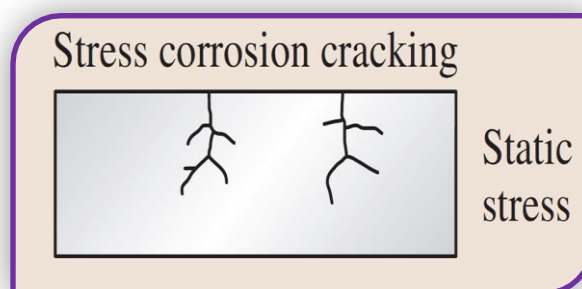


Figure 1.10. Schematic representation of stress corrosion cracking [20].

In aluminium alloys, stress corrosion can be promoted by a film of moisture on the surface of metal which exposed to the atmosphere, or by

contaminants (such as chlorides). Only a prolonged surface tension, stress will cause SCC [16].

1.5.7 Corrosion Fatigue

Corrosion fatigue (CF) is crack formation due to varying stresses combined with corrosion (**Figure 1.11.**). Alternatively, it may be defined as fatigue stimulated and accelerated by corrosion. The problem is caused by tensile stresses, just as for SCC. The external difference between these two forms of deterioration is only that CF develops under varying stresses, with regard to SCC which is under static stresses [25].

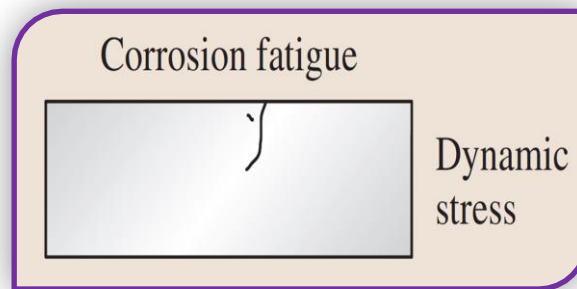


Figure 1.11. Schematic representation of corrosion fatigue [20].

Fatigue strengths of aluminium alloys are lower in corrosive environments such as seawater and other salt solutions than in air, especially when evaluated by low – stress, long – duration tests. This corrosive environments produce smaller reductions in fatigue strength in the more corrosion – resistant alloys, such as the 5xxx and 6xx series, than in the less resistant alloys, 2xxx and 7xxx series [13].

1.5.8 Erosion – Corrosion

Erosion is accelerated corrosion resulting from the conjoint action of corrosion and erosion in the presence of a moving corrosive fluid (**Figure 1.12.**). This type of attack is highly dependent on fluid flow rate and corrosivity [26].

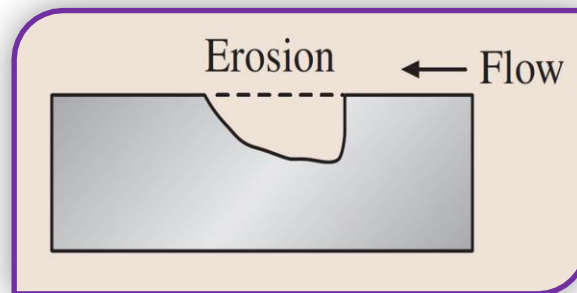


Figure 1.12. Schematic representation of erosion – corrosion [20].

In noncorrosive environments (high – purity water) the stronger aluminium alloys have the greatest resistance to erosion – corrosion, because resistance is controlled almost entirely by the mechanical components of the system [13].

1.5.9 Exfoliation Corrosion

Exfoliation corrosion, sometimes referred to as layer, stratified, or lamellar corrosion, is a form of corrosion resulting from a relatively rapid lateral attack along electrochemically anodic strata parallel to the metal surface (**Figure 1.13**) [16].

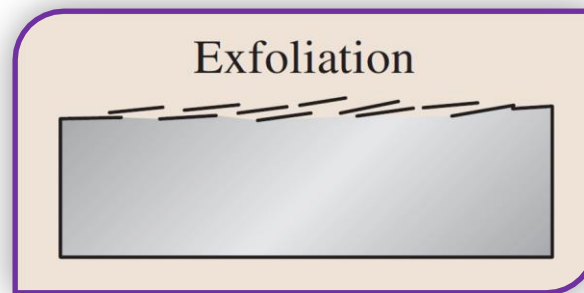


Figure 1.13. Schematic representation of exfoliation corrosion[31].

Exfoliation is a related type of anodic path corrosion in which attack of rolled or extruded aluminium alloy results in surface blisters followed by separation of elongated slivers or laminae of metal. It occurs in various types of aluminium alloys in addition to the copper - bearing series. Proper heat treatment may alleviate such attack [26].

1.5.10 Filiform Corrosion

This corrosion occurs under some coatings in the form of randomly distributed threadlike filaments, sometimes known as under film corrosion. It appears as a narrow from 0.05 to 3 mm wide network of tunnels or filaments either under thin film, thick coating or native oxide film of alloy on the surface[28].

Usually such type of corrosion starts in flaws, micro defects or scratches present in organic coatings. However, poor adhesion of paint and coatings to aluminium substrate can also be a reason for the appearance of such corrosion activity. The factors that accelerate filiform corrosion are the increase of

relative humidity and temperature. It was shown that the most rapid growth of filaments occurs at the relative humidity about 80 % and the temperature around 40°C. Penetration of water inside the defects forms differential aeration cells with localized anodic and cathodic activity [29]. The mechanism of the filiform corrosion is presented in **Figure 1.14.**

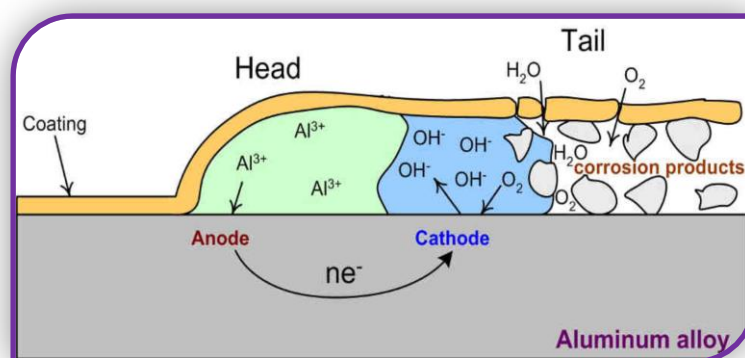


Figure 1.14. Schematic representation of the filiform corrosion mechanism [23].

The filament is separated into head and tail corrosion parts. At the head there is an anodic reaction of aluminium dissolution, equation (1.33) with the formation of aluminium cations. The reaction of hydrolysis of aluminium species in chloride containing solution decreases pH that assists further propagation of corrosion, equation (1.36). Atmospheric constituents like sulfates, sulfides and carbon dioxide also assist acidification. During the corrosion process the head of filament is moving forward while the tail stays behind. Corrosion products of aluminium stay in the tail of the filament and assists migration of soluble species (oxygen and water). The cathodic process of oxygen reduction takes place in the tail of the filament, equation (1.35), which makes localized alkali environment nearby [20].

1.5.11 Stray – Current Corrosion

Stray-current corrosion, or stray-current electrolysis, is different from natural corrosion because it is caused by an externally induced electrical current (alternating, AC, or direct current, DC). It is basically independent of environmental factors as oxygen concentration or pH [16].

Whenever an electric current is conducted from aluminium to an environment such as water, soil, or concrete, the aluminium is corroded in the area of anodic reaction proportion to the current. At low current densities, the corrosion may be in the form of pitting, while at higher current rates dimities the corrosion do not diminish with time [13].

1.5.12 Deposition Corrosion

Deposition corrosion is a special form of galvanic corrosion that causes pitting. It occurs when particles of a more cathodic metal plate out of solution on the aluminium surface, setting up local galvanic cells. The ions aggressive to aluminium are copper, lead, mercury, nickel and tin, often referred to as heavy metals. Their effects are greater in acidic solutions and are much less severe in alkaline solutions in which their solubility is low [16].

Copper ions most commonly cause this type of corrosion in applications of aluminium. For example, rain runoff from copper roof flashing can cause corrosion of aluminium gutters with no electrical contact between the two metals. Very small amounts of copper in solution (as low as 0.05 ppm) can be detrimental. The inferior general corrosion resistance of alloys containing

copper is attributed to deposition corrosion by copper repleted from the dissolved corrosion products [16].

Mercury is the ion most aggressive to aluminium, and even traces can cause serious problems. Liquid mercury does not wet aluminium, but if the natural oxide film on the aluminium surface is broken, aluminium dissolves in mercury, forming amalgam, and the corrosion reaction becomes catastrophic. In corrosive solutions, any concentration of mercury greater than a few parts per billion should be cause for concern [16].

1.5.13 Hydrogen Embrittlement

Only recently it has been determined that hydrogen embrittles aluminium. For many years, all environments cracking of aluminium and aluminium alloys was represented as SCC. However, testing in specific hydrogen environments revealed that aluminium is susceptible to hydrogen damage [13] **Figure 1.15.**

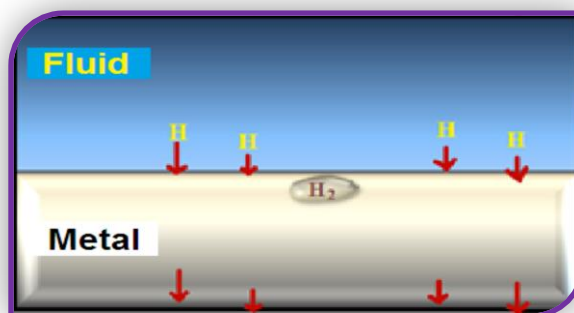


Figure 1.15. Corrosion by hydrogen embrittlement [30].

Hydrogen damage in aluminium alloys may take the form of intergranular or transgranular cracking or blistering. Blistering is most often associated with the melting or heat treatment of aluminium, in which reaction with water vapor produces hydrogen. Blistering due to hydrogen is frequently associated with grain-boundary precipitates or the formation of small voids [13].

1.6 Corrosion Inhibitors

1.6.1 Definition of Inhibitors

Inhibitors got their names from the Latin word *inhibere* which means *to suppress, to hold, or to retain* [31]. An inhibitor is a chemical substance or combination of substances that when present in the environment, prevents or reduces corrosion without significant reaction with the components of the environment [32]. Corrosion inhibitors can be solids, liquids, and gases (vapor-phase inhibitors), and can be used in solid, liquid, and gaseous media. Solid media can be concrete, coal slurries or organic coatings (paints). Liquids may be water, aqueous solutions, or organic solvents. A gaseous medium is an atmosphere or water vapor [31].

Inhibitors slow the corrosion processes by [33].

- ◆ Increasing the anodic or cathodic polarization behaviour (Tafel slopes).
- ◆ Reducing the movement or diffusion of ions to the metallic surface.
- ◆ Increasing the electrical resistance of the metallic surface.

Inhibitors can be used at pH values of acid from near neutral to alkaline. They can be classified in many different ways according to [34]

1. Their chemical nature (organic or inorganic substances).
2. Their characteristics (oxidizing or nonoxidizing compounds).
3. Their technical field of application (pickling, descaling, acid cleaning, cooling water systems, and the like).

1.6.2 Classification of Inhibitors

Inhibitor selection is based on the metal and the environment. A qualitative classification of inhibitors is presented in **Figure 1.16**. Inhibitors can be classified into environmental conditioners, and interface inhibitors [24].

1.6.2.1 Environmental Conditioners (Scavengers)

Corrosion can be controlled by removing the corrosive species in the medium. Inhibitors that decrease corrosivity of the medium by scavenging the aggressive substances are called environmental conditioners or scavengers. In near-neutral and alkaline solutions, oxygen reduction is a common cathodic reaction. In such situations, corrosion can be controlled by decreasing the oxygen content using scavengers [24]. Examples of this type of inhibitors hydrazine which removed oxygen from aqueous solutions as follows [35]:



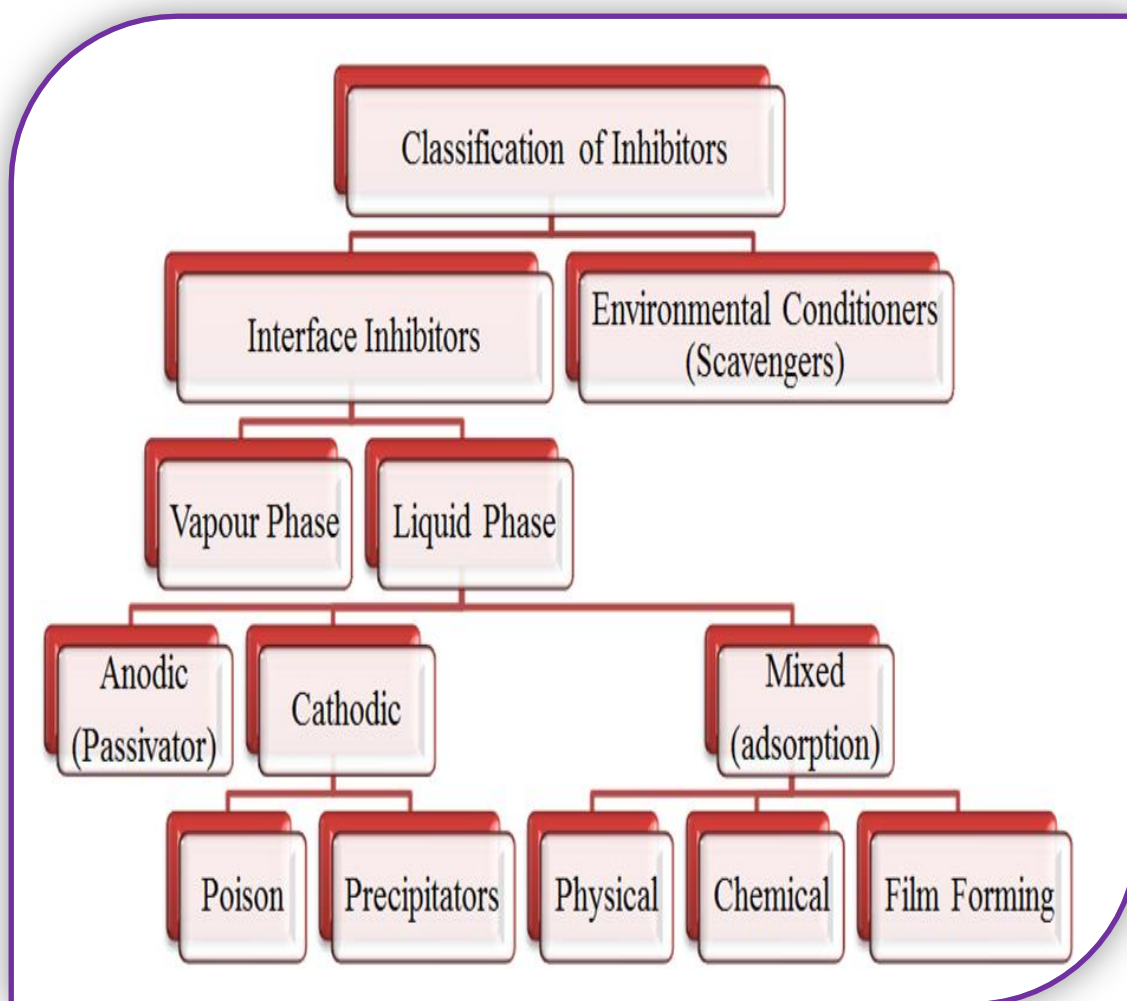


Figure 1.16. Classification of inhibitors [24].

1.6.2.2 *Interface Inhibitors*

Interface inhibitors control corrosion by forming a film at the metal/environment interface. Interface inhibitors can be classified into vapour-phase and liquid-inhibitors [24].

1.6.2.2.1 Liquid-Phase Inhibitors

Liquid-phase inhibitors are classified as anodic, cathodic, or mixed inhibitors, depending on whether they inhibit the anodic, cathodic, or both electrochemical reactions [24].

1.6.2.2.1.1 Anodic Inhibitors (Passivator)

Passivating inhibitors cause a large anodic shift of the corrosion potential, forcing the metallic surface into the passivation range [34], **Figure 1.17**. Passivation inhibitors are chemical oxidizing materials such as chromate ($\text{Cr}_2\text{O}_4^{2-}$) and nitrite (NO_2^-) or substances such as (Na_3PO_4) or (NaBrO_7). These materials favour adsorbed on the metal surface of dissolved oxygen [34] **Figure 1.18**.

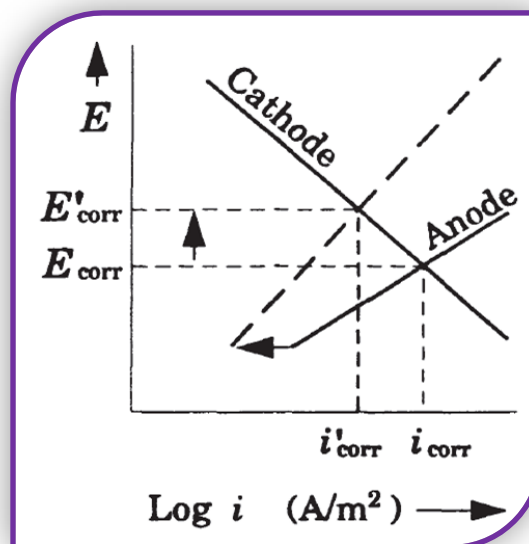


Figure 1.17. Effect of adding an anodic inhibitor. Dash lines show inhibitor addition [26].

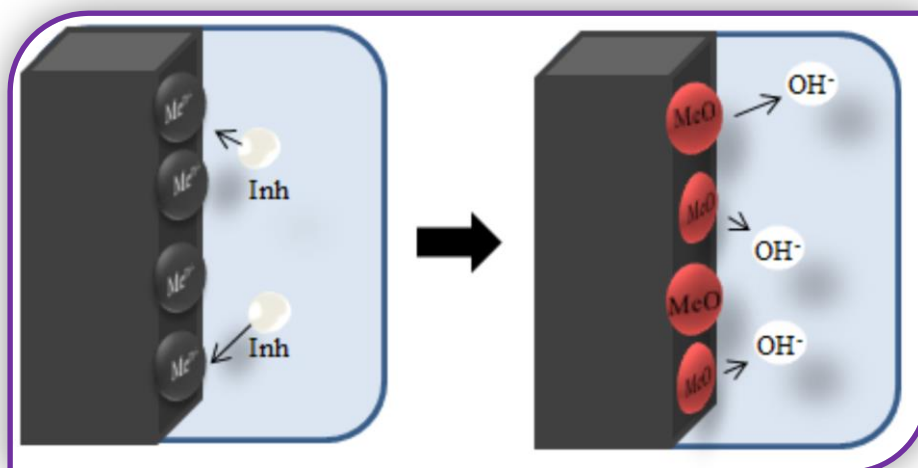


Figure 1.18. The mechanism of actuation of the anodic inhibitors [36].

In general, passivation inhibitors are considered dangerous because they can actually cause pitting and accelerate corrosion when concentrations fall below minimum limits (insufficient concentrations). For this reason it is essential that monitoring of the inhibitor concentration be performed [33].

1.6.2.2.1.2 Cathodic Inhibitors

Cathodic inhibitors either slow the cathodic reaction itself or selectively precipitate on cathodic areas to increase the surface impedance and limit the diffusion of reducible species to these areas [33] (**Figure 1.19**). Cathodic inhibitors are effective when they slow down the cathodic reaction rate. A cathodic inhibitor reduces the cathode exchange current density and often increases the activation of polarization [26], **Figure 1.20.**, by reducing the hydrogen reduction reaction rate and, lowering the overall corrosion rate [31].

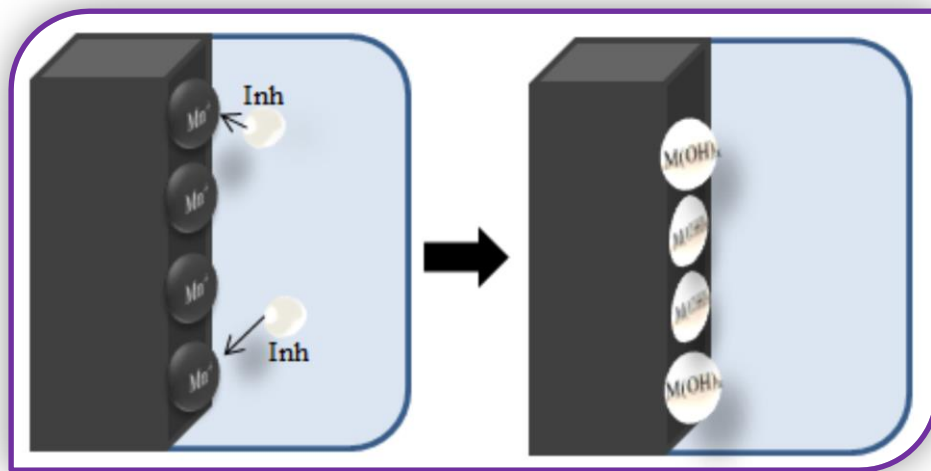


Figure 1.19. The mechanism of actuation of the cathodic inhibitors [36].

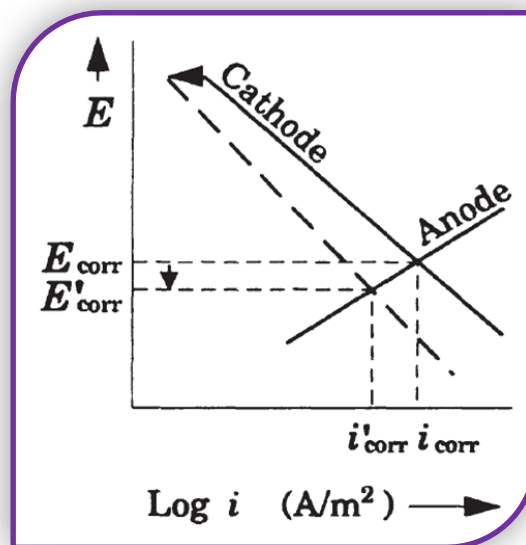


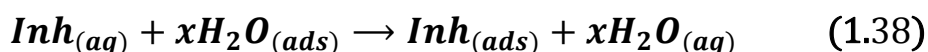
Figure 1.20. Effect of adding a cathodic inhibitor. Dash lines show inhibitor addition [26].

1.6.2.2.1.3 Mixed inhibitors

Mixed inhibitors are compounds that retard the anodic and cathodic corrosion processes simultaneously by general adsorption covering the entire surface [2] (**Figure 1.21.**). A mixed inhibitor affects both anode and cathode, with only a minor effect, either to positive or negative direction, on the corrosion potential (**Figure 1.22.**).

About 80% of inhibitors are organic compounds that cannot be designated specifically as anodic or cathodic and are known as mixed inhibitors. The effectiveness of organic inhibitors is related to the extent to which they adsorb and cover the metal surface. Adsorption depends on the structure of the inhibitor, on the surface charge of the metal, and the type of electrolyte [24].

Metal and oxide surfaces that are in contact with an aqueous solution are covered by adsorbed water. Any other species, inhibitors or electrolyte anions that adsorb on the surface must replace one or several water molecules. Therefore the adsorption reaction of an inhibitor occurring in the following general way [37]:



The (*Inh*) is assigned for the inhibitor molecule, and the subscripts (*aq*) and (*ads*) designate species in the aqueous phase and adsorbed at the surface, respectively. The stoichiometric coefficient *x* depends on the size of the inhibitor molecule and the structure of the metal surface [37].

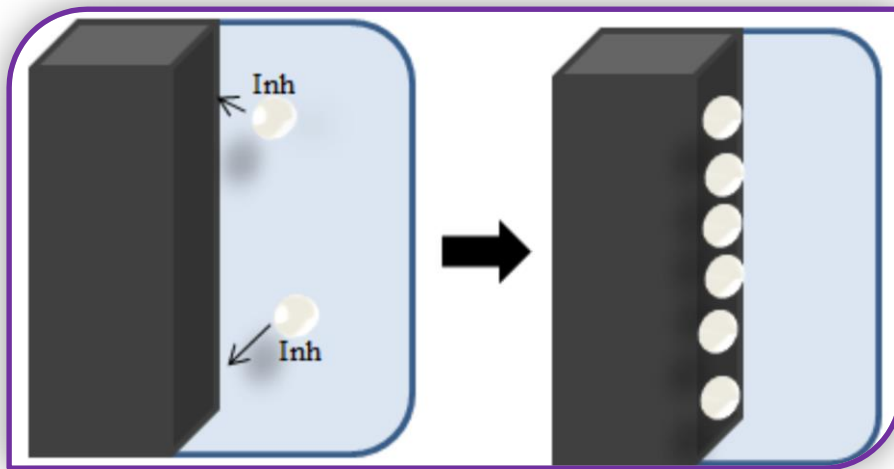


Figure 1.21. The mechanism of actuation of the mixed inhibitors: acting through adsorption of the inhibitor on the metal surface [36].

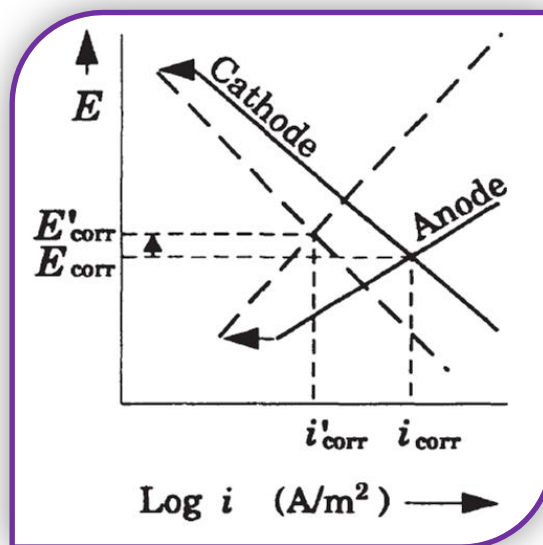


Figure 1.22. Adding a mixed inhibitor. The dash lines show the inhibitor addition effect [26].

Mixed inhibitors protect the metal in three possible ways: physical adsorption, chemisorption and film formation. Physical (or electrostatic) adsorption is a result of electrostatic attraction between the inhibitor and the metal surface. Physically adsorbed inhibitors interact rapidly, but they are also easily removed from the surface. Increase in temperature generally facilitates desorption of physically adsorbed inhibitor molecules [24].

The most effective inhibitors are those that chemically adsorb (chemisorb), a process that involves charge sharing or charge transfer between the inhibitor molecules and the metal surface. Chemisorption takes place more slowly than physical adsorption. As temperature increases, adsorption and inhibition also increase. Chemisorption is specific and is not completely reversible [24].

The adsorbed species must have a dipole in the molecule. Chemisorption usually occurs through electron donation to a metal surface. Compounds which contain sulphur atom such as sulfoxides. Furthermore nitrogen, atom such as aliphatic, aromatic or heterocyclic amines and compounds containing double or triple bonds such as hydrocarbon chain can be used in this type of inhibitors. The tendency to stronger co-ordinate bond formation between the inhibitor molecule and metal surface and hence stronger adsorption increases with decreasing electronegativity in following the order [38]:



← Increasing inhibition

→ Increasing electronegativity

The adsorption of organic compounds is influenced by the electronic structure of inhibiting molecules, steric factor, aromatic, and electron density at donor site, presence of functional group such as $-\text{CHO}$, $-\text{N}=\text{N}$, $\text{R}-\text{OH}$ etc., molecular area and molecular weight of the inhibitor molecule [39].

Adsorbed inhibitor molecules may undergo surface reactions, producing polymeric films. Corrosion protection increases markedly as the films grow from nearly two-dimensional adsorbed layers to three-dimension films up to several hundred angstroms thick. Inhibition is effective only when the films are adherent, are not soluble, and prevent access of the solution to the metal. Protective films may be nonconducting (sometimes called ohmic inhibitors because they increase the resistance of the circuit, thereby inhibiting the corrosion process) or conducting (self-healing films) [24].

1.6.2.2.2 Vapor-Phase Inhibitors

The process of vapor-phase inhibition involves two steps: transport of inhibitor to the metal surface and interaction of inhibitor on the surface. AVPI may vaporize either in the molecular form or it may first dissociate and then vaporize. Both in molecular and in dissociated forms VPIs adsorb either physically or chemically on the metal surface to inhibit corrosion [24].

1.7 Green Corrosion Inhibitors

There is increasing concern about the toxicity, biodegradability, and bioaccumulation of corrosion inhibitors discharged into the environment. A noteworthy example consists of oilfield chemicals used as inhibitors discharged into the environment from offshore production platforms. Corrosion inhibitors in the aqueous phase are discharged into the ocean; these become an environmental hazard to marine life [40].

Organic compounds with functional groups containing nitrogen, sulfur, and oxygen atoms are generally used as corrosion inhibitors. Most of these organic compounds are not only expensive, but also harmful to the environment. Thus, efforts have been directed toward the development of cost effective and nontoxic corrosion inhibitors [40].

Consequently, the search for effective as well as environmentally acceptable corrosion inhibitors as alternatives to these toxic inhibitors is considered to be important for prevention of corrosion of metal and its alloys in an aggressive medium. In the past few years, attempts have been made to use plant extracts as *green inhibitors* [5]. Because of their natural origin, as well as their non-toxic characteristics and negligible negative impacts on the aquatic environment, drugs (chemical medicines) seem to be ideal candidates to replace traditional toxic corrosion inhibitors [41]. The choice of some drugs as corrosion inhibitors is based on the following points [42-44]:

- Drug molecules containing oxygen, nitrogen and sulphur as active centres.

- Drugs are reported environmentally friendly and important in biological reactions (i.e. non-hazardous).
- They are biodegradable
- Drugs can be easily produced and purified.

Thus, such investigations are found to be very fruitful and encouraging in saving not only metals and energy but also the environment [5].

Some investigations have been reported on the use of antibacterial drugs as corrosion inhibitors [45-48]. Most of the used drugs play important roles in biological reactions because of their anticonvulsant, antibacterial, and anti diabetic, inhibitive to *Mycobacterium tuberculosis* and other properties [49-50].

Carbocyclic and heterocyclic systems are ubiquitous in drug structure. The five- and six-membered rings are the most common, but small ring systems occur with reasonable frequency (for example, the cyclopropane ring in ciprofloxacin and the aziridine ring in mitomycin C). In the five- and six-membered systems, the majority are aromatic or pseudo-aromatic. Hence, substituted benzene rings are very frequent, and heterocycles such as pyridines, furans, thiophenes, imidazoles, isoxazoles and others occur commonly in drug structure. Due to above-mentioned structural closeness, corrosion protection properties of many drugs have attracted so much attention in recent years [41].

1.8 Quantum Chemistry and Corrosion Inhibitor Studies

Quantum chemical methods have already proven to be very useful in determining the molecular structure as well as elucidating the electronic structure and reactivity. Thus, it has become a common practice to carry out quantum chemical calculations in corrosion inhibition studies. The concept of assessing the efficiency of a corrosion inhibitor with the help of computational chemistry is to search for compounds with desired properties, using chemical intuition and experience into a mathematically quantified and computerized form [51].

Quantum mechanics (QM) is the correct mathematical description of the behaviour of electrons and thus of chemistry. In theory, QM can predict any property of an individual atom or molecule exactly. In practice, the QM equations have only been solved exactly for one electron systems. A myriad collection of methods has been developed for approximating the solution for multiple electron systems [52].

Nearly all computational chemistry methods based on the Schrödinger equation

$$\hat{H} \Psi = E \Psi \quad (1.39)$$

Where \hat{H} is the Hamiltonian operator, Ψ a wave function, and E the energy. In the language of mathematics, an equation of this form is called an eigen equation. Ψ is then called the eigenfunction and E an eigenvalue [52].

The wave function Ψ is a function of the electron and nuclear positions. It can describe the probability of electrons being in certain locations, but it cannot predict exactly where electrons are located. The wave function Ψ is

also called a probability amplitude because it is the square of the wave function that yields the probabilities [52].

Several attempts have been made to predict corrosion inhibition efficiency using a number of individual quantum chemical parameters give enough information. These trial were aimed at finding possible correlations between corrosion inhibition efficiency and some quantum molecular properties such as dipole moment, the energy of the highest occupied molecular orbital (E_{HOMO}), the energy of the lowest unoccupied molecular orbital (E_{LUMO}), Mulliken charges as well as some structural parameters [53].

According to DFT-Koopmans' theorem, the ionization potential (I) can be approximated as the negative of the highest occupied molecular orbital (HOMO) energy [54],

$$I = -E_{HOMO} \quad (1.40)$$

The negative of the lowest unoccupied molecular orbital (LUMO) energy is similarly related to the electron affinity A,

$$A = -E_{LUMO} \quad (1.41)$$

The values of I and A can be used to obtained the electronegativity χ , and the global hardness η in each of the tested molecule according to the following relations:

$$\chi = \frac{A+I}{2} \quad (1.42)$$

$$\eta = \frac{A-I}{2} \quad (1.43)$$

During the interaction of the inhibitor molecule with bulk metal, electrons flow from the lower electronegativity molecule to the higher electronegativity metal until the chemical potential becomes equalized. The fraction of the transferred electron, ΔN , was estimated according to the following equation:

$$\Delta N = \frac{\chi_M - \chi_{Inh}}{2(\eta_M - \eta_{Inh})} \quad (1.44)$$

Where χ_M and χ_{Inh} denote the absolute electronegativity of metal and the inhibitor molecule, respectively; η_M and η_{Inh} denote the absolute hardness of metal and the inhibitor molecule, respectively.

1.9 The Literature Survey

According to the attractive applications of aluminium and its alloys in industry, many investigations about their corrosion and its inhibition have been done.

Gerengi et al. [55] investigated the inhibition effect of mad honey on corrosion of 2007-type aluminium alloy in 3.5% NaCl solution by Tafel extrapolation (TP), electrochemical impedance spectroscopy (EIS) and dynamic electrochemical impedance spectroscopy (DEIS). All the studied parameters exhibited good anti-corrosive properties against corrosion of 2007-type aluminium alloy in the test solution. Corrosion rates decreased with the increase of the mad honey concentration.

Popoola et al. [56] studied the corrosion of aluminium in saline environment in the presence of ferrous gluconate using weight loss and linear polarization methods. The corrosion rates were studied in different

concentrations of ferrous gluconate 0.5, 1.0, 1.5, and 2.0 g/mL at 28°C. Experimental results revealed that ferrous gluconate in saline environment reduced the corrosion rate of aluminium alloy at the different concentrations studied. The minimum inhibition efficiency was obtained at 1.5 g/mL concentration, while the optimum inhibition efficiency was achieved with 1.0 g/mL.

Chen et al. [57] studied the relationships between corrosion inhibition performance of four kinds of Schiff base inhibitors and their molecular electronic properties using quantum chemistry method, at the level of DFT/B3LYP with the 6-31+G (d, p) base sets. The study of the interaction between inhibitors and Al (100) surface shows that there are some electrons transferred from inhibitors to the surface, so after adsorption the inhibitor cannot capture electron from Al and lead to corrosion, and it could play a protective effect on the metal surface.

Singh et al. [58] investigated the inhibition behaviour of 5,6-dihydro-9,10-dimethoxybenzo[g]-1,3-benzodioxolo[5,6-a]quinolizinium (berberine) as an environment-benign corrosion inhibitor for AA7075 aluminium alloy in 3.5 wt.% NaCl solution by means of potentiodynamic polarization, AC impedance, scanning electrochemical spectroscopy (SECM) and scanning electron microscopy (SEM). The results showed that berberine can inhibit the corrosion of 7075 Al alloy at a different immersion time. The surface analysis also revealed that the retardation of corrosion due to adsorption of inhibitor molecules on the Al alloy surface.

Sherif [59] reported Corrosion of aluminium in aerated Arabian Gulf seawater (AGS) and 3.5% NaCl solutions and its inhibition by 3-amino-5-mercapto-1,2,4-triazole (AMTA). The study was carried out using cyclic potentiodynamic polarization (CPP), current-time at constant potential (CT), and electrochemical impedance spectroscopy (EIS) measurements. The results indicated that the presence of AMTA molecules inhibit the general and pitting corrosion of Al in both AGS and NaCl solutions by shifting the corrosion and pitting potentials of Al to the more noble values. This decreasing the corrosion, passivation currents and corrosion rate, by increasing the surface, and charge transfer resistances.

Shi et al. [60] studied the corrosion protection of Al 2024-T3 in 0.05 M NaCl by cerium cinnamate. Polarization measurements demonstrate that cerium cinnamate is markedly effective for suppressing anodic process of the alloy corrosion during the initial 72 h of immersion. The protection mechanism during the immersion period appears to involve two stages: the deposition of cerium cinnamate, and then hydrolysis of cerium ions forming a cerium oxide/hydroxide, prevailing over the foregoing deposition.

Sherif et al. [61] investigated the effects of 1,4-naphthoquinone (NQ) as a corrosion inhibitor for aluminium in aerated and de-aerated solutions of 0.50 M NaCl. These measurements revealed that the presence of NQ shifted the corrosion and pitting potentials to more noble values and decreased the anodic currents in the passive region in both aerated and de-aerated chloride solutions. The surface and polarization resistances are increased as the concentration of NQ is increased. The most effective concentration was found to be 1.0×10^{-3} M in both aerated and de-aerated chloride solutions.

1.10 *The Aim of the Research*

This research includes a number of important aims which may be summarized as:

1. Potentiostatic polarization studies for the corrosion behaviour of pure aluminium, 5052 aluminium and 2024 aluminium alloys, in saline solution at five different temperatures in the range of (283-323) K.
2. Studying the inhibition effect of three various concentrations of ampicillin, amoxicillin and cephalexin to inhibiting the corrosion, the effect of these inhibitors over the temperatures range (283 - 323) K by using potentiostatic polarization method. .
3. Calculate some quantum parameters for the ampicillin, amoxicillin and cephalexin to ascertain any correlation between the inhibitive effect and their molecular structures.
4. Studying the surface morphologies of pure aluminium in sodium chloride solution containing 7.5×10^{-4} M of ampicillin by using scanning electron microscope (SEM) to show the effect of adding inhibitor on aluminium surface.



CHAPTER TWO
EXPERIMENTAL



2.1 Materials and Chemicals

2.1.1 Aluminium Alloys

Aluminium and its alloys were used as test specimens have the following composition.

Table 2.1. Composition of aluminium alloys, wt. %.

Aluminium and its Alloys	Si	Fe	Cu	Mn	Mg	Cr	Ni	Zn	Al, min.*
1100 (Pure)	0.95 Si+Fe		0.05-0.2	0.05	-	-	-	0.10	99.0
2024	0.5	0.5	3.8-4.9	0.3-0.9	1.2-1.8	0.1	-	0.25	bal.*
5052	0.25	0.4	0.1	0.1	2.2-2.8	-	0.15-0.35	0.1	bal.*

* *min.* = minimum, *bal.* = balance

2.1.2 Chemicals

Many chemical were used in this work include some reagents which are listed in **Table 2.2.** with their purity and origin

Table 2.2. List of reagents used.

Reagent name	%Purity	Producer
sodium chloride	99	EDUTEK
Acetone	95	BDH
diamond product spray	High quality diamond product	Struers

2.1.3 Inhibitors

The inhibitors used for testing the corrosion protection of the alloys are

2.1.3.1 Ampicillin

(2S,5R,6R)-6-((R)-2-amino-2-phenylacetamido)-3,3-dimethyl-7-oxo-4-thia-1-azabicyclo[3.2.0]heptane-2-carboxylic acid, more commonly known as Ampicillin, obtained from Samarra Drugs Industry (SDI) with a purity exceeding 99%.

Physical Properties	
Abbreviation	AMP.
Appearance	White Crystals or Powder
Molecular Formula	C ₁₆ H ₁₉ N ₃ O ₄ S
Molecular Weight	349.40476 g /mol
Melting Point	208 °C
Solubility	13 mg/mL in water at 20°C

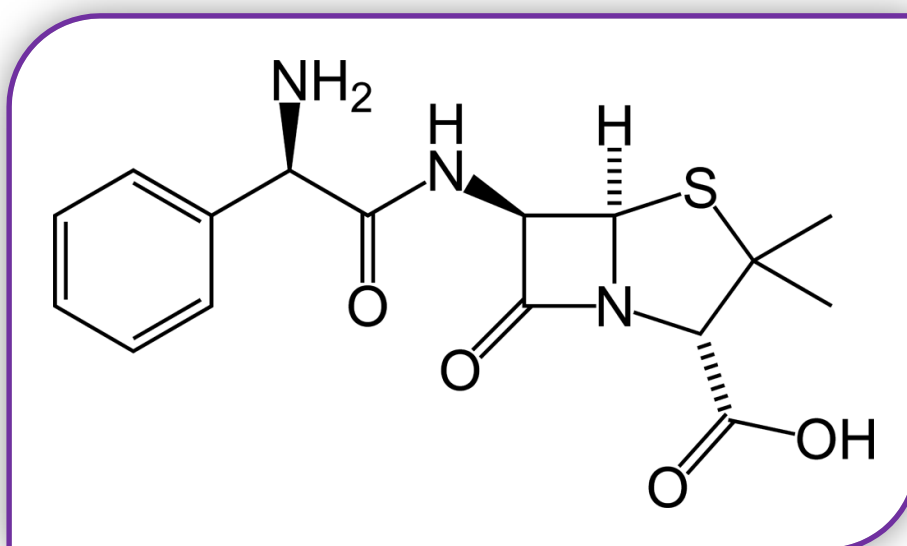


Figure 2.1. The chemical Structure of ampicillin.

2.1.3.2 Amoxicillin

(2S,5R,6R)- 6-[[[(2R)-2-amino- 2-(4-hydroxyphenyl)- acetyl]amino]- 3,3-dimethyl-7-oxo- 4-thia- 1-azabicyclo[3.2.0]heptane- 2-carboxylic acid, more commonly known as Amoxicillin, obtained from Samarra Drugs Industry (SDI) with a purity exceeding 99%.

Physical Properties	
Abbreviation	AMOX.
Appearance	White Crystals or Powder
Molecular Formula	C ₁₆ H ₁₉ N ₃ O ₅ S
Molecular Weight	365.40416 g/mol
Melting Point	194°C
Solubility	3.430 mg/mL in water at 20°C

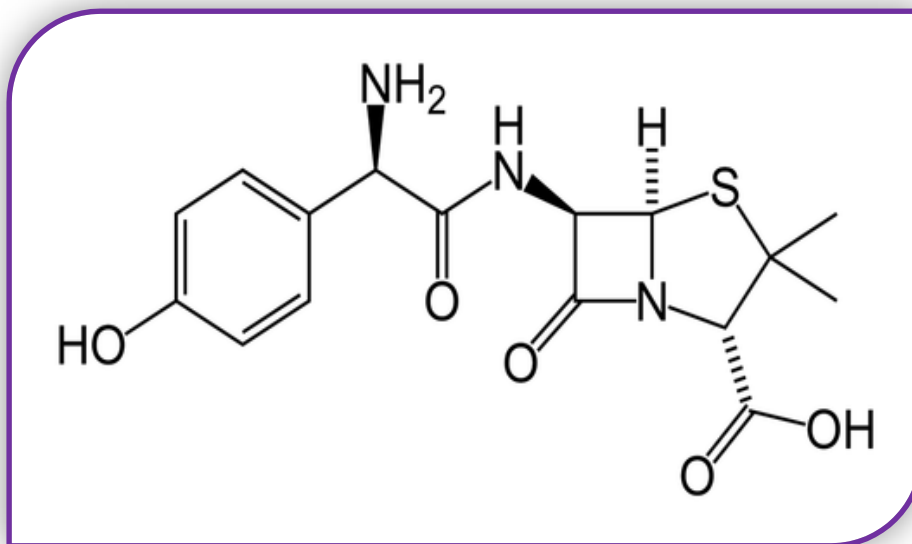


Figure 2.2. The Chemical Structure of Amoxicillin.

2.1.3.3 Cephalexin

(6R,7R)-7-[(2R)-2-amino-2-phenylacetamido]-3-methyl-8-oxo-5-thia-1-azabicyclo[4.2.0]oct-2-ene-2-carboxylic acid, more commonly known as Cephalexin, obtained from Samarra Drugs Industry (SDI) with a purity exceeding 99%.

Physical Properties	
Abbreviation	CEX.
Appearance	White to Off-White Crystals or Powder
Molecular Formula	$C_{16}H_{17}N_3O_4S$
Molecular Weight	347.38888 g/mol
Melting Point	326.8 °C
Solubility	1.789 mg/mL in water at 20°C

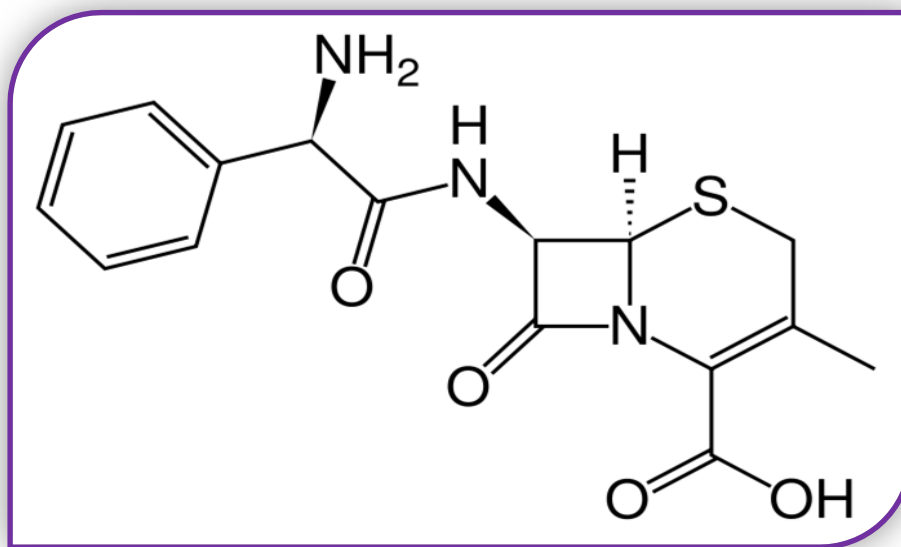


Figure 2.3. The chemical Structure of Cephalexin.

2.2 Sample Preparation

Circular shape samples of aluminium alloys were mechanically cut with dimensions of 2.5 cm diameter and 0.5 mm thickness. Prior to each electrochemical experiment, the test specimens were polished with emery paper (SiC paper) in different grades (320, 500, 1000, 2400, 4000) with diamond product sprays that contain ethanol with different size of the diamond particles (1 μ m, 3 μ m, 6 μ m, 9 μ m), then washed with acetone and finally rinsed with distilled water and keep in a desiccator for further use.

2.3 Preparation of Solutions

(3.5%) NaCl was prepared by dissolving (35 g) of NaCl pellets in 1000 ml distilled water. To prepare the inhibitor solutions, in each experiment, (1.5×10^{-4} , 3×10^{-4} , 4.5×10^{-4} , 6×10^{-4} and 7.5×10^{-4} M) of each inhibitor dissolved respectively in freshly prepared 3.5% NaCl solution.

2.4 The Experimental Equipment and Procedures

2.4.1 Electrochemical System

The electrochemical system consists of:

2.4.1.1 Potentiostat/Galvanostat

The polarization can be carried by using a potentiostat , A manually operated potentiostat is a stepwise instrument for measuring potential E and current density(i) and develop E vs. $\log (i)$ plots. Commercially programmable potentiostat, together with an electrometer, logarithmic

converter, and data acquisition device is an automated instrument that provides variability of continuous sweep (scan) over a desired potential range, including the cathodic and anodic regions. This automated procedure is called potentiodynamic polarization technique, which provides a polarization curve at desired scan rates [62].

The potentiostat measurements were carried out using M lab potentiostat / galvanostat 200 (2007) (Germany), was obtained from Bank Elektronik – Intelligent Controls GmbH as shown in **Figure 2.4.**



Figure 2.4. The front panel of M Lab 200 potentiostat/galvanostat.

2.4.1.2 Host Computer

The M Lab 200 potentiostat/galvanostat was connected to an external computer (type acer) via the RS 332 interface. M lab is controlled from computer software. The M lab software cares for control of the potentiostats, recording of data and also data processing.

2.4.1.3 Corrosion Cell

A suitable jacket vessel cell made of Pyrex with (1L) capacity consists of two vessels, internal and external, with enough cover openings to insert the electrodes, thermometer to measure the temperature of the solution inside the cell, gas inlets and outlet tubes, was used in this investigation, as shown in **Figure 2.5.**

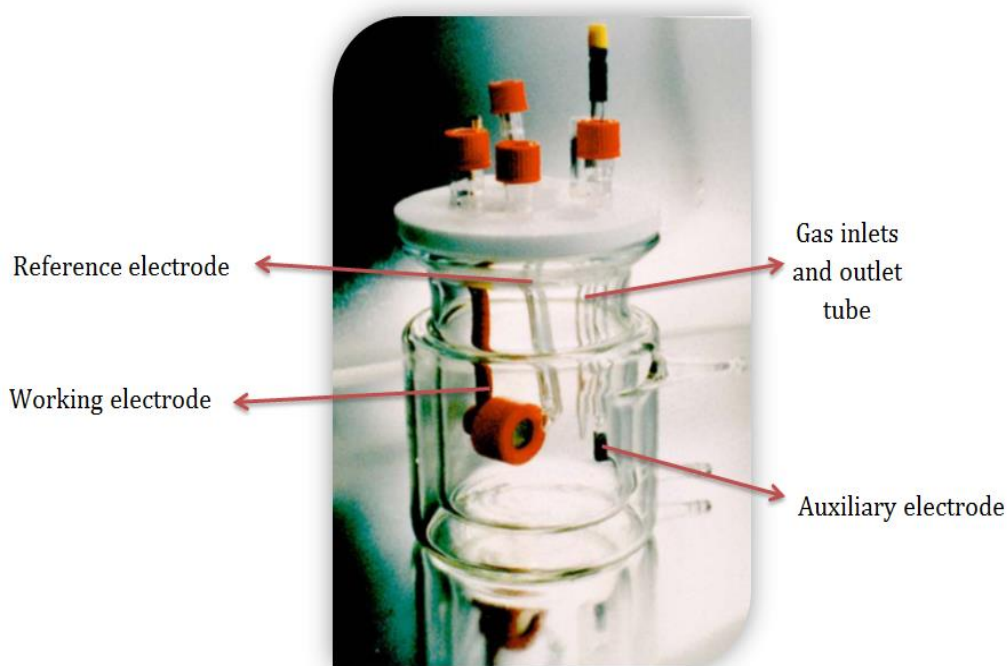


Figure 2.5. Set up the corrosion cell and three electrodes.

2.4.1.4 Three-Electrode System

This system is shown in **Figure 2.5.** The working electrode potential is measured against the reference electrode, provided that an ohmic resistance gradient is significantly reduced and current flows only between the auxiliary electrode and the working electrode. The electrochemical cell components and their functions are described below.

2.4.1.4.1 Working Electrode

Circular working electrode with 20 cm length metallic wire were made of (2.5) cm diameter, disk fix working electrode used for flat specimens in this investigation as shown in **Figure 2.6.**



Figure 2.6. Working electrode.

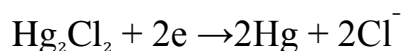
The specimen is placed between a mask with around opening and an electrically contacted brass plate, the backside of the specimen and the whole interior of the disk fix are sealed by washer to keep it dry. The exposed measuring surface of the specimen is determined by the mask of opening size, there are different mask size available. The aluminium alloys specimens with an exposed area of 1 cm^2 functions as the working electrode, where the anodic and cathodic reactions take place on the surface of the alloys.

2.4.1.4.2 Reference Electrodes

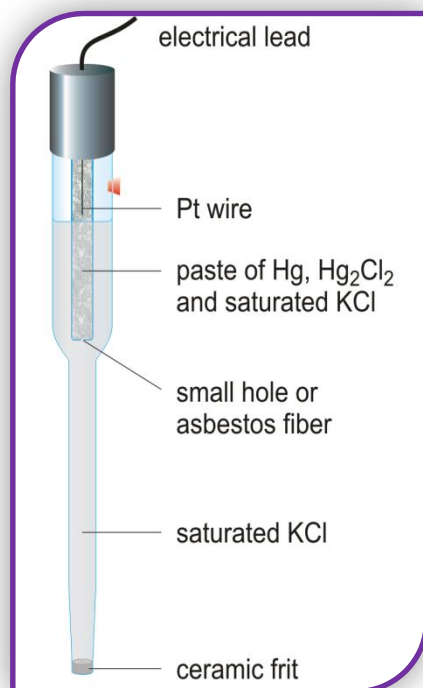
A saturated calomel reference electrode (SCE) was used throughout the whole work (**Figure 2.7.**). The calomel element consisted of mercury, mercurous chloride (calomel), and chloride ion.



The reduction reaction which occurs at the calomel electrode may be represented as:



Reference electrode is used to determine the working electrode potential according to the potential of reference electrode. The potential of reference electrode is well known and accurate (0.241 V, at 25°C). The electrode is usually brought in contact with the electrolyte through a glass tubing known as "Luggin capillary" the tip of the Luggin capillary is placed at the distance 1-2 mm from working electrode, Such arrangement of the Luggin capillary eliminated any ohmic potential drop (IR drop) that may develop in the solution separating the calomel electrode and the working electrode in the cell solution [63].



(a)



(b)

Figure 2.7. (a) Schematic diagram of reference electrode [64] (b) Reference electrode in Luggin capillary.

2.4.1.4.3 Auxiliary Electrode

Platinum electrode was used for this purpose. This electrode was prepared from high-purity rod stock with length (10 cm). It was preferred to use as an auxiliary electrode due to its large surface area and high catalytic activity. It passes the current to the working electrode (specimen) to be studied.

2.4.1.5 The Thermostat

The thermostat device used to make the temperature of water which flows through the external vessel of corrosion cell constant at required temperatures. Thermostat used in this study was HETOFRIG type DT. Accuracy of temperature adjustment was to within + 0.01°C of the required temperature in the experimental range 10 - 50°C.

2.4.1.6 Magnetic Stirrer

A magnetic stirrer is a laboratory device that employs a rotating magnetic field to cause a stir bar immersed in a liquid, thus stirring it. Magnetic Stirrer used in this study was Tacussel type AGIMAX.

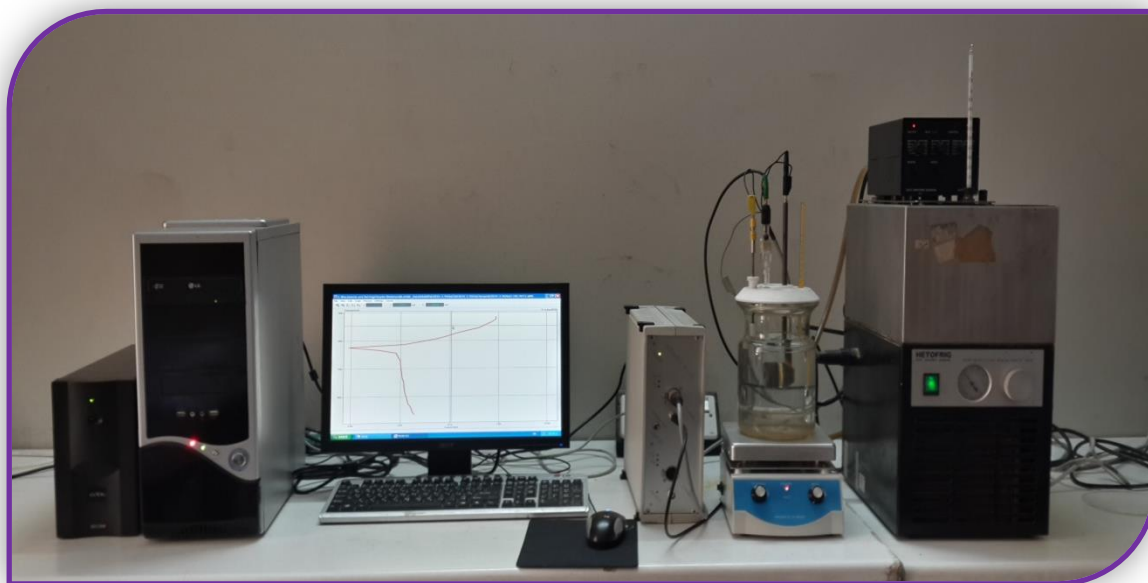


Figure 2.8. Complete system set up for polarization measurements.

2.4.2 Corrosion Measurement Procedures:

The corrosion behaviour of the aluminium alloy with and without inhibitors in 3.5% NaCl solution at different temperatures to understand their inhibition mechanism and to estimate the inhibition efficiency were measured by Tafel method.

2.4.2.1 Open Circuit Potential

To determine the open circuit potential (OCP) of the specimens corrosion, in each experiment the specimen have been immersed in the solution in different temperatures (10, 20, 30,40 and 50) °C to reach the steady state between the specimen's material and electrolytic solution. The open circuit potential assumed by the metal in the absence of applied

electrical connections. The change in potential according to the current were determined during (30min), and time step equal to 60 seconds for each specimen. After reaching the steady state condition, the determined potential is known as corrosion potential or free potential or open circuit potential.

2.4.2.2 *Tafel Extrapolation*

After determining the open circuit potential of the system, the cell will subject to potentiostatic scan ranging about (± 200) mV from the open circuit with scan rate (10 mV/s). The potential of according metal (WE) is varied (polarized) from its equilibrium value (E_{corr}) firstly in the negative and then in the positive direction and the current response to the applied potential is recorded. The voltage/current density data pairs produced from the polarization, WE can then be used to construct polarization diagram similar to **Figure 2.8**. [65-66].

2.5 *Quantum Chemical Calculation*

The molecular sketches of the inhibitors were drawn using the GaussView 5.08. All the quantum calculations were performed with complete geometry optimization using standard Gaussian 09 software package [67]. The quantum chemical parameters were calculated using the density functional theory (DFT) method (B3LYP) with 6-31G basis set. The evaluated quantum chemical parameters were: total energy (TE), the energy of the highest occupied molecular orbital (E_{HOMO}), the energy of the lowest unoccupied molecular orbital (E_{LUMO}), the energy gap between $E_{\text{LUMO}} - E_{\text{HOMO}}$ (ΔE_{gap}), dipole moment (μ), The number of electrons transferred from the molecule to the surface (ΔN), and Mulliken atomic charges of molecules.

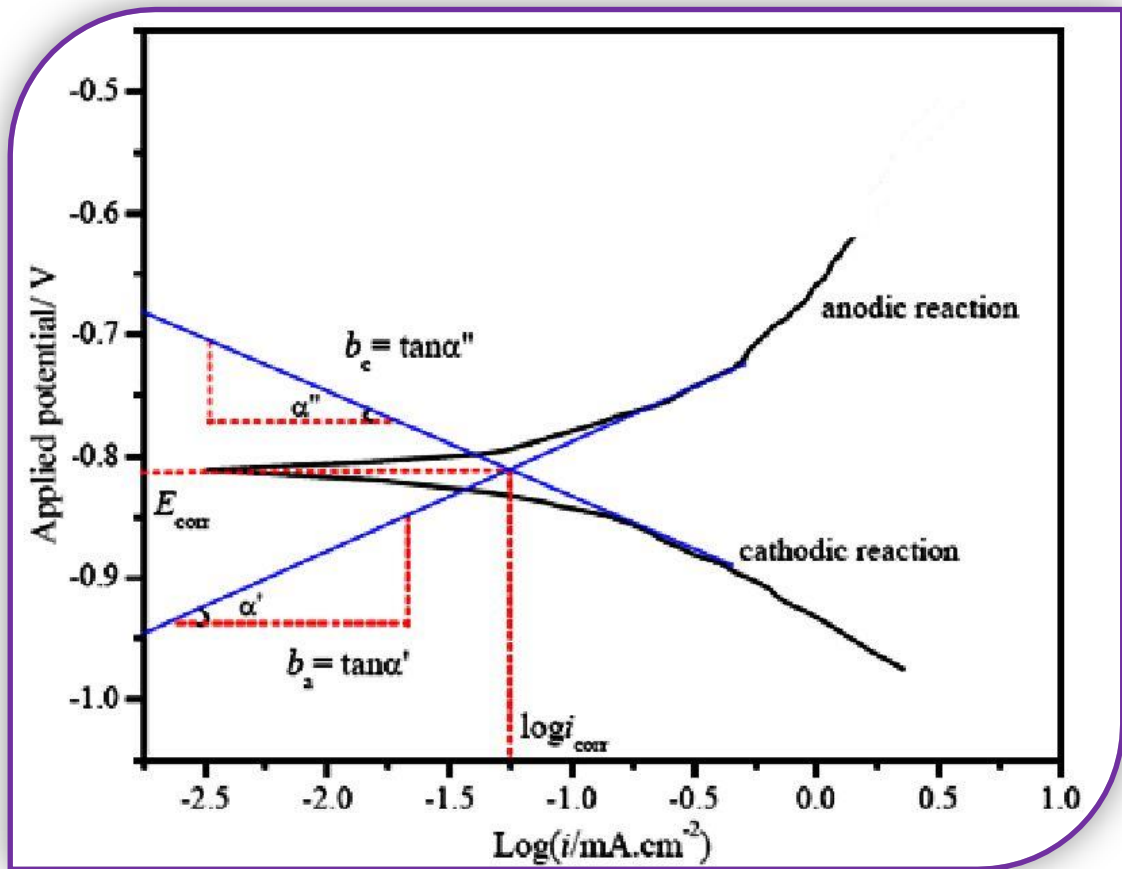


Figure 2.9. Schematic polarization curve showing Tafel extrapolation [68].

2.6 Scanning Electron Microscopy (SEM) Analysis

SEM is an analytical tool measuring surface topography using energetic electron beams. The electron beam can be focused by a magnetic field from micro nanometer level, thus enabling measurement of surface topography.

The scanning electron microscope images of the aluminium samples were recorded via FEI Inspect-S50 scanning electron microscope.



CHAPTER THREE

RESULTS

AND

DISCUSSION



3.1 Potentiodynamic Polarization Measurements

Figures 3.1., 3.2. and 3.3. show the polarization curves for pure aluminium, 5052 and 2024 aluminium alloys respectively in 3.5% NaCl solution, in the absence and presence of 7.5×10^{-4} M of ampicillin, cephalexin and amoxicillin, over the temperature range (283-323) K. The corrosion current densities i_{corr} and the corrosion potentials E_{corr} have been obtained by extrapolation of the linear logarithmic sections of cathodic and anodic Tafel lines to the point of intersection.

The polarization data, including the corrosion potential (E_{corr}), corrosion current densities (i_{corr}), anodic (b_a), cathodic (b_c) Tafel slopes, corrosion rates (C_R), and penetration rates (P_R), for pure Al, in the absence and presence of different concentrations of ampicillin, cephalexin, amoxicillin are given in Tables 3.1., 3.2. and 3.3. respectively. Tables 3.4. - 3.9. give the polarization data of 5052 and 2024 Al alloys without and with different concentrations of ampicillin, cephalexin, amoxicillin respectively, at five different temperatures in the range 283-323 K.

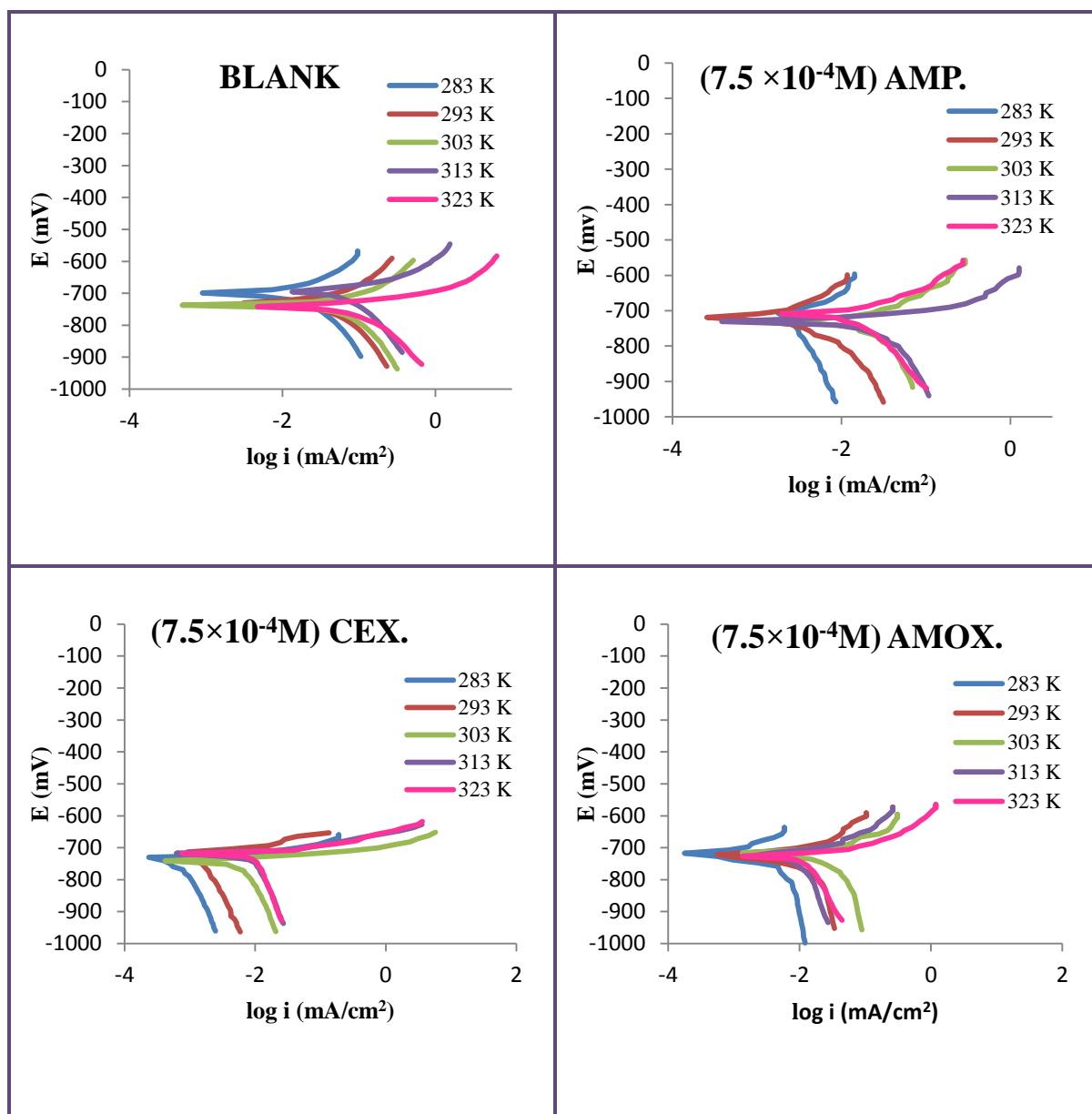


Figure 3.1. Polarization plots for the corrosion of **Pure Aluminium** in 3.5% NaCl in the absence and presence of ($7.5 \times 10^{-4} \text{M}$) **Ampicillin**, **Cephalexin** and **Amoxicillin**, at different temperature 283-323K.

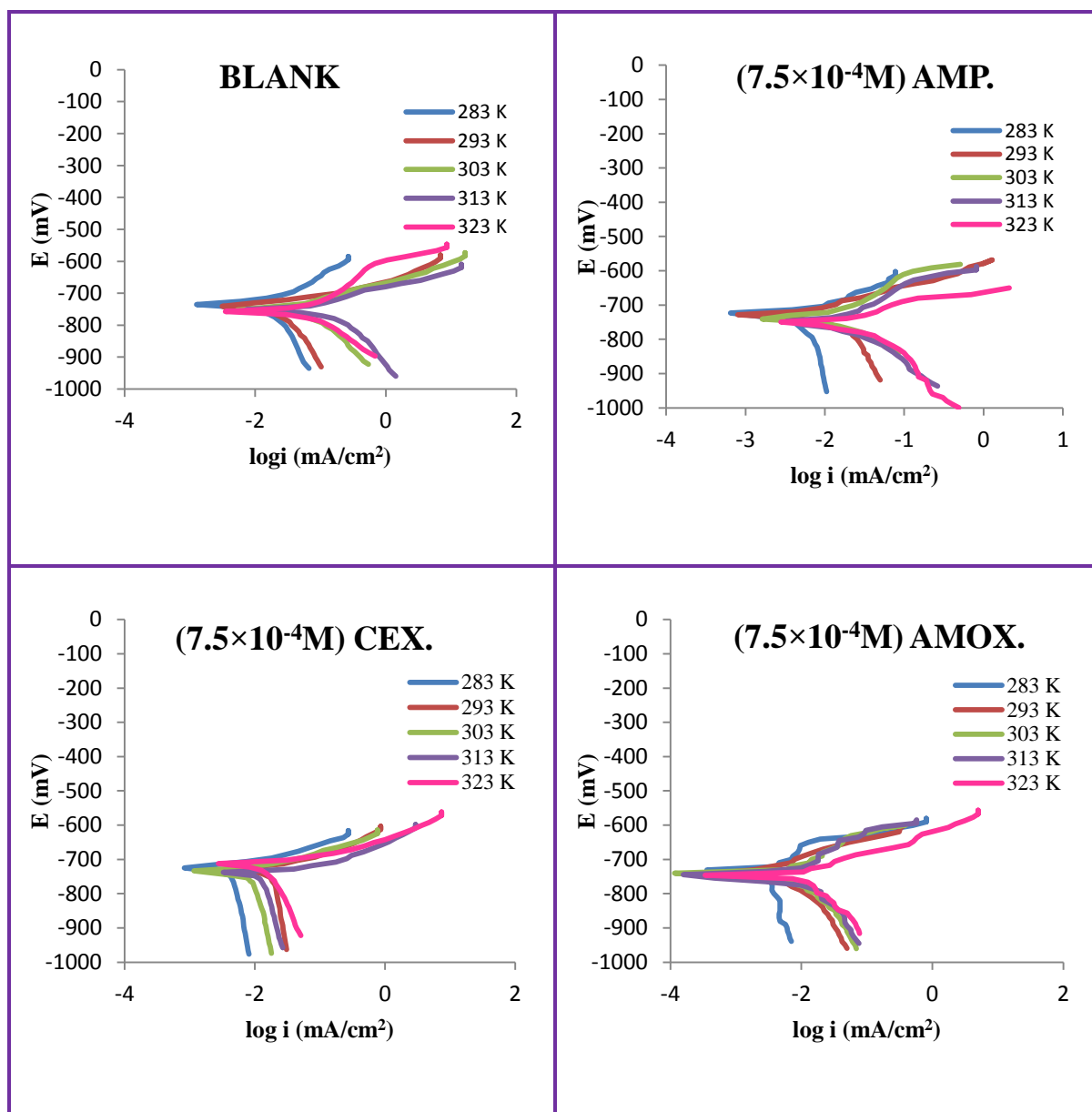


Figure 3.2. Polarization plots for the corrosion of **5052 Aluminium** in 3.5% NaCl in the absence and presence ($7.5 \times 10^{-4} \text{M}$) **Ampicillin**, **Cephalexin**, **Amoxicillin**, at different temperature 283-323K.

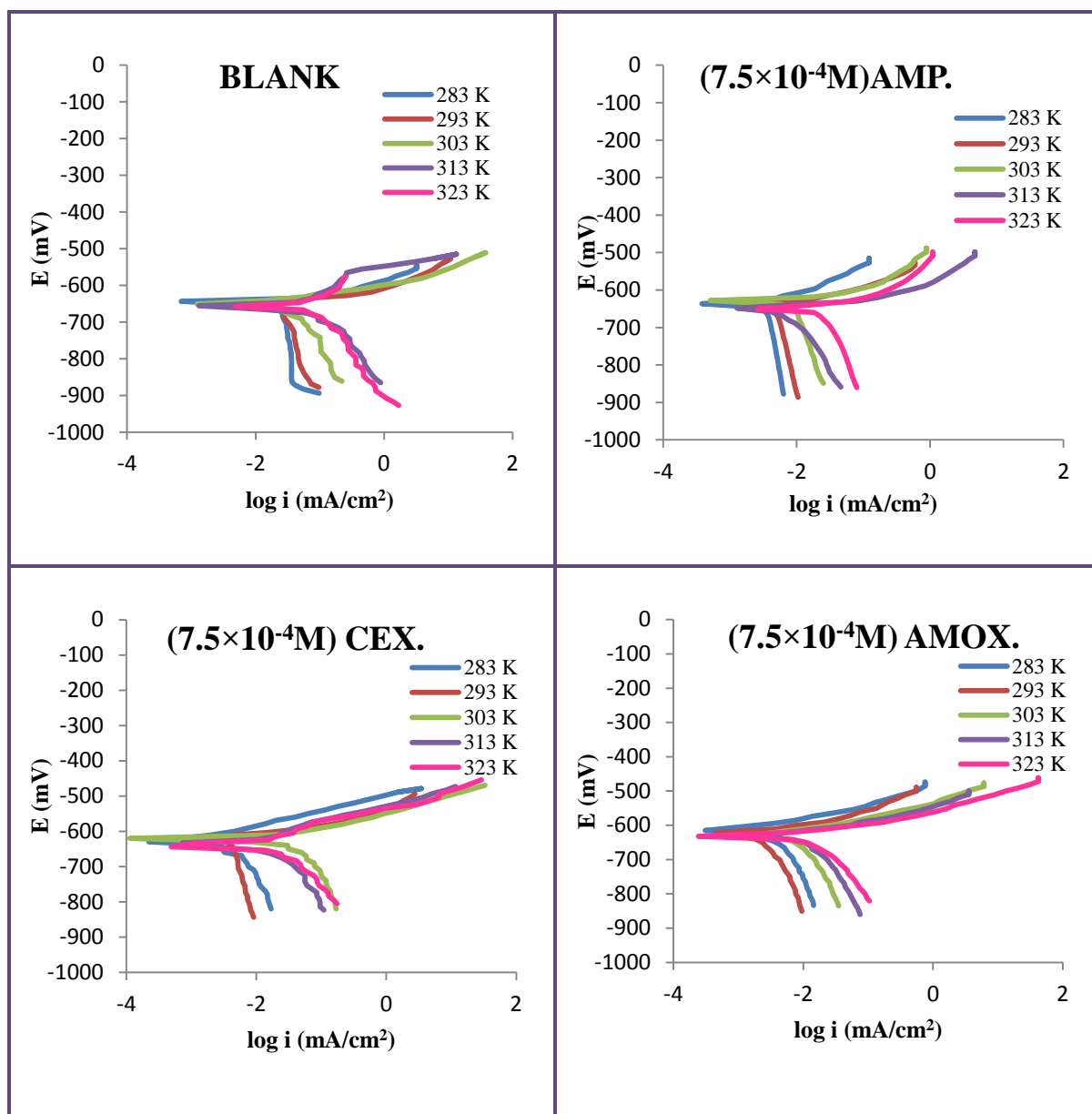


Figure 3.3. Polarization plots for the corrosion of **2024 Aluminium** in 3.5% NaCl in the absence and presence $7.5 \times 10^{-4} \text{M}$ Ampicillin, Cephalexin, Amoxicillin, at different temperature 283-323K.

CHAPTER THREE RESULTS AND DISCUSSION

Table 3.1. Potentiodynamic polarization parameters for **Pure Aluminium** without and with various concentrations of **Ampicillin** in 3.5% of NaCl aqueous solution at different temperatures.

Conc. [M]	T [K]	$-E_{\text{corr}}$ [mV]	i_{corr} [$\mu\text{A}/\text{cm}^2$]	$-b_c$ [mV/Dec]	b_a [mV/Dec]	C_R [g/($\text{m}^2\cdot\text{d}$)]	P_R [mm/y]
0 (Blank)	283	727.3	13.33	146.8	41.9	1.07	0.145
	293	731.1	16.42	164.2	44.6	1.32	0.178
	303	737.8	36.65	165.1	96.2	2.95	0.398
	313	739.4	47.88	337.5	100.1	3.85	0.520
	323	742.4	54.47	385.7	104.2	4.38	0.592
1.5×10^{-4}	283	705.0	3.72	149.1	48.6	0.30	0.040
	293	713.0	4.78	289.2	52.3	0.38	0.052
	303	717.0	11.98	305.0	73.0	0.96	0.130
	313	718.7	17.10	358.8	99.2	1.38	0.186
	323	722.2	19.90	419.0	105.2	1.60	0.216
3×10^{-4}	283	709.6	3.49	142.2	48.3	0.28	0.038
	293	716.2	4.46	229.6	56.2	0.36	0.049
	303	725.8	11.32	233.7	75.0	0.91	0.123
	313	727.2	15.37	316.3	90.5	1.24	0.167
	323	731.4	17.91	402.3	100.4	1.44	0.195
4.5×10^{-4}	283	705.6	2.36	130.2	33.7	0.19	0.026
	293	710.0	3.24	135.3	49.0	0.26	0.035
	303	715.9	8.57	138.1	69.9	0.69	0.093
	313	719.2	11.31	241.1	75.6	0.91	0.123
	323	720.8	14.48	367.0	93.7	1.17	0.157
6×10^{-4}	283	707.3	2.12	128.4	30.3	0.17	0.023
	293	711.8	2.89	123.5	45.0	0.23	0.031
	303	714.2	7.74	126.8	66.4	0.62	0.084
	313	722.4	11.12	224.1	78.4	0.89	0.121
	323	726.1	13.22	382.6	84.6	1.06	0.144
7.5×10^{-4}	283	708.1	1.92	118.1	28.2	0.15	0.021
	293	718.5	2.51	102.4	45.3	0.20	0.027
	303	726.4	5.67	112.4	51.9	0.46	0.062
	313	728.2	8.85	173.4	65.8	0.71	0.096
	323	730.0	10.64	302.7	71.0	0.86	0.116

CHAPTER THREE RESULTS AND DISCUSSION

Table 3.2. Potentiodynamic polarization parameters for **Pure Aluminium** without and with various concentrations of **Cephalexin** in 3.5% of NaCl aqueous solution at different temperatures.

Conc. [M]	T [K]	$-E_{\text{corr}}$ [mV]	i_{corr} [$\mu\text{A}/\text{cm}^2$]	$-b_c$ [mV/Dec]	b_a [mV/Dec]	C_R [g/($\text{m}^2\cdot\text{d}$)]	P_R [mm/y]
0 (Blank)	283	727.3	13.33	146.8	41.9	1.07	0.145
	293	731.1	16.42	164.2	44.6	1.32	0.178
	303	737.8	36.65	165.1	96.2	2.95	0.398
	313	739.4	47.88	337.5	100.1	3.85	0.520
	323	742.4	54.47	385.7	104.2	4.38	0.592
1.5×10^{-4}	283	704.5	2.71	368.2	28.5	0.22	0.029
	293	714.2	4.15	326.5	37.8	0.33	0.045
	303	722.7	9.49	308.4	56.0	0.76	0.103
	313	724.9	14.62	291.4	68.4	1.18	0.159
	323	729.1	17.52	266.4	40.6	1.41	0.190
3×10^{-4}	283	708.4	2.14	258.2	32.8	0.17	0.023
	293	717.6	3.47	231.6	44.2	0.28	0.038
	303	722.4	7.82	325.2	61.0	0.63	0.085
	313	728.5	9.42	348.1	45.9	0.76	0.102
	323	729.4	13.91	215.0	43.6	1.12	0.151
4.5×10^{-4}	283	701.9	1.92	120.7	38.9	0.15	0.021
	293	712.7	2.65	131.2	32.8	0.21	0.029
	303	713.3	7.32	237.3	64.8	0.59	0.080
	313	714.5	9.11	119.3	71.0	0.73	0.099
	323	720.4	12.54	246.5	74.9	1.01	0.136
6×10^{-4}	283	706.5	1.92	181.3	42.0	0.15	0.021
	293	715.6	2.53	159.8	47.3	0.20	0.027
	303	717.7	6.43	204.6	94.8	0.52	0.070
	313	723.6	8.73	201.8	84.6	0.70	0.095
	323	726.4	11.4	393.9	78.5	0.92	0.124
7.5×10^{-4}	283	709.8	1.57	441.5	35.0	0.13	0.017
	293	712.3	1.99	402.1	34.5	0.16	0.022
	303	716.5	4.82	388.2	60.3	0.39	0.052
	313	719.1	8.02	439.2	69.5	0.65	0.087
	323	723.0	10.85	572.0	80.2	0.87	0.118

CHAPTER THREE RESULTS AND DISCUSSION

Table 3.3. Potentiodynamic polarization parameters for **Pure Aluminium** without and with various concentrations of **Amoxicillin** in 3.5% of NaCl aqueous solution at different temperatures.

Conc. [M]	T [K]	$-E_{\text{corr}}$ [mV]	i_{corr} [$\mu\text{A}/\text{cm}^2$]	$-b_c$ [mV/Dec]	b_a [mV/Dec]	C_R [g/($\text{m}^2 \cdot \text{d}$)]	P_R [mm/y]
0 (Blank)	283	727.3	13.33	146.8	41.9	1.07	0.145
	293	731.1	16.42	164.2	44.6	1.32	0.178
	303	737.8	36.65	165.1	96.2	2.95	0.398
	313	739.4	47.88	337.5	100.1	3.85	0.520
	323	742.4	54.47	385.7	104.2	4.38	0.592
1.5×10^{-4}	283	702.8	1.99	114.3	33.3	0.16	0.022
	293	703.9	3.23	169.3	49.4	0.26	0.035
	303	707.0	7.69	137.4	60.1	0.62	0.084
	313	708.7	12.66	109.6	94.4	1.02	0.138
	323	709.2	15.64	115.5	96.8	1.26	0.170
3×10^{-4}	283	704.9	1.62	66.1	25.8	0.13	0.018
	293	705.4	2.95	161.6	46.6	0.24	0.032
	303	714.7	6.87	269.2	52.3	0.55	0.075
	313	716.1	11.21	462.6	82.5	0.90	0.122
	323	720.2	14.00	312.3	85.4	1.13	0.152
4.5×10^{-4}	283	708.1	1.35	89.4	35.3	0.11	0.015
	293	709.8	2.43	199.9	45.3	0.20	0.026
	303	712.0	6.43	140.4	69.8	0.52	0.070
	313	714.1	9.16	190.1	72.7	0.74	0.100
	323	715.0	11.59	179.8	109.3	0.93	0.126
6×10^{-4}	283	712.8	1.28	118.1	34.8	0.10	0.014
	293	715.0	2.45	267.0	44.2	0.20	0.027
	303	719.9	6.08	178.2	70.8	0.49	0.066
	313	721.3	8.98	168.5	83.6	0.72	0.098
	323	726.4	11.05	132.0	90.8	0.89	0.120
7.5×10^{-4}	283	715.6	1.04	98.3	31.0	0.08	0.011
	293	716.4	1.84	155.9	45.4	0.15	0.020
	303	721.7	4.45	130.8	61.2	0.36	0.048
	313	725.3	7.15	238.4	76.7	0.58	0.078
	323	726.0	10.40	240.6	77.4	0.84	0.113

CHAPTER THREE RESULTS AND DISCUSSION

Table 3.4. Potentiodynamic polarization parameters for **5052 Aluminium** without and with various concentrations of **Ampicillin** in 3.5% of NaCl aqueous solution at different temperatures.

Conc. [M]	T [K]	$-E_{\text{corr}}$ [mV]	i_{corr} [$\mu\text{A}/\text{cm}^2$]	$-b_c$ [mV/Dec]	b_a [mV/Dec]	C_R [g/($\text{m}^2\cdot\text{d}$)]	P_R [mm/y]
0 (Blank)	283	736.4	16.60	191.6	46.8	1.34	0.181
	293	742.0	18.58	123.6	60.7	1.50	0.203
	303	750.3	38.36	119.6	61.6	3.09	0.418
	313	753.1	49.19	119.2	113.9	3.96	0.536
	323	759.0	61.26	89.5	127.6	4.94	0.668
1.5×10^{-4}	283	720.0	5.39	482.0	60.1	0.43	0.059
	293	722.0	7.08	416.3	82.2	0.57	0.077
	303	725.0	14.99	376.2	93.8	1.21	0.163
	313	728.0	19.89	286.1	139.4	1.60	0.217
	323	735.0	24.84	284.3	170.5	2.00	0.271
3×10^{-4}	283	721.6	4.65	450.8	61.1	0.38	0.051
	293	725.5	6.20	194.8	95.6	0.50	0.068
	303	728.9	13.54	209.0	103.4	1.09	0.148
	313	732.6	17.46	198.9	149.6	1.41	0.190
	323	739.7	22.29	247.0	162.2	1.80	0.243
4.5×10^{-4}	283	713.3	4.59	372.4	62.6	0.37	0.050
	293	721.6	5.33	168.9	94.3	0.43	0.058
	303	729.4	11.69	156.2	98.7	0.94	0.127
	313	735.3	16.58	235.2	132.9	1.34	0.181
	323	740.2	21.00	251.6	148.8	1.69	0.229
6×10^{-4}	283	726.7	3.76	260.1	56.2	0.30	0.041
	293	728.3	4.39	255.0	63.4	0.35	0.048
	303	732.0	9.95	199.4	74.9	0.80	0.109
	313	740.4	13.24	170.2	120.6	1.07	0.144
	323	741.1	17.96	199.2	144.9	1.45	0.196
7.5×10^{-4}	283	724.6	3.07	198.0	58.3	0.25	0.033
	293	727.6	3.85	171.2	79.2	0.31	0.042
	303	739.7	8.98	121.3	87.6	0.72	0.098
	313	747.1	11.88	164.3	112.1	0.96	0.130
	323	749.4	14.87	174.6	121.5	1.20	0.162

CHAPTER THREE RESULTS AND DISCUSSION

Table 3.5. Potentiodynamic polarization parameters for **5052 Aluminium** without and with various concentrations of **Cephalexin** in 3.5% of NaCl aqueous solution at different temperatures.

Conc. [M]	T [K]	$-E_{\text{corr}}$ [mV]	i_{corr} [$\mu\text{A}/\text{cm}^2$]	$-b_c$ [mV/Dec]	b_a [mV/Dec]	C_R [g/($\text{m}^2\cdot\text{d}$)]	P_R [mm/y]
0 (Blank)	283	736.4	16.60	191.6	46.8	1.34	0.181
	293	742.0	18.58	123.6	60.7	1.50	0.203
	303	750.3	38.36	119.6	61.6	3.09	0.418
	313	753.1	49.19	119.2	113.9	3.96	0.536
	323	759.0	61.26	89.5	127.6	4.94	0.668
1.5×10^{-4}	283	711.0	4.87	203.5	69.5	0.39	0.053
	293	719.6	5.82	266.5	79.7	0.47	0.063
	303	726.1	13.43	283.5	94.4	1.08	0.146
	313	727.2	18.11	359.2	115.0	1.46	0.197
	323	728.5	23.03	297.0	153.3	1.86	0.251
3×10^{-4}	283	713.3	4.46	202.2	93.5	0.36	0.049
	293	716.5	5.29	215.7	76.9	0.43	0.058
	303	719.3	12.40	289.6	113.7	1.00	0.135
	313	728.7	16.62	293.6	119.2	1.34	0.181
	323	735.0	21.08	297.6	146.2	1.70	0.230
4.5×10^{-4}	283	617.1	3.25	131.7	85.5	0.26	0.035
	293	618.2	3.75	220.1	58.7	0.30	0.041
	303	619.3	9.57	405.2	79.3	0.77	0.104
	313	619.7	12.50	234.1	107.6	1.01	0.136
	323	621.5	14.71	240.6	117.0	1.19	0.160
6×10^{-4}	283	719.0	3.00	308.3	66.2	0.24	0.033
	293	721.8	3.50	496.4	57.4	0.28	0.038
	303	729.8	8.11	258.0	111.7	0.65	0.088
	313	738.0	10.51	313.8	132.4	0.85	0.115
	323	742.5	13.27	223.2	125.3	1.07	0.145
7.5×10^{-4}	283	723.7	2.57	142.8	85.7	0.21	0.028
	293	726.2	3.48	162.1	89.5	0.28	0.038
	303	732.3	7.40	191.3	128.6	0.60	0.081
	313	637.2	10.04	194.8	119.9	0.81	0.109
	323	741.6	12.96	256.6	135.6	1.04	0.141

CHAPTER THREE RESULTS AND DISCUSSION

Table 3.6. Potentiodynamic polarization parameters for **5052 Aluminium** without and with various concentrations of **Amoxicillin** in 3.5% of NaCl aqueous solution at different temperatures.

Conc. [M]	T [K]	$-E_{\text{corr}}$ [mV]	i_{corr} [$\mu\text{A}/\text{cm}^2$]	$-b_c$ [mV/Dec]	b_a [mV/Dec]	C_R [g/($\text{m}^2\cdot\text{d}$)]	P_R [mm/y]
0 (Blank)	283	736.4	16.60	191.6	46.8	1.34	0.181
	293	742.0	18.58	123.6	60.7	1.50	0.203
	303	750.3	38.36	119.6	61.6	3.09	0.418
	313	753.1	49.19	119.2	113.9	3.96	0.536
	323	759.0	61.26	89.5	127.6	4.94	0.668
1.5×10^{-4}	283	710.0	4.87	134.9	51.2	0.39	0.053
	293	715.0	5.82	236.2	59.5	0.47	0.063
	303	724.7	13.43	284.9	82.2	1.08	0.146
	313	732.7	18.11	474.1	99.6	1.46	0.197
	323	738.6	23.03	496.2	117.6	1.86	0.251
3×10^{-4}	283	721.7	4.46	210.0	43.0	0.36	0.049
	293	725.0	5.29	158.0	50.1	0.43	0.058
	303	732.6	12.40	275.0	93.3	1.00	0.135
	313	734.2	16.62	291.6	122.3	1.34	0.181
	323	734.6	21.08	326.7	138.6	1.70	0.230
4.5×10^{-4}	283	727.9	3.25	147.4	53.8	0.26	0.035
	293	735.4	3.75	291.6	56.2	0.30	0.041
	303	736.7	9.57	232.1	91.7	0.77	0.104
	313	736.9	12.50	207.8	93.2	1.01	0.136
	323	740.8	14.71	375.2	122.3	1.19	0.160
6×10^{-4}	283	728.8	3.00	139.0	67.4	0.24	0.033
	293	731.8	3.50	119.9	78.8	0.28	0.038
	303	735.7	8.11	224.5	117.4	0.65	0.088
	313	736.2	10.51	283.2	98.9	0.85	0.115
	323	743.3	13.27	265.8	102.6	1.07	0.145
7.5×10^{-4}	283	721.1	2.57	131.1	62.9	0.21	0.028
	293	727.6	3.48	171.1	61.7	0.28	0.038
	303	730.6	7.40	185.7	92.9	0.60	0.081
	313	733.5	10.04	216.5	155.6	0.81	0.109
	323	736.2	12.96	175.9	181.0	1.04	0.141

CHAPTER THREE RESULTS AND DISCUSSION

Table 3.7. Potentiodynamic polarization parameters for **2024 Aluminium** without and with various concentrations of **Ampicillin** in 3.5% of NaCl aqueous solution at different temperatures.

Conc. [M]	T [K]	$-E_{\text{corr}}$ [mV]	i_{corr} [$\mu\text{A}/\text{cm}^2$]	$-b_c$ [mV/Dec]	b_a [mV/Dec]	C_R [g/($\text{m}^2\cdot\text{d}$)]	P_R [mm/y]
0 (Blank)	283	645.2	27.87	252.1	51.3	2.25	0.304
	293	647.8	30.42	142.3	60.8	2.45	0.332
	303	651.4	59.42	166.5	108.6	4.79	0.648
	313	656.4	62.25	245.9	93.4	5.02	0.679
	323	658	73.41	145.7	94.3	5.92	0.800
1.5×10^{-4}	283	617.9	6.65	298.4	87.9	0.54	0.072
	293	621	8.76	487.9	101.1	0.71	0.095
	303	627	18.77	411.7	208.9	1.51	0.205
	313	629.2	21.87	381.3	199.6	1.76	0.238
	323	632.8	25.88	490.9	116.7	2.09	0.282
3×10^{-4}	283	627.9	5.73	282.4	95.4	0.46	0.062
	293	630.7	7.96	293	102.3	0.64	0.087
	303	631.3	17.88	297.3	183.6	1.44	0.195
	313	634.2	19.97	299.7	197.1	1.61	0.218
	323	640.2	23.66	441.8	164.5	1.91	0.258
4.5×10^{-4}	283	630	4.87	254.9	88.2	0.39	0.053
	293	634.4	5.68	495.8	76.8	0.46	0.062
	303	636.3	13.54	457.1	115.6	1.09	0.148
	313	639.9	15.27	232.5	146	1.23	0.166
	323	643	18.73	228	168.2	1.51	0.204
6×10^{-4}	283	635	4.05	178.3	99.1	0.33	0.044
	293	638.1	4.93	140.7	113.7	0.40	0.054
	303	643	12.53	305	182.8	1.01	0.137
	313	648.4	14.65	370.5	121	1.18	0.160
	323	650.4	17.65	300.2	133.3	1.42	0.192
7.5×10^{-4}	283	636.6	3.37	158.5	83.3	0.27	0.037
	293	637	4.57	244.5	94.6	0.37	0.050
	303	638.5	9.37	347.3	119.6	0.76	0.102
	313	648.6	10.76	259	99.1	0.87	0.117
	323	649.2	13.70	334.5	107.2	1.10	0.149

CHAPTER THREE RESULTS AND DISCUSSION

Table 3.8. Potentiodynamic polarization parameters for **2024 Aluminium** without and with various concentrations of **Cephalexin** in 3.5% of NaCl aqueous solution at different temperatures.

Conc. [M]	T [K]	$-E_{\text{corr}}$ [mV]	i_{corr} [$\mu\text{A}/\text{cm}^2$]	$-b_c$ [mV/Dec]	b_a [mV/Dec]	C_R [g/($\text{m}^2\cdot\text{d}$)]	P_R [mm/y]
0 (Blank)	283	645.2	27.87	252.1	51.3	2.25	0.304
	293	647.8	30.42	142.3	60.8	2.45	0.332
	303	651.4	59.42	166.5	108.6	4.79	0.648
	313	656.4	62.25	245.9	93.4	5.02	0.679
	323	658.0	73.41	145.7	94.3	5.92	0.800
1.5×10^{-4}	283	618.4	5.51	283.1	79.3	0.44	0.060
	293	619.4	6.83	271.5	94.6	0.55	0.074
	303	625.6	18.23	313.4	178.7	1.47	0.199
	313	627.2	20.26	381.5	142.7	1.63	0.221
	323	629.7	24.83	396.2	165.3	2.00	0.271
3×10^{-4}	283	616.8	3.84	127.5	98.8	0.31	0.042
	293	624.1	7.01	192.0	125.4	0.56	0.076
	303	631.4	17.29	289.3	179.8	1.39	0.188
	313	633.0	19.06	260.8	193.0	1.54	0.208
	323	634.1	23.62	292.5	190.4	1.90	0.257
4.5×10^{-4}	283	618.0	3.26	131.4	90.9	0.26	0.036
	293	622.0	4.11	172.0	85.8	0.33	0.045
	303	624.5	11.70	273.1	126.1	0.94	0.127
	313	628.0	14.01	249.4	154.9	1.13	0.153
	323	629.8	17.74	265.1	181.2	1.43	0.193
6×10^{-4}	283	614.7	2.93	198.7	69.4	0.24	0.032
	293	624.2	3.79	169.6	91.1	0.31	0.041
	303	628.3	9.63	287.6	142.1	0.78	0.105
	313	635.7	12.42	291.8	177.7	1.00	0.135
	323	636.0	15.67	281.1	196.4	1.26	0.171
7.5×10^{-4}	283	613.8	2.77	208.2	94.4	0.22	0.030
	293	620.4	3.63	419.9	85.8	0.29	0.040
	303	621.8	8.81	309.0	131.6	0.71	0.096
	313	632.7	9.47	202.3	152.7	0.76	0.103
	323	637.5	13.55	290.0	192.6	1.09	0.148

CHAPTER THREE RESULTS AND DISCUSSION

Table 3.9. Potentiodynamic polarization parameters for **2024 Aluminium** without and with various concentrations of **Amoxicillin** in 3.5% of NaCl aqueous solution at different temperatures.

Conc. [M]	T [K]	$-E_{\text{corr}}$ [mV]	i_{corr} [$\mu\text{A}/\text{cm}^2$]	$-b_c$ [mV/Dec]	b_a [mV/Dec]	C_R [g/($\text{m}^2\cdot\text{d}$)]	P_R [mm/y]
0 (Blank)	283	645.2	27.87	252.1	51.3	2.25	0.304
	293	647.8	30.42	142.3	60.8	2.45	0.332
	303	651.4	59.42	166.5	108.6	4.79	0.648
	313	656.4	62.25	245.9	93.4	5.02	0.679
	323	658.0	73.41	145.7	94.3	5.92	0.800
1.5×10^{-4}	283	613.0	4.45	209.3	99.3	0.36	0.048
	293	615.5	6.25	271.8	106.1	0.50	0.068
	303	616.1	16.53	340.0	175.0	1.33	0.180
	313	621.4	18.54	405.2	156.2	1.49	0.202
	323	623.1	22.99	419.8	177.1	1.85	0.251
3×10^{-4}	283	616.3	2.37	207.2	55.2	0.19	0.026
	293	618.7	5.26	253.8	91.5	0.42	0.057
	303	625.5	12.60	244.8	145.7	1.02	0.137
	313	627.2	15.99	386.5	151.0	1.29	0.174
	323	630.3	21.81	392.4	165.6	1.76	0.238
4.5×10^{-4}	283	619.4	2.32	209.7	61.2	0.19	0.025
	293	625.4	3.29	222.5	87.4	0.27	0.036
	303	627.2	9.63	298.6	108.0	0.78	0.105
	313	630.9	12.94	341.0	132.4	1.04	0.141
	323	632.8	16.36	366.4	154.2	1.32	0.178
6×10^{-4}	283	619.2	2.07	173.5	83.1	0.17	0.023
	293	620.0	2.45	186.8	91.2	0.20	0.027
	303	624.4	8.47	244.8	173.3	0.68	0.092
	313	627.8	11.67	287.5	181.4	0.94	0.127
	323	630.7	14.68	380.1	194.3	1.18	0.160
7.5×10^{-4}	283	612.5	1.64	116.0	91.2	0.13	0.018
	293	621.7	1.65	176.1	59.1	0.13	0.018
	303	625.9	6.68	276.4	90.2	0.54	0.073
	313	629.8	10.15	304.8	150.4	0.82	0.111
	323	633.7	11.67	318.3	155.3	0.94	0.127

CHAPTER THREE RESULTS AND DISCUSSION

3.1.1 Corrosion Current Density and Corrosion Potential

The corrosion current density (i_{corr}) is a kinetic parameter and its value reflects the kinetic behaviour of the corrosion process. Generally, the data in the **Tables 3.1 - 3.9.** indicates that (i_{corr}) for 2024 alloy higher than (i_{corr}) of 5052 alloy and (i_{corr}) for 5052 alloy is higher than (i_{corr}) for pure Al. also the (i_{corr}) increases with increasing temperature as shown in **Tables 3.1 - 3.9.** The sequence of (i_{corr}) value may be put as:

$$2024 \text{ Al} > 5052 \text{ Al} > \text{Pure Al}$$

The corrosion potential (E_{corr}) sequence for pure Al and its alloys under study in saline solution to noble direction was as follows:

$$5052 \text{ Al} > \text{Pure Al} > 2024 \text{ Al}$$

It is obvious from the results that the addition of inhibitors caused a decrease in the corrosion current densities for pure Al as well as Al alloys under study as the concentration of inhibitors increased at constant temperatures. Increasing the temperature at constant inhibitors concentration lead to increase in the (i_{corr}) values.

The kinetic effects should be reflected in the change of the corrosion current density of the specimen and the tendency of the specimen for corrosion under the specified conditions is expected to decrease on purely thermodynamic grounds when its corrode [69].

The corrosion potential (E_{corr}) generally shifted to the noble direction (or to less negative potential) in the presence of inhibitors, while its values generally vary with increasing inhibitor concentration. For inhibited system, if the displacement in E_{corr} value is greater than 85 mV relative to uninhibited

CHAPTER THREE RESULTS AND DISCUSSION

system then the inhibitor is classified as cathodic or anodic type while if displacement in E_{corr} is less than 85mV, it could be recognized as mixed-type [70-72]. In this work, the maximum displacement of E_{corr} value is less than 85mV hence the inhibitors were classified as mixed-type inhibitors.

3.1.2 Corrosion Rate and Penetration Rate

The corrosion process involves a simultaneous charge transfer and mass transfer across the metal/solution interface. So the rate of electron flow (current, I) to and from an electrode is a measure of reaction rate. The proportionality between I (in Ampere, A) and mass reacted, m , in an electrochemical reaction is given by Faraday's law [73]:

$$m = \frac{I t a}{n F} \quad (3.1)$$

where F is the Faraday's constant (96500C/equivalent), t is the time in seconds, a is the atomic weight of the metal, and n is the number of valence.

The corrosion rate, C_R , i.e. mass dissolved per unit surface area SA , in a unit time, can be expressed as [6]:

$$C_R = \frac{m}{t \cdot SA} = \frac{i a}{n F} \quad (3.2)$$

Where, $i = I/SA$, i is defined as the current density [37].

Penetration rate in millimeters per year (mm/y) can be calculated from the following equation [74]:

$$P_R = 3.27 * 10^{-3} (e/\rho) i \quad (3.3)$$

CHAPTER THREE RESULTS AND DISCUSSION

where (e) is the chemical equivalent of the metal (ρ) its density and (i) is the current density corresponding to the equilibrium state of the metal (i_{corr}) [40].

The results of corrosion rate (C_R) and penetration rate (P_R) can be summarized as follows:

1. C_R and P_R values increased with increasing temperature for pure Al and 5052 and 2024 Al alloys.
2. C_R and P_R decreased with increasing corrosion inhibitors concentration.

3.1.3 Surface Coverage and Inhibition Efficiency

The surface coverage (θ) and inhibition efficiency (%IE) of pure Al and 5052,2024 Al alloys in 3.5% NaCl containing different concentration of the inhibitors could be estimated using equations (3.4) and (3.5) respectively [75], at five experimental temperatures. The results are given in **Tables 3.10. - 3.12..**

$$\theta = 1 - (i_2 - i_1) \quad (3.4)$$

$$\%IE = 100 \times [1 - (i_2/i_1)] \quad (3.5)$$

Where i_1 and i_2 , are the corrosion current densities in the absence and presence of inhibitors in 3.5 % of NaCl aqueous solution respectively.

CHAPTER THREE RESULTS AND DISCUSSION

Table 3.10. Values of surface coverages and protection efficiencies for various concentrations of **Ampicillin**, **Amoxicillin** and **Cephalexin** in 3.5% of NaCl aqueous solution at five different temperatures on **Pure Aluminium** surface.

Conc. [M]	T [K]	AMP.		CEX.		AMOX.	
		θ	%IE	θ	%IE	θ	%IE
1.5×10^{-4}	283	0.72	72.09	0.80	79.67	0.85	85.07
	293	0.71	70.91	0.75	74.73	0.80	80.35
	303	0.67	67.32	0.74	74.11	0.79	79.03
	313	0.64	64.29	0.69	69.47	0.74	73.55
	323	0.63	63.47	0.68	67.84	0.71	71.29
3×10^{-4}	283	0.74	73.82	0.84	83.95	0.88	87.82
	293	0.73	72.81	0.79	78.87	0.82	82.06
	303	0.69	69.12	0.79	78.66	0.81	81.26
	313	0.68	67.89	0.80	80.33	0.77	76.58
	323	0.67	67.12	0.74	74.46	0.74	74.30
4.5×10^{-4}	283	0.82	82.30	0.86	85.60	0.90	89.87
	293	0.80	80.28	0.84	83.86	0.85	85.20
	303	0.77	76.62	0.80	80.03	0.82	82.46
	313	0.76	76.38	0.81	80.97	0.81	80.87
	323	0.73	73.41	0.77	76.98	0.79	78.72
6×10^{-4}	283	0.84	84.10	0.86	85.60	0.90	90.40
	293	0.82	82.39	0.85	84.59	0.85	85.08
	303	0.79	78.87	0.82	82.46	0.83	83.41
	313	0.77	76.79	0.82	81.77	0.81	81.25
	323	0.76	75.73	0.79	79.07	0.80	79.71
7.5×10^{-4}	283	0.86	85.60	0.88	88.22	0.92	92.20
	293	0.85	84.71	0.88	87.88	0.89	88.79
	303	0.85	84.54	0.87	86.85	0.88	87.87
	313	0.82	81.51	0.83	83.25	0.85	85.07
	323	0.80	80.47	0.80	80.08	0.81	80.92

CHAPTER THREE RESULTS AND DISCUSSION

Table 3.11. Values of surface coverages and protection efficiencies for various concentrations of **Ampicillin**, **Amoxicillin** and **Cephalexin** in 3.5% of NaCl aqueous solution at five different temperatures on **5052 Aluminium** surface.

Conc. [M]	T [K]	AMP.		CEX.		AMOX.	
		θ	%IE	θ	%IE	θ	%IE
1.5×10^{-4}	283	0.68	67.54	0.71	70.68	0.83	83.04
	293	0.62	61.90	0.69	68.66	0.79	78.99
	303	0.61	60.93	0.65	64.99	0.70	69.61
	313	0.60	59.56	0.63	63.18	0.67	66.61
	323	0.59	59.45	0.62	62.40	0.66	66.49
3×10^{-4}	283	0.72	71.96	0.73	73.14	0.87	86.68
	293	0.67	66.65	0.72	71.55	0.84	83.64
	303	0.65	64.71	0.68	67.68	0.74	73.82
	313	0.65	64.51	0.66	66.22	0.71	70.68
	323	0.64	63.62	0.66	65.59	0.69	69.25
4.5×10^{-4}	283	0.72	72.36	0.80	80.41	0.88	87.63
	293	0.71	71.30	0.80	79.82	0.86	85.60
	303	0.70	69.53	0.75	75.06	0.78	77.54
	313	0.66	66.30	0.75	74.58	0.76	76.26
	323	0.66	65.72	0.76	75.98	0.76	76.19
6×10^{-4}	283	0.77	77.34	0.82	81.93	0.88	88.36
	293	0.76	76.40	0.81	81.15	0.86	86.48
	303	0.74	74.05	0.79	78.87	0.79	79.38
	313	0.73	73.09	0.79	78.64	0.79	78.72
	323	0.71	70.68	0.78	78.33	0.78	77.72
7.5×10^{-4}	283	0.82	81.53	0.84	84.50	0.90	89.65
	293	0.79	79.29	0.81	81.29	0.88	88.44
	303	0.77	76.59	0.81	80.72	0.83	83.41
	313	0.76	75.85	0.80	79.60	0.80	80.43
	323	0.76	75.73	0.79	78.85	0.80	79.83

CHAPTER THREE RESULTS AND DISCUSSION

Table 3.12. Values of surface coverages and protection efficiencies for various concentrations of **Ampicillin**, **Amoxicillin** and **Cephalexin** in 3.5% of NaCl aqueous solution at five different temperatures on **2024 Aluminium** surface.

Conc. [M]	T [K]	AMP.		CEX.		AMOX.	
		θ	%IE	θ	%IE	θ	%IE
1.5×10^{-4}	283	0.76	76.14	0.80	80.24	0.84	84.04
	293	0.71	71.21	0.78	77.56	0.79	79.44
	303	0.68	68.40	0.69	69.32	0.72	72.18
	313	0.65	64.87	0.67	67.45	0.70	70.22
	323	0.65	64.74	0.66	66.17	0.69	68.69
3×10^{-4}	283	0.79	79.46	0.86	86.20	0.92	91.51
	293	0.74	73.84	0.77	76.96	0.83	82.72
	303	0.70	69.92	0.71	70.91	0.79	78.79
	313	0.68	67.92	0.69	69.38	0.74	74.32
	323	0.68	67.78	0.68	67.83	0.70	70.29
4.5×10^{-4}	283	0.83	82.53	0.88	88.31	0.92	91.69
	293	0.81	81.32	0.86	86.49	0.89	89.18
	303	0.77	77.22	0.80	80.32	0.84	83.79
	313	0.75	75.46	0.77	77.50	0.79	79.22
	323	0.74	74.49	0.76	75.84	0.78	77.72
6×10^{-4}	283	0.85	85.48	0.89	89.47	0.93	92.59
	293	0.84	83.80	0.88	87.55	0.92	91.93
	303	0.79	78.91	0.84	83.80	0.86	85.74
	313	0.76	76.47	0.80	80.04	0.81	81.26
	323	0.76	75.96	0.79	78.65	0.80	80.00
7.5×10^{-4}	283	0.88	87.89	0.90	90.06	0.94	94.10
	293	0.85	84.98	0.88	88.05	0.95	94.56
	303	0.84	84.23	0.85	85.17	0.89	88.76
	313	0.83	82.72	0.85	84.79	0.84	83.70
	323	0.81	81.34	0.82	81.54	0.84	84.10

CHAPTER THREE RESULTS AND DISCUSSION

The results show the highest value of surface coverage for the three inhibitors on the surface of the pure aluminium and 2024, 5052 alloys were achieved by using amoxicillin. The surface coverages of inhibitors on the pure and two other alloys have the following order;

$$2024 \text{ Al} > \text{Pure Al} > 5052 \text{ Al}$$

This may be due to composition of alloys.

Generally for all examined alloys the higher protection efficiency achieved by amoxicillin followed it cephalixin and ampicillin.

$$\text{AMOX.} > \text{CEX.} > \text{AMP.}$$

The characteristics of inhibitors can be explained in the terms of inhibitor concentration, and temperature. The values of the inhibition efficiency (%IE) were highly dependent on temperature and inhibitors concentrations. Among the compound studied AMOX. exhibited the best performance, giving more than 94% inhibition efficiency at 283K for 2024Al alloy. **Figure 3.4.** shows the relationship between the protection efficiencies and various concentrations of amoxicillin in five different temperatures for pure Al, 5052 Al, and 2024 Al. The values of inhibition efficiency decrease with temperature, and the capacity of inhibition increased with increasing concentration (this true for all inhibitors). This means that the inhibitors are physical inhibitors for pure Al, 5052 and 2024 Al alloys. And may be due to the physical adsorption mechanism. Since the inhibition efficiency of an inhibitor decreases with temperature, while for a chemical adsorption mechanism, values of inhibition efficiency increase with temperature [76].

CHAPTER THREE RESULTS AND DISCUSSION

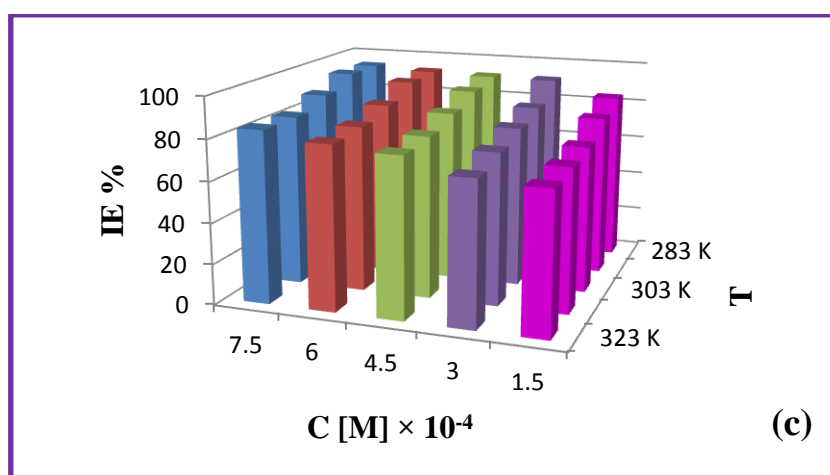
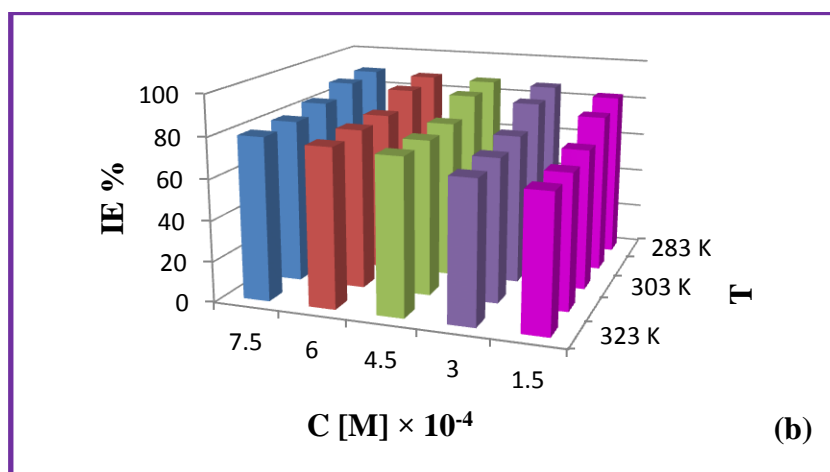
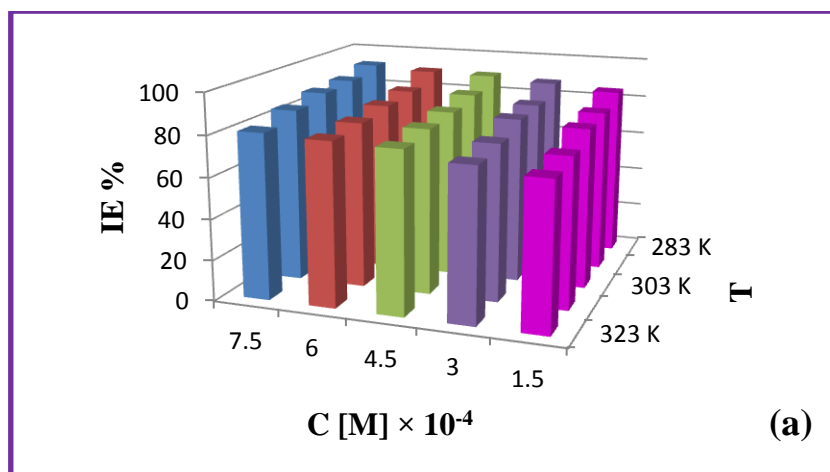


Figure 3.4. Inhibition efficiencies of Amoxicillin for (a) Pure Al (b) 5052 Al (c) 2024 Al, in 3.5% NaCl at different temperatures and concentrations of Amoxicillin.

3.1.4 The Tafel Slopes and Transfer Coefficients

The cathodic (b_c) and anodic (b_a) Tafel slopes, which were obtained from the slopes of the anodic and cathodic Tafel region of the polarization curves are given in the **Tables 3.1. - 3.9.** The tables show that the cathodic and anodic Tafel slopes change in the presence of inhibitors, this indicates for the inhibitors used in this study of a mixed-type nature [39].

The values of the transfer coefficients for the cathodic (α_c) and anodic (α_a), processes have been calculated from the corresponding cathodic (b_c) and anodic (b_a) Tafel slopes using equations (3.6) and (3.7) respectively which are derived from equation (1.13) and (1.15) [77]:

$$\alpha_a = \frac{2.303 RT}{b_a n F} \quad (3.6)$$

$$\alpha_c = -\frac{2.303 RT}{b_c n F} \quad (3.7)$$

The obtained results are presented in **Tables 3.13. - 3.21.** The result was the relatively some higher or lower values of the Tafel slopes (b_a and b_c) or the transfer coefficients (α_a and α_c) for the specimens in 3.5% NaCl electrolyte. Increasing the temperature from 283 to 323K has caused only a slight change in the values of b_a and b_c .

A cathodic Tafel slope approximately equal -0.120 V (or of $\alpha_c = 0.5$) in general diagnostic of a discharge – chemical desorption mechanism for hydrogen evolution reaction a cathode in which the proton discharge is the rate – determining step. If a chemical desorption is the rate – determining step, the rate will then be independent on the overpotential. Since no charge transfer occurs so rate becomes directly proportional to the concentration or

CHAPTER THREE RESULTS AND DISCUSSION

the coverage (θ) of the adsorbed hydrogen atoms, which may occur at coverage ranging from very small values to almost full surface layer formation [69]. The expected Tafel slope in such step would then be ($-0.03 \text{ V.decade}^{-1}$) and ($\alpha_c = 2$). When an electrochemical desorption becomes the rate – determining step for the hydrogen evolution reaction on the cathode, the expected value of b_c is ($-0.05 \text{ V.decade}^{-1}$) and ($\alpha_c = 1.5$). The results of the tables indicate that the variation of the cathodic Tafel slopes and of the corresponding transfer coefficients could be interpreted in terms of the variation of rate – determining step from charge transfer process to either chemical – desorption or to electrochemical desorption. The variation of the anodic Tafel slope and transfer coefficients (α_a) could be interpreted in terms of the variation of the rate-determining step from charge transfer process to either chemical–desorption or to electrochemical desorption. The variation of the anodic transfer coefficient (α_a) may be attributed to the variation of the rate-determining step in the metal dissolution reaction. A change in mechanism as well as in the rate-determining step cannot be ignored throughout the anodic processes [11].

3.1.5 The Exchange Current Densities and Polarization Resistances

The polarization resistance (R_p) values have been calculated using the following equation:

$$R_p = \frac{b_a b_c}{2.303(b_a + b_c) i_{corr}} \quad (3.8)$$

For low field approximation ($\eta \leq 20 \text{ mV}$), the Tafel equation may be reduced to the form [78]:

CHAPTER THREE RESULTS AND DISCUSSION

$$\eta = \left[\frac{RT}{i_o F} \right] i \quad (3.9)$$

where i_o is the equilibrium exchange current density. The term η/i correspond to the resistance R_p of the interface to the charge transfer reaction as in equation (1.22). so i_o values can be calculated from the following equation:

$$i_o = \frac{RT}{R_p F} \quad (3.10)$$

Values of R_p and i_o are presented in **Tables 3.13. - 3.21.**

The results of R_p can be summarized as follows:

- the values of the R_p in the absence of inhibitors of pure Al and its alloys under investigation can sequence as follow:

Pure Al > 5052 Al > 2024 Al

- R_p decreased with increasing temperature
- R_p increased with increasing inhibitors concentration
- the values of the polarization resistance in the presence of inhibitors of pure Al and its alloys can sequence as follow:

2024 Al > 5052 Al > Pure Al

- The greatest values of the polarization resistance which have been observed in the presence amoxicillin

CHAPTER THREE RESULTS AND DISCUSSION

Table 3.13. Values of transfer coefficients (α_c , α_a), the polarization resistance (R_p) and equilibrium exchange current density (i_o) for corrosion of **Pure Aluminium** in 3.5%NaCl solution without and with **Ampicillin** at temperature range 283-323K.

Conc. [M]	T [K]	α_c	α_a	$R_p/10^3$ [Ω/cm^2]	$i_o/10^{-5}$ [A/cm^2]
0 (Blank)	283	0.383	1.341	1.062	2.297
	293	0.354	1.304	0.927	2.722
	303	0.364	0.625	0.720	3.626
	313	0.184	0.621	0.700	3.852
	323	0.166	0.615	0.654	4.256
1.5×10^{-4}	283	0.377	1.156	4.278	0.570
	293	0.201	1.112	4.026	0.627
	303	0.197	0.824	2.135	1.223
	313	0.173	0.626	1.973	1.367
	323	0.153	0.609	1.835	1.517
3×10^{-4}	283	0.395	1.163	4.486	0.544
	293	0.253	1.035	4.396	0.574
	303	0.257	0.802	2.178	1.199
	313	0.196	0.686	1.988	1.357
	323	0.159	0.638	1.948	1.429
4.5×10^{-4}	283	0.432	1.667	4.926	0.495
	293	0.430	1.187	4.821	0.524
	303	0.435	0.860	2.351	1.110
	313	0.258	0.822	2.210	1.221
	323	0.175	0.684	2.238	1.243
6×10^{-4}	283	0.438	1.854	5.021	0.486
	293	0.471	1.292	4.956	0.509
	303	0.474	0.906	2.445	1.068
	313	0.277	0.792	2.268	1.189
	323	0.168	0.758	2.276	1.223
7.5×10^{-4}	283	0.476	1.993	5.148	0.474
	293	0.568	1.284	5.433	0.465
	303	0.535	1.159	2.719	0.960
	313	0.358	0.944	2.340	1.152
	323	0.212	0.903	2.347	1.186

CHAPTER THREE RESULTS AND DISCUSSION

Table 3.14. Values of transfer coefficients (α_c , α_a), the polarization resistance (R_p) and equilibrium exchange current density (i_o) for corrosion of **Pure Aluminium** in 3.5%NaCl solution without and with **Cephalexin** at temperature range 283-323K.

Conc. [M]	T [K]	α_c	α_a	$R_p/10^3$ [Ω/cm^2]	$i_o/10^{-5}$ [A/cm^2]
0 (Blank)	283	0.383	1.341	1.062	2.297
	293	0.354	1.304	0.927	2.722
	303	0.364	0.625	0.720	3.626
	313	0.184	0.621	0.700	3.852
	323	0.166	0.615	0.654	4.256
1.5×10^{-4}	283	0.153	1.971	4.238	0.575
	293	0.178	1.538	3.545	0.712
	303	0.195	1.074	2.169	1.204
	313	0.213	0.908	1.645	1.639
	323	0.241	1.579	0.873	3.188
3×10^{-4}	283	0.218	1.712	5.905	0.413
	293	0.251	1.315	4.645	0.544
	303	0.185	0.986	2.852	0.915
	313	0.178	1.353	1.869	1.443
	323	0.298	1.470	1.132	2.460
4.5×10^{-4}	283	0.465	1.444	6.653	0.367
	293	0.443	1.773	4.300	0.587
	303	0.253	0.928	3.019	0.865
	313	0.521	0.875	2.122	1.271
	323	0.260	0.856	1.989	1.399
6×10^{-4}	283	0.310	1.337	7.712	0.316
	293	0.364	1.229	6.264	0.403
	303	0.294	0.634	4.375	0.597
	313	0.308	0.734	2.965	0.910
	323	0.163	0.817	2.493	1.116
7.5×10^{-4}	283	0.127	1.605	8.969	0.464
	293	0.145	1.685	6.933	0.613
	303	0.155	0.997	4.702	0.922
	313	0.141	0.894	3.249	1.361
	323	0.112	0.799	2.815	1.601

CHAPTER THREE RESULTS AND DISCUSSION

Table 3.15. Values of transfer coefficients (α_c , α_a), the polarization resistance (R_p) and equilibrium exchange current density (i_o) for corrosion of **Pure Aluminium** in 3.5%NaCl solution without and with **Amoxicillin** at temperature range 283-323K.

Conc. [M]	T [K]	α_c	α_a	$R_p/10^3$ [Ω/cm^2]	$i_o/10^{-5}$ [A/cm^2]
0 (Blank)	283	0.383	1.341	1.062	2.297
	293	0.354	1.304	0.927	2.722
	303	0.364	0.625	0.720	3.626
	313	0.184	0.621	0.700	3.852
	323	0.166	0.615	0.654	4.256
1.5×10^{-4}	283	0.491	1.686	5.627	0.433
	293	0.343	1.177	5.148	0.490
	303	0.438	1.000	2.362	1.105
	313	0.567	0.658	1.739	1.551
	323	0.555	0.662	1.462	1.904
3×10^{-4}	283	0.850	2.177	4.964	0.491
	293	0.360	1.248	5.331	0.474
	303	0.223	1.150	2.769	0.943
	313	0.134	0.753	2.711	0.995
	323	0.205	0.751	2.080	1.338
4.5×10^{-4}	283	0.628	1.591	8.140	0.511
	293	0.291	1.284	6.599	0.644
	303	0.428	0.861	3.148	1.377
	313	0.327	0.854	2.494	1.773
	323	0.356	0.586	2.547	1.770
6×10^{-4}	283	0.476	1.614	9.118	0.645
	293	0.218	1.315	6.721	0.888
	303	0.337	0.849	3.619	1.674
	313	0.369	0.743	2.703	2.273
	323	0.486	0.706	2.114	2.947
7.5×10^{-4}	283	0.571	1.812	9.840	0.773
	293	0.373	1.281	8.297	0.927
	303	0.460	0.983	4.071	1.911
	313	0.261	0.810	3.524	2.232
	323	0.266	0.828	2.446	3.251

CHAPTER THREE RESULTS AND DISCUSSION

Table 3.16. Values of transfer coefficients (α_c , α_a), the polarization resistance (R_p) and equilibrium exchange current density (i_o) for corrosion of **5052 Aluminium** in 3.5%NaCl solution without and with **Ampicillin** at temperature range 283-323K.

Conc. [M]	T [K]	α_c	α_a	$R_p/10^3$ [Ω/cm^2]	$i_o/10^{-5}$ [A/cm^2]
0 (Blank)	283	0.293	1.200	0.984	2.479
	293	0.470	0.958	0.951	2.654
	303	0.503	0.976	0.460	5.673
	313	0.521	0.545	0.514	5.246
	323	0.716	0.502	0.373	7.465
1.5×10^{-4}	283	0.117	0.934	4.307	0.566
	293	0.140	0.707	4.211	0.600
	303	0.160	0.641	2.175	1.200
	313	0.217	0.446	2.046	1.318
	323	0.225	0.376	1.863	1.494
3×10^{-4}	283	0.125	0.919	5.020	0.486
	293	0.298	0.608	4.494	0.562
	303	0.288	0.582	2.219	1.177
	313	0.312	0.415	2.124	1.270
	323	0.260	0.395	1.907	1.459
4.5×10^{-4}	283	0.151	0.897	5.071	0.481
	293	0.344	0.617	4.928	0.512
	303	0.385	0.609	2.247	1.162
	313	0.264	0.467	2.224	1.213
	323	0.255	0.431	1.933	1.440
6×10^{-4}	283	0.216	0.999	5.334	0.457
	293	0.228	0.917	5.027	0.502
	303	0.302	0.803	2.375	1.099
	313	0.365	0.515	2.315	1.165
	323	0.322	0.442	2.028	1.372
7.5×10^{-4}	283	0.284	0.963	6.380	0.382
	293	0.340	0.734	6.109	0.413
	303	0.496	0.686	2.459	1.062
	313	0.378	0.554	2.435	1.107
	323	0.367	0.528	2.092	1.330

CHAPTER THREE RESULTS AND DISCUSSION

Table 3.17. Values of transfer coefficients (α_c , α_a), the polarization resistance (R_p) and equilibrium exchange current density (i_o) for corrosion of **5052 Aluminium** in 3.5%NaCl solution without and with **Cephalexin** at temperature range 283-323K.

Conc. [M]	T [K]	α_c	α_a	$R_p/10^3$ [Ω/cm^2]	$i_o/10^{-5}$ [A/cm^2]
0 (Blank)	283	0.293	1.200	0.984	2.479
	293	0.470	0.958	0.951	2.654
	303	0.503	0.976	0.460	5.673
	313	0.521	0.545	0.514	5.246
	323	0.716	0.502	0.373	7.465
1.5×10^{-4}	283	0.276	0.808	4.621	0.528
	293	0.218	0.730	4.575	0.552
	303	0.212	0.637	2.290	1.140
	313	0.173	0.540	2.088	1.292
	323	0.216	0.418	1.906	1.460
3×10^{-4}	283	0.474	1.025	6.226	0.447
	293	0.454	1.272	4.656	0.598
	303	0.345	0.878	2.859	0.973
	313	0.347	0.854	2.215	1.256
	323	0.349	0.710	2.020	1.378
4.5×10^{-4}	283	0.728	1.121	6.924	0.402
	293	0.444	1.667	5.368	0.519
	303	0.246	1.259	3.011	0.925
	313	0.435	0.946	2.560	1.087
	323	0.431	0.887	2.323	1.198
6×10^{-4}	283	0.311	1.448	7.887	0.353
	293	0.197	1.704	6.377	0.436
	303	0.387	0.894	4.176	0.666
	313	0.324	0.769	3.848	0.723
	323	0.465	0.828	2.625	1.060
7.5×10^{-4}	283	0.671	1.118	9.038	0.308
	293	0.604	1.093	7.204	0.386
	303	0.522	0.776	4.515	0.616
	313	0.523	0.849	3.211	0.867
	323	0.404	0.765	2.973	0.936

CHAPTER THREE RESULTS AND DISCUSSION

Table 3.18. Values of transfer coefficients (α_c , α_a), the polarization resistance (R_p) and equilibrium exchange current density (i_o) for corrosion of **5052 Aluminium** in 3.5%NaCl solution without and with **Amoxicillin** at temperature range 283-323K.

Conc. [M]	T [K]	α_c	α_a	$R_p/10^3$ [Ω/cm^2]	$i_o/10^{-5}$ [A/cm^2]
0 (Blank)	283	0.293	1.200	0.984	2.479
	293	0.470	0.958	0.951	2.654
	303	0.503	0.976	0.460	5.673
	313	0.521	0.545	0.514	5.246
	323	0.716	0.502	0.373	7.465
1.5×10^{-4}	283	0.416	1.097	5.726	0.426
	293	0.246	0.977	5.287	0.478
	303	0.211	0.731	2.376	1.099
	313	0.131	0.624	2.176	1.239
	323	0.129	0.545	2.011	1.384
3×10^{-4}	283	0.267	1.306	7.010	0.348
	293	0.368	1.161	5.435	0.465
	303	0.219	0.644	3.012	0.867
	313	0.213	0.508	2.594	1.040
	323	0.196	0.462	2.243	1.241
4.5×10^{-4}	283	0.381	1.044	8.336	0.293
	293	0.199	1.035	7.648	0.330
	303	0.259	0.656	3.313	0.788
	313	0.299	0.666	2.392	1.128
	323	0.171	0.524	2.746	1.014
6×10^{-4}	283	0.404	0.833	10.201	0.408
	293	0.485	0.738	8.222	0.517
	303	0.268	0.512	4.231	1.024
	313	0.219	0.628	3.040	1.454
	323	0.241	0.625	2.355	1.914
7.5×10^{-4}	283	0.428	0.893	10.740	0.388
	293	0.340	0.942	9.170	0.463
	303	0.324	0.647	4.225	1.026
	313	0.287	0.399	4.083	1.083
	323	0.364	0.354	3.135	1.438

CHAPTER THREE RESULTS AND DISCUSSION

Table 3.19. Values of transfer coefficients (α_c , α_a), the polarization resistance (R_p) and equilibrium exchange current density (i_o) for corrosion of **2024 Aluminium** in 3.5%NaCl solution without and with **Ampicillin** at temperature range 283-323K.

Conc. [M]	T [K]	α_c	α_a	$R_p/10^3$ [Ω/cm^2]	$i_o/10^{-5}$ [A/cm^2]
0 (Blank)	283	0.223	1.095	0.664	3.672
	293	0.409	0.956	0.608	4.152
	303	0.361	0.554	0.480	5.436
	313	0.253	0.665	0.472	5.712
	323	0.440	0.680	0.339	8.219
1.5×10^{-4}	283	0.188	0.639	4.435	0.550
	293	0.119	0.575	4.152	0.608
	303	0.146	0.288	3.205	0.815
	313	0.163	0.311	2.602	1.037
	323	0.131	0.549	1.582	1.760
3×10^{-4}	283	0.199	0.589	5.408	0.451
	293	0.198	0.568	4.138	0.610
	303	0.202	0.328	2.757	0.947
	313	0.207	0.315	2.585	1.043
	323	0.145	0.390	2.200	1.265
4.5×10^{-4}	283	0.220	0.637	5.844	0.417
	293	0.117	0.757	5.083	0.497
	303	0.132	0.520	2.959	0.882
	313	0.267	0.425	2.549	1.058
	323	0.281	0.381	2.244	1.240
6×10^{-4}	283	0.315	0.567	6.836	0.357
	293	0.413	0.511	5.541	0.456
	303	0.197	0.329	3.960	0.659
	313	0.168	0.513	2.704	0.998
	323	0.214	0.481	2.272	1.225
7.5×10^{-4}	283	0.354	0.674	7.026	0.347
	293	0.238	0.615	6.484	0.389
	303	0.173	0.503	4.122	0.633
	313	0.240	0.627	2.893	0.932
	323	0.192	0.598	2.574	1.081

CHAPTER THREE RESULTS AND DISCUSSION

Table 3.20. Values of transfer coefficients (α_c , α_a), the polarization resistance (R_p) and equilibrium exchange current density (i_o) for corrosion of **2024 Aluminium** in 3.5%NaCl solution without and with **Cephalexin** at temperature range 283-323K.

Conc. [M]	T [K]	α_c	α_a	$R_p/10^3$ [Ω/cm^2]	$i_o/10^{-5}$ [A/cm^2]
0 (Blank)	283	0.223	1.095	0.664	3.672
	293	0.409	0.956	0.608	4.152
	303	0.361	0.554	0.480	5.436
	313	0.253	0.665	0.472	5.712
	323	0.440	0.680	0.339	8.219
1.5×10^{-4}	283	0.198	0.708	4.885	0.499
	293	0.214	0.615	4.462	0.566
	303	0.192	0.336	2.710	0.963
	313	0.163	0.435	2.226	1.212
	323	0.162	0.388	2.040	1.365
3×10^{-4}	283	0.440	0.568	6.287	0.388
	293	0.303	0.464	4.700	0.537
	303	0.208	0.334	2.785	0.937
	313	0.238	0.322	2.527	1.067
	323	0.219	0.337	2.120	1.313
4.5×10^{-4}	283	0.427	0.618	7.163	0.340
	293	0.338	0.678	6.049	0.417
	303	0.220	0.477	3.203	0.815
	313	0.249	0.401	2.962	0.911
	323	0.242	0.354	2.635	1.056
6×10^{-4}	283	0.283	0.809	7.610	0.547
	293	0.343	0.638	6.797	0.625
	303	0.209	0.423	4.289	1.010
	313	0.213	0.350	3.860	1.145
	323	0.228	0.326	3.203	1.407
7.5×10^{-4}	283	0.270	0.595	10.181	0.409
	293	0.138	0.678	8.511	0.499
	303	0.195	0.457	4.547	0.953
	313	0.307	0.407	3.992	1.107
	323	0.221	0.333	3.708	1.215

CHAPTER THREE RESULTS AND DISCUSSION

Table 3.21. Values of transfer coefficients (α_c , α_a), the polarization resistance (R_p) and equilibrium exchange current density (i_o) for corrosion of **2024 Aluminium** in 3.5%NaCl solution without and with **Amoxicillin** at temperature range 283-323K.

Conc. [M]	T [K]	α_c	α_a	$R_p/10^3$ [Ω/cm^2]	$i_o/10^{-5}$ [A/cm^2]
0 (Blank)	283	0.223	1.095	0.664	3.672
	293	0.409	0.956	0.608	4.152
	303	0.361	0.554	0.480	5.436
	313	0.253	0.665	0.472	5.712
	323	0.440	0.680	0.339	8.219
1.5×10^{-4}	283	0.268	0.566	6.574	0.371
	293	0.214	0.548	5.298	0.477
	303	0.177	0.344	3.035	0.860
	313	0.153	0.398	2.641	1.021
	323	0.153	0.362	2.353	1.183
3×10^{-4}	283	0.271	1.017	7.999	0.305
	293	0.229	0.635	5.555	0.454
	303	0.246	0.413	3.147	0.830
	313	0.161	0.411	2.949	0.914
	323	0.163	0.387	2.318	1.200
4.5×10^{-4}	283	0.268	0.918	8.882	0.275
	293	0.261	0.665	8.278	0.305
	303	0.201	0.557	3.575	0.730
	313	0.182	0.469	3.201	0.842
	323	0.175	0.416	2.881	0.966
6×10^{-4}	283	0.324	0.676	11.814	0.206
	293	0.311	0.638	10.839	0.233
	303	0.246	0.347	5.200	0.502
	313	0.216	0.342	4.140	0.651
	323	0.169	0.330	3.803	0.732
7.5×10^{-4}	283	0.484	0.616	13.483	0.181
	293	0.330	0.984	11.611	0.217
	303	0.218	0.667	4.421	0.591
	313	0.204	0.413	4.310	0.626
	323	0.201	0.413	3.883	0.717

3.1.6 Activation Parameters of Corrosion

Inspection of **Tables 3.1. - 3.9.** show that corrosion rate increased with increasing temperature both in uninhibited and inhibited solutions. For corrosion systems that in which corrosion rate increase with a temperature, kinetics parameters can be calculated by using Arrhenius equation [79]:

$$r = A e^{\left(\frac{-E_a}{RT}\right)} \quad (3.11)$$

where r is corrosion rate, A and E_a are the pre- exponential factor and energy of activation of the corrosion process respectively, R the gas constant and T the absolute temperature.

The rate (r) of corrosion in a given environment is directly proportional with its corrosion current density (i_{corr}) in accordance with Faraday's law (equation (3.2)), so is reasonable to write Arrhenius equation as [80]:

$$\log i_{\text{corr}} = \log A - \frac{E_a}{2.303 RT} \quad (3.12)$$

Values of E_a were derived from the slopes of the ($\log i_{\text{corr}}$) versus ($1/T$) linear plots as in **Figures 3.5. to 3.7.**, while those of (A) were obtained from the intercepts of the plots; values of (A) expressed in term of ($\text{Amper} \cdot \text{m}^{-2}$), have then been converted into ($\text{molecules per m}^2 \text{ per second}$).

In order to calculate activation thermodynamic parameters of the corrosion reaction such as activated entropy ΔS^* and enthalpy ΔH^* , the Arrhenius equation and its alternative formulation called transition state equation were employed [81]:

$$C_R = \frac{RT}{Nh} e^{\left(\frac{\Delta S^*}{R}\right)} e^{\left(\frac{-\Delta H^*}{RT}\right)} \quad (1.13)$$

CHAPTER THREE RESULTS AND DISCUSSION

$$\log \frac{C_R}{T} = \log \frac{R}{N h} + \frac{\Delta S^*}{2.303 R} - \frac{\Delta H^*}{2.303 R T} \quad (3.14)$$

where C_R is the corrosion rate, N is the Avogadro's number, h is the Planck's constant. A plot of $\log (C_R/T)$ as a function of $1/T$ was made for pure aluminium and two other Al alloys under study in 3.5% NaCl in the absence and presence of different concentrations of inhibitors. Straight lines are obtained with a slope $(-\Delta H^*/R)$ and intercept $(\log R/Nh + \Delta S^*/2.303R)$ from which the ΔH^* and ΔS^* values are calculated.

Tables 3.22. - 3.30. present the values of activation energy (E_a), pre-exponential factor (A), enthalpy of activation (ΔH^*), entropy of activation (ΔS^*) of pure Al, 5052 Al and 2024 Al in the 3.5% NaCl without and with presence of AMP., CEX. and AMOX. as inhibitors. Examination of these data reveals that the values of pre-exponential factor and activation energy varies in the same way. The E_a values were greater than 20 kJ mol^{-1} in both the absence and presence of the inhibitor, which reveals that the entire process is controlled by the surface reaction [82], E_a in the presence of inhibitors is higher than that in the uninhibited solution, this indicate that the corrosion reaction of aluminium and two others alloys is inhibited by AMP., CEX. and AMOX. By physical adsorption on surface [83].

Higher values of E_a in the presence of inhibitor can be correlated with increasing thickness of the double layer which enhances the E_a of the corrosion process [84]. It is also an indication of a strong inhibitive action of inhibitors by increasing energy barrier for the corrosion process, emphasizing the electrostatic character of the inhibitor's adsorption on the aluminium and two other alloys surface (physisorption) [85].

CHAPTER THREE RESULTS AND DISCUSSION

The positive sign of ΔH^* show the endothermic nature of the corrosion process suggesting that the dissolution of aluminium and two other alloys is slow, which indicates that inhibition efficiencies decrease with increase in temperature [86].

The large negative value of ΔS^* for aluminium and two other alloys in 3.5% NaCl implies that the activated complex is the rate determining step, rather than the dissociation step. In the presence of the inhibitor, the values of ΔS^* increases and is generally interpreted as an increase in disorder as the reactants are converted to the activated complex [87].

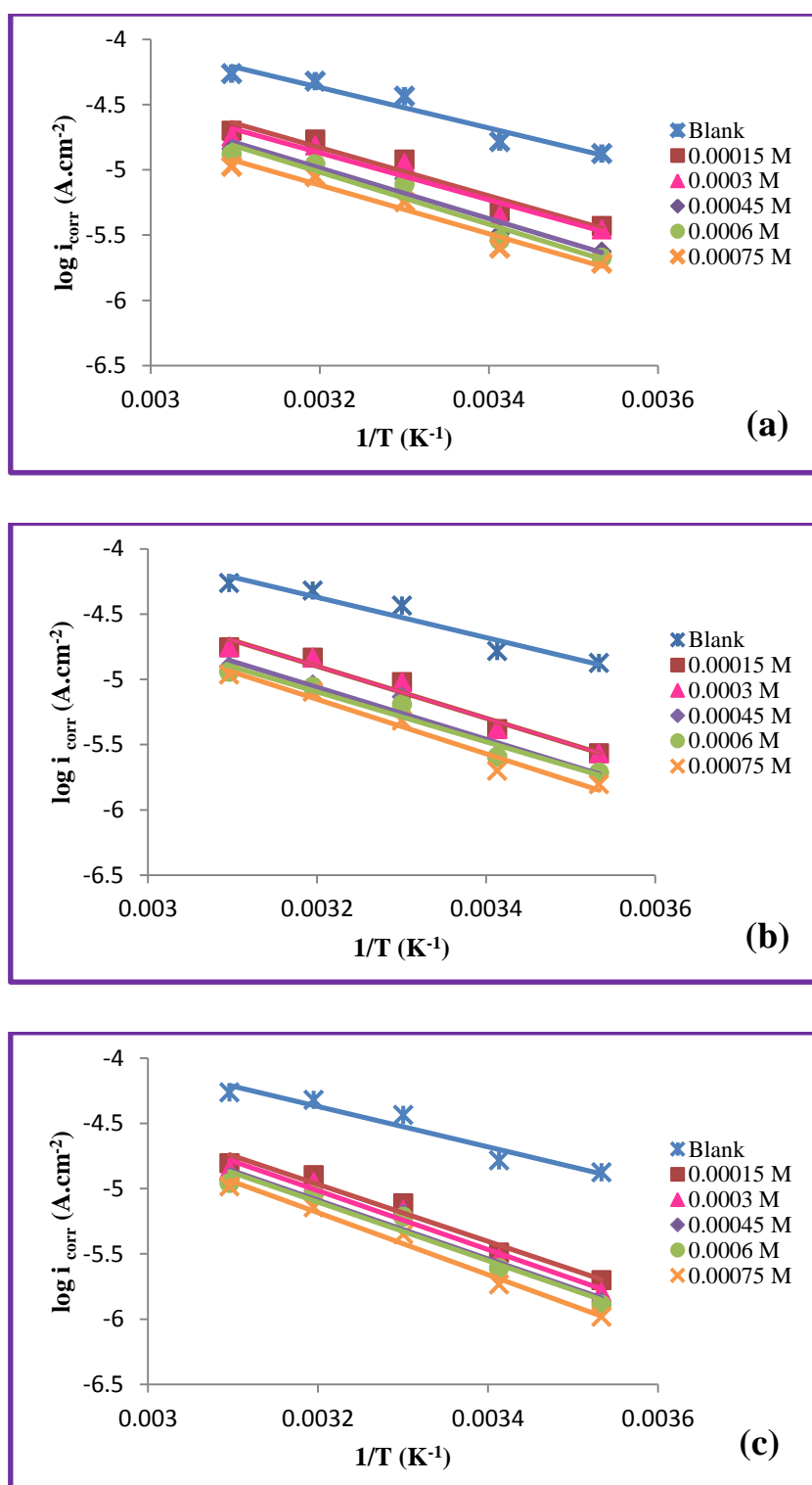


Figure 3.5. Arrhenius Plots of $\log i_{\text{corr}}$ versus $1/T$ for the corrosion of **Pure Aluminium** in 3.5% NaCl containing various concentrations of (a) **Ampicillin** (b) **Cephalexin** (c) **Amoxicillin**.

CHAPTER THREE RESULTS AND DISCUSSION

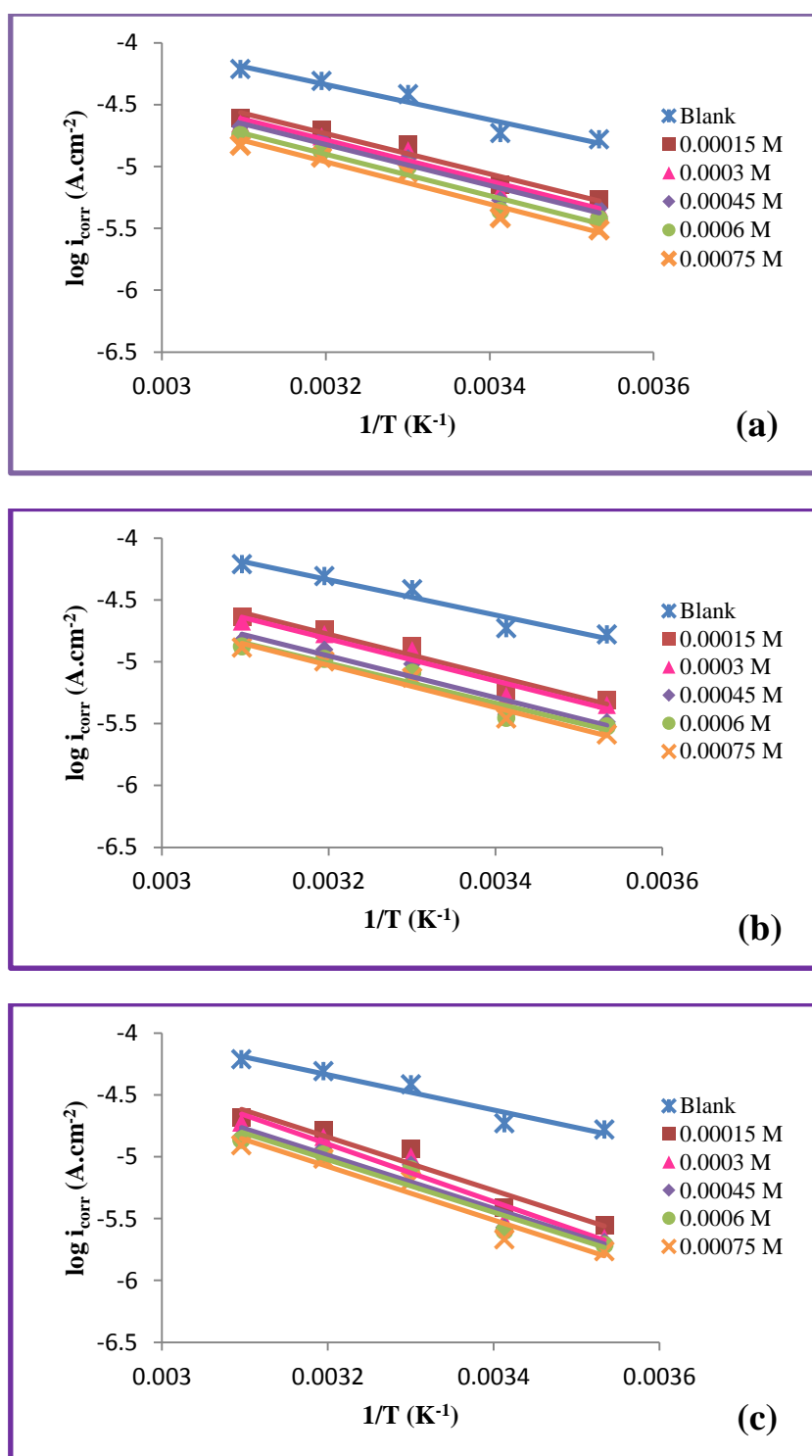


Figure 3.6. Arrhenius Plots of $\log i_{\text{corr}}$ versus $1/T$ for the corrosion of **5052 Aluminium** in 3.5% NaCl containing various concentrations of (a) **Ampicillin** (b) **Cephalexin** (c) **Amoxicillin**.

CHAPTER THREE RESULTS AND DISCUSSION

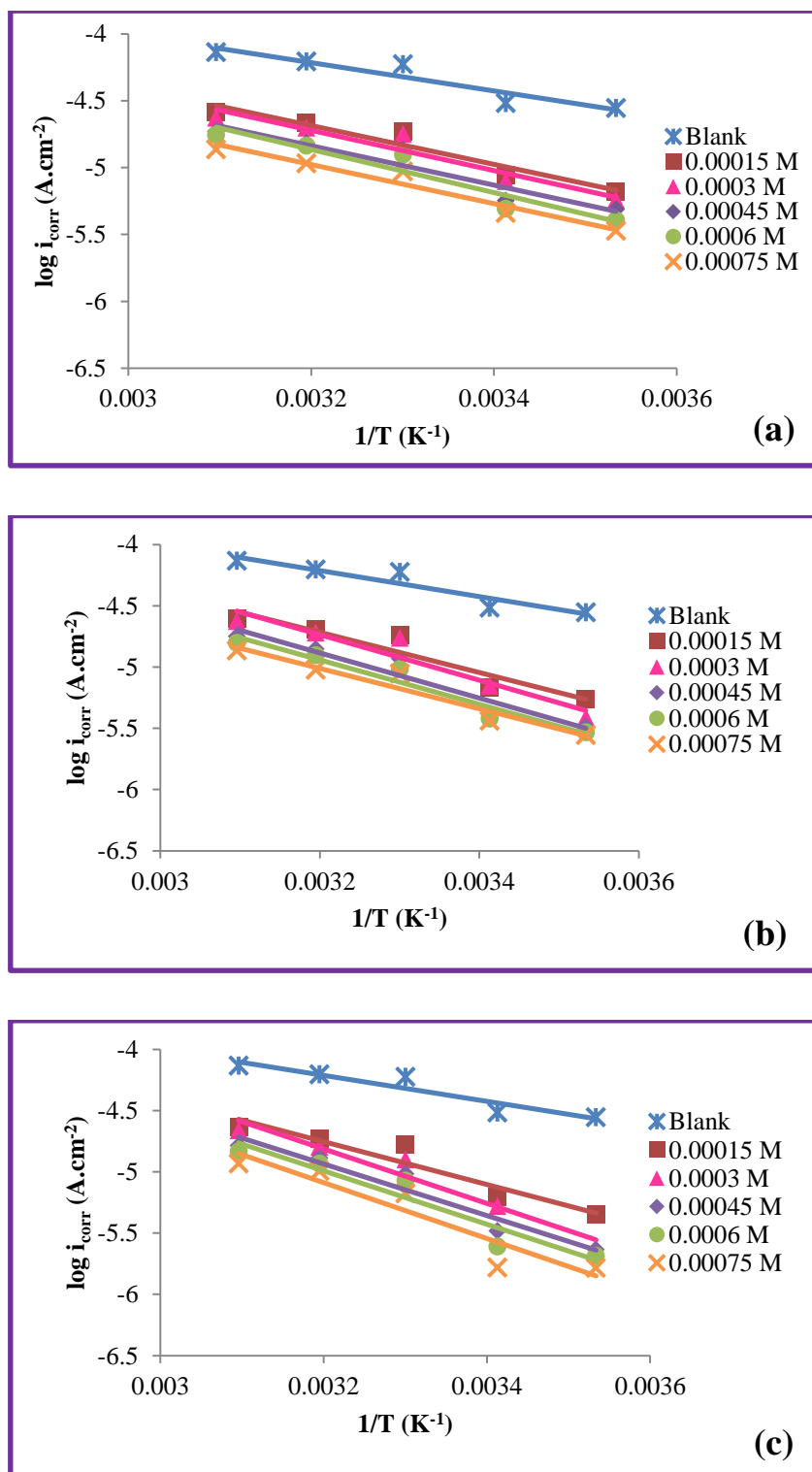


Figure 3.7. Arrhenius Plots of $\log i_{\text{corr}}$ versus $1/T$ for the corrosion of **2024 Aluminium** in 3.5% NaCl containing various concentrations of (a) **Ampicillin** (b) **Cephalexin** (c) **Amoxicillin**.

CHAPTER THREE RESULTS AND DISCUSSION

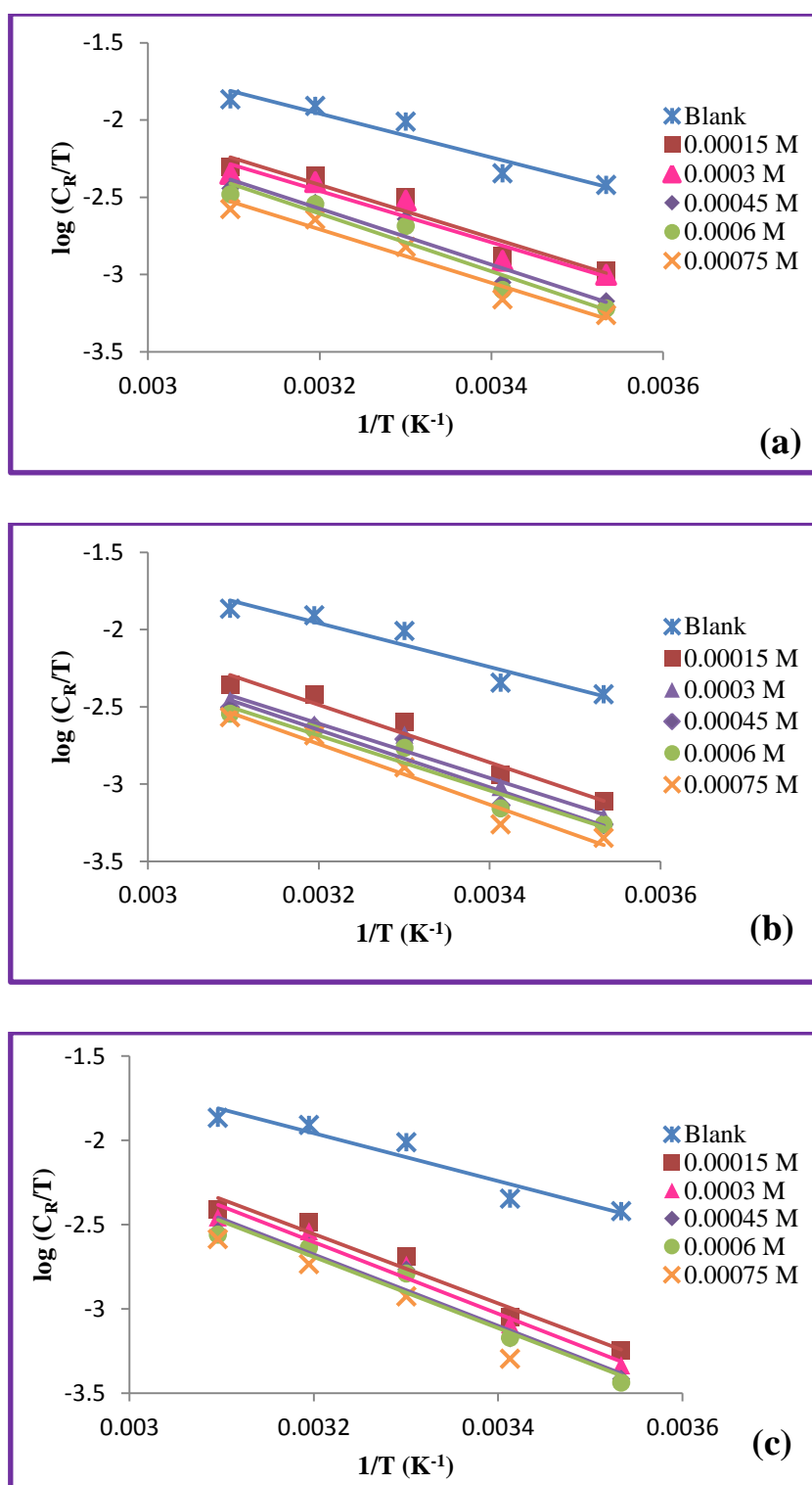


Figure 3.8. Plots of $\log C_R/T$ versus $1/T$ for the corrosion of **Pure Aluminium** in 3.5% NaCl containing various concentrations of (a) **Ampicillin** (b) **Cephalixin** (c) **Amoxicillin**.

CHAPTER THREE RESULTS AND DISCUSSION

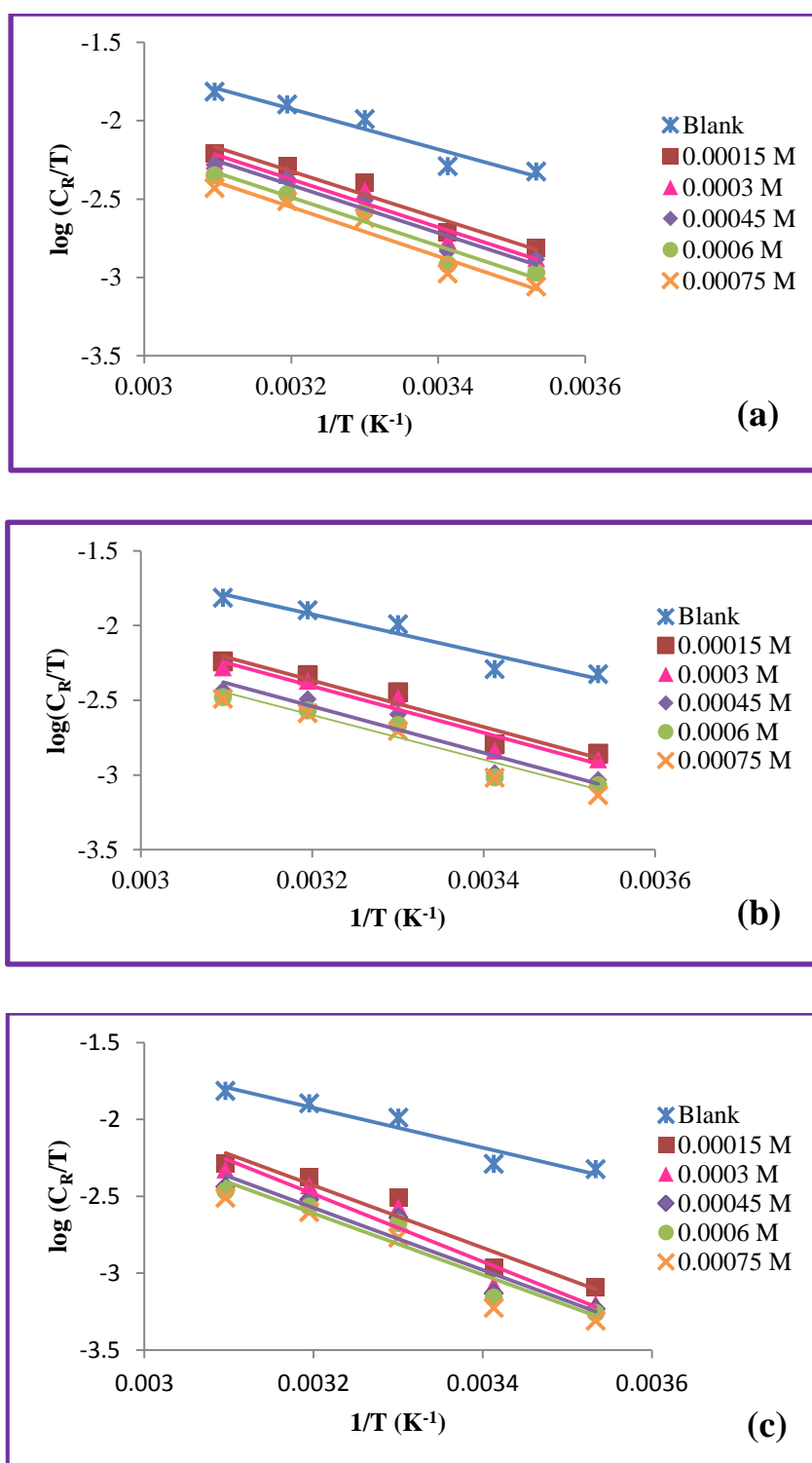


Figure 3.9. Plots of $\log C_R/T$ versus $1/T$ for the corrosion of **5052 Aluminium** in 3.5% NaCl containing various concentrations of (a) **Ampicillin** (b) **Cephalexin** (c) **Amoxicillin**.

CHAPTER THREE RESULTS AND DISCUSSION

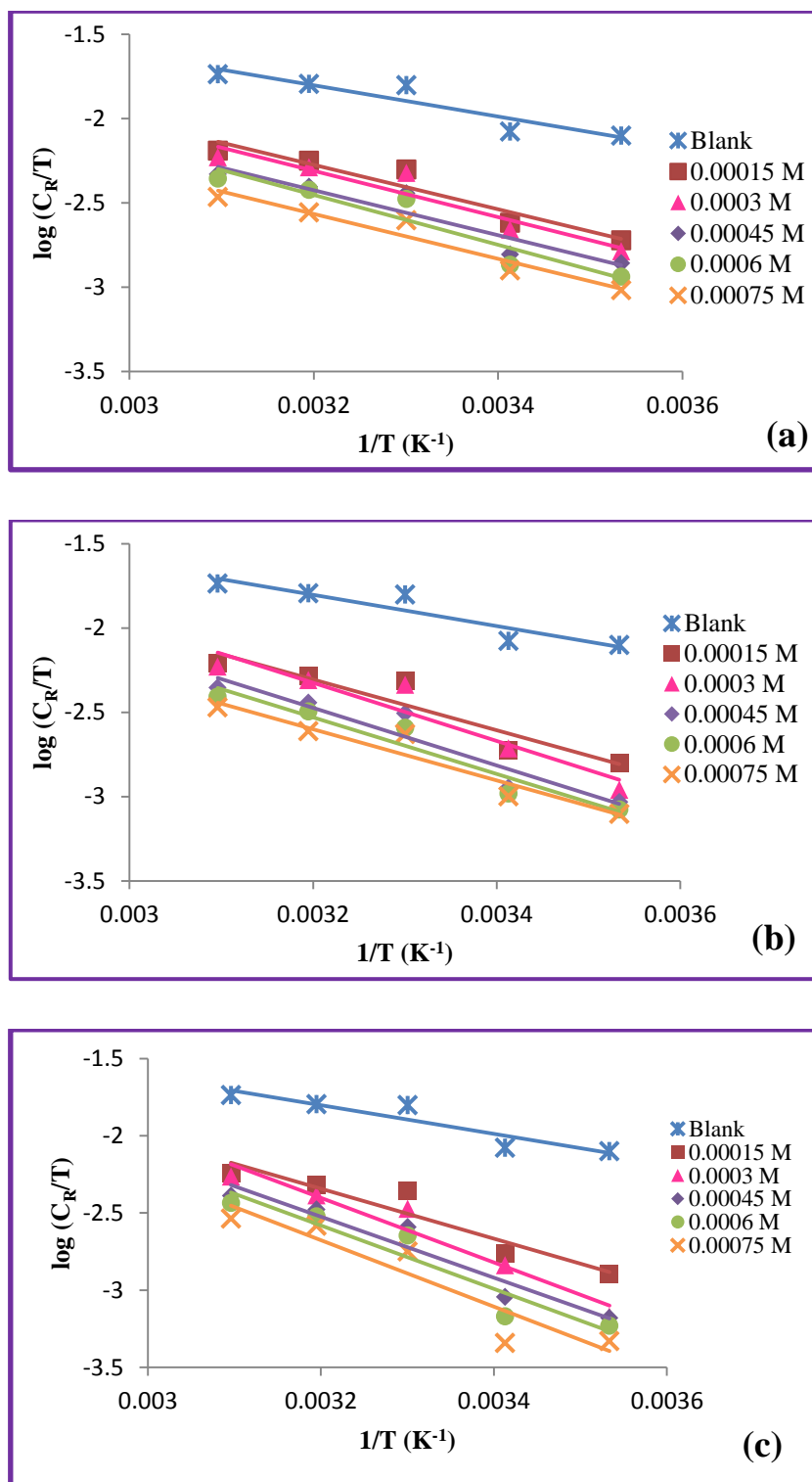


Figure 3.10. Plots of $\log C_R/T$ versus $1/T$ for the corrosion of **2024 Aluminium** in 3.5% NaCl containing various concentrations of (a) **Ampicillin** (b) **Cephalixin** (c) **Amoxicillin**.

CHAPTER THREE RESULTS AND DISCUSSION

Table 3.22. Activation parameters of the corrosion of **Pure Aluminium** in 3.5%NaCl in the absence and presence of different concentrations of **Ampicillin, Cephalexin, Amoxicillin** inhibitors.

inhibitor	Conc. [M]	E_a [kJ.mol ⁻¹]	A [molecule.cm ⁻² .s ⁻¹]	ΔH^* [kJ.mol ⁻¹]	ΔS^* [J.K ⁻¹ .mol ⁻¹]
AMP.	0	29.67	2.41×10^{19}	27.16	-148.15
	1.5×10^{-4}	35.34	7.39×10^{19}	32.83	-138.85
	3×10^{-4}	34.43	4.79×10^{19}	31.92	-142.51
	4.5×10^{-4}	37.25	1.08×10^{20}	34.74	-135.69
	6×10^{-4}	38.25	1.47×10^{20}	35.74	-133.11
	7.5×10^{-4}	35.70	4.39×10^{19}	33.19	-143.18
CEX.	0	29.67	2.41×10^{19}	27.16	-148.15
	1.5×10^{-4}	38.13	1.85×10^{20}	35.62	-131.24
	3×10^{-4}	36.22	6.68×10^{19}	33.71	-139.68
	4.5×10^{-4}	38.08	1.25×10^{20}	35.57	-134.50
	6×10^{-4}	36.62	6.55×10^{19}	34.11	-139.85
	7.5×10^{-4}	40.00	2.11×10^{20}	37.49	-130.10
AMOX.	0	29.67	2.41×10^{19}	27.16	-148.15
	1.5×10^{-4}	41.92	6.79×10^{20}	39.41	-120.40
	3×10^{-4}	43.15	9.74×10^{20}	40.64	-117.40
	4.5×10^{-4}	43.06	7.95×10^{20}	40.55	-119.09
	6×10^{-4}	42.95	7.36×10^{20}	40.44	-119.74
	7.5×10^{-4}	45.47	1.61×10^{21}	42.96	-113.21

CHAPTER THREE RESULTS AND DISCUSSION

Table 3.23. Activation parameters of the corrosion of **5052 Aluminium** in 3.5%NaCl in the absence and presence of different concentrations of **Ampicillin, Cephalexin, Amoxicillin** inhibitors.

inhibitor	Conc. [M]	E_a [kJ.mol ⁻¹]	A [molecule.cm ⁻² .s ⁻¹]	ΔH^* [kJ.mol ⁻¹]	ΔS^* [J.K ⁻¹ .mol ⁻¹]
AMP.	0	27.29	1.04×10^{19}	24.78	-155.16
	1.5×10⁻⁴	31.20	1.87×10^{19}	28.69	-150.27
	3×10⁻⁴	31.81	2.10×10^{19}	29.29	-149.29
	4.5×10⁻⁴	31.78	1.91×10^{19}	29.27	-150.09
	6×10⁻⁴	32.18	1.86×10^{19}	29.67	-150.30
	7.5×10⁻⁴	32.68	1.96×10^{19}	30.17	-149.87
CEX.	0	27.29	1.04×10^{19}	24.78	-155.16
	1.5×10⁻⁴	32.32	2.61×10^{19}	29.81	-147.50
	3×10⁻⁴	32.39	2.45×10^{19}	29.88	-148.01
	4.5×10⁻⁴	32.23	1.68×10^{19}	29.72	-151.15
	6×10⁻⁴	31.03	9.27×10^{18}	28.52	-151.10
	7.5×10⁻⁴	32.73	1.71×10^{19}	30.22	-150.99
AMOX.	0	27.29	1.04×10^{19}	24.78	-155.16
	1.5×10⁻⁴	41.32	7.21×10^{20}	38.813	-119.89
	3×10⁻⁴	44.59	2.23×10^{21}	42.083	-110.50
	4.5×10⁻⁴	41.20	4.91×10^{20}	38.692	-123.09
	6×10⁻⁴	40.75	3.79×10^{20}	38.23	-125.24
	7.5×10⁻⁴	41.50	4.48×10^{20}	38.99	-123.85

CHAPTER THREE RESULTS AND DISCUSSION

Table 3.24. Activation parameters of the corrosion of **2024 Aluminium** in 3.5%NaCl in the absence and presence of different concentrations of **Ampicillin, Cephalexin, Amoxicillin** inhibitors.

inhibitor	Conc. [M]	Ea [kJ.mol ⁻¹]	A [molecule.cm ⁻² .s ⁻¹]	ΔH* [kJ.mol ⁻¹]	ΔS* [J.K ⁻¹ .mol ⁻¹]
AMP.	0	20.26	9.22 × 10 ¹⁷	17.75	-175.29
	1.5×10 ⁻⁴	27.80	5.65 × 10 ¹⁸	25.28	-160.21
	3×10 ⁻⁴	28.79	7.63 × 10 ¹⁸	26.28	-157.72
	4.5×10 ⁻⁴	28.13	4.55 × 10 ¹⁸	25.62	-162.02
	6×10 ⁻⁴	30.84	1.21 × 10 ¹⁹	28.32	-153.92
	7.5×10 ⁻⁴	27.96	3.07 × 10 ¹⁸	25.44	-165.29
CEX.	0	20.26	9.22 × 10 ¹⁷	17.75	-175.29
	1.5×10 ⁻⁴	31.36	2.07 × 10 ¹⁹	28.84	-149.41
	3×10 ⁻⁴	35.57	1.00 × 10 ²⁰	33.05	-136.31
	4.5×10 ⁻⁴	35.26	6.34 × 10 ¹⁹	32.75	-140.12
	6×10 ⁻⁴	34.64	4.37 × 10 ¹⁹	32.13	-143.20
	7.5×10 ⁻⁴	31.54	1.13 × 10 ¹⁹	29.03	-154.47
AMOX.	0	20.26	9.22 × 10 ¹⁷	17.75	-175.29
	1.5×10 ⁻⁴	33.47	4.29 × 10 ¹⁹	30.96	-143.35
	3×10 ⁻⁴	42.59	1.25 × 10 ²¹	40.08	-115.33
	4.5×10 ⁻⁴	40.33	3.96 × 10 ²⁰	37.82	-124.88
	6×10 ⁻⁴	41.82	6.16 × 10 ²⁰	39.31	-121.20
	7.5×10 ⁻⁴	43.70	1.02 × 10 ²¹	41.19	-117.02

3.1.7 Thermodynamic Quantities of corrosion

Thermodynamic quantities can be explain a corrosion situation in terms of the stability of chemical species and the reactions associated with corrosion processes [35].

The change in the Gibbs free energy (ΔG) for the corrosion of a metal in an environment at a given temperature may be related to the corrosion potential (E_{corr}) of the metal by the well-known relation [88]:

$$\Delta G = -nFE \quad (3.15)$$

where n is the number of electrons involved in the corrosion reaction, F is the Faraday constant, E equals the cell potential ($E=E_{corr}$) its sign is reversed prior to its use in equation (3.19) to represent the potential of the reversibly operating cell and not the applied potential from the potentiostat.

From the values of ΔG at different temperatures, for each inhibitors concentration, it has been possible to estimate ΔS values using the well – known thermodynamic relation:

$$\Delta S = -\frac{d(\Delta G)}{dT} \quad (3.16)$$

The change in free energy, ΔG , is related to ΔH , the change in the enthalpy, and ΔS , the change in entropy of the corrosion reaction at a constant temperature, T , by the equation:

$$\Delta G = \Delta H - T\Delta S \quad (1.17)$$

ΔS correspond to the slope of the plot of values of ΔG against temperatures (Figures 3.8. - 3.10.); by using the values of ΔG and ΔS , it is possible to

CHAPTER THREE RESULTS AND DISCUSSION

calculate the corresponding values of the change in the enthalpy ΔH of the corrosion reaction at each temperature.

Values of ΔG , ΔH and ΔS have been determined for different concentrations of AMP., CEP., and AMOX. over the temperature range (293-323) K for pure Al and its alloys under investigation; the resulting data have been arranged as in **Tables 3.25. - 3.34.** The results in the tables indicate negative values of ΔG that mean, these reactions are occurring spontaneously.

The enthalpy changes ΔH of the corrosion reaction of aluminium and two others alloys in different concentrations AMP., CEP., and AMOX. at temperatures range 283- 323 K have negative values indicating the exothermic nature for this reaction.

The values of ΔS reflect the change in the order and orientation of the solvent molecules around the hydrated metal ions in the corrosion medium when metal atoms were corroded and subsequently hydrated in the solution. Values of ΔS were generally positive due to negativity of ΔG ; this suggests a lower order in the solvated states of the metal ions as compared with the state of metal atoms in the crystal lattice of the corroding electrodes [89].

CHAPTER THREE RESULTS AND DISCUSSION

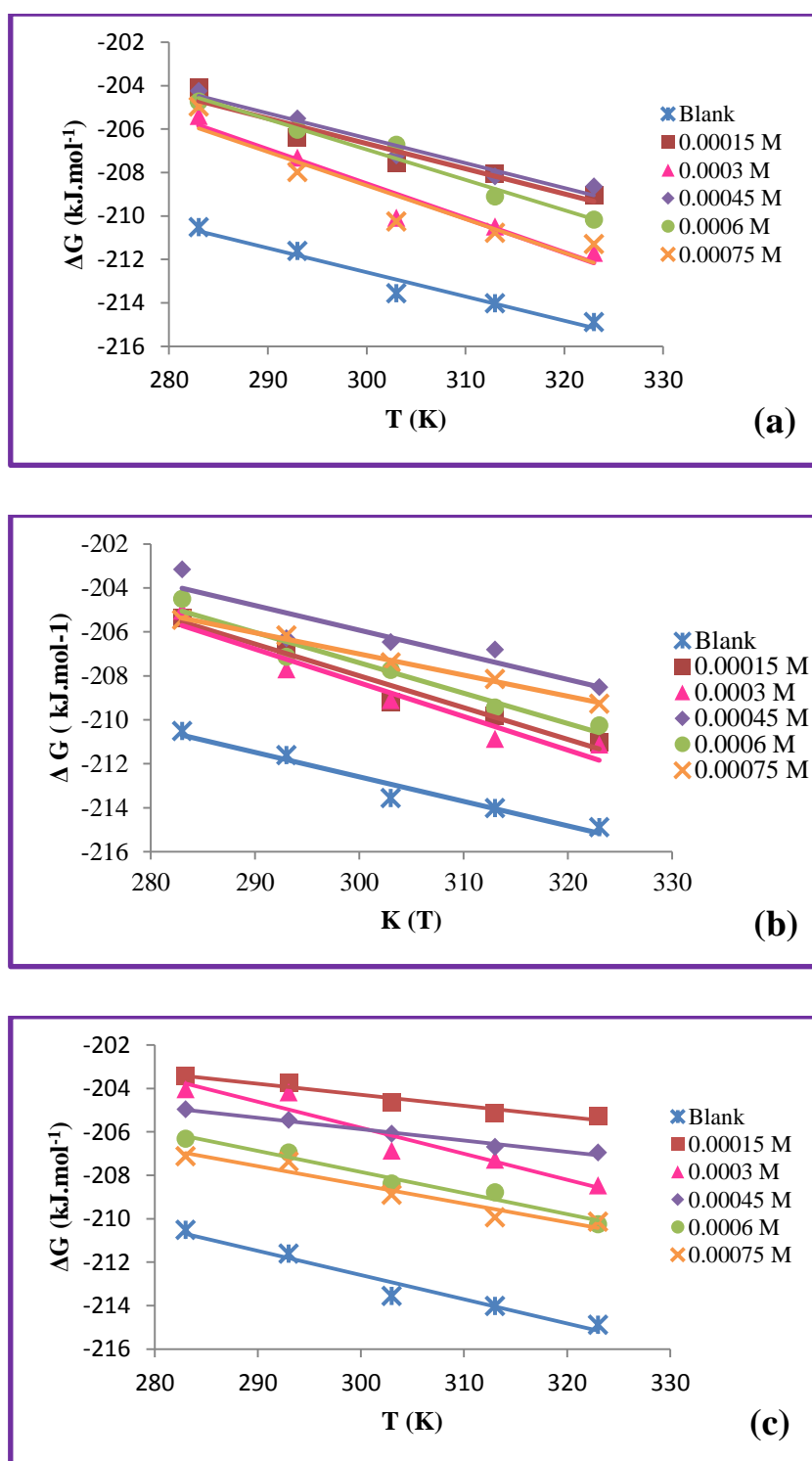


Figure 3.11. The variation of Gibbs free energies (ΔG) with temperature for the corrosion of **Pure Aluminium** in 3.5% NaCl at absence and presence different concentrations of (a) **Ampicillin** (b) **Cephalexin** (c) **Amoxicillin**.

CHAPTER THREE RESULTS AND DISCUSSION

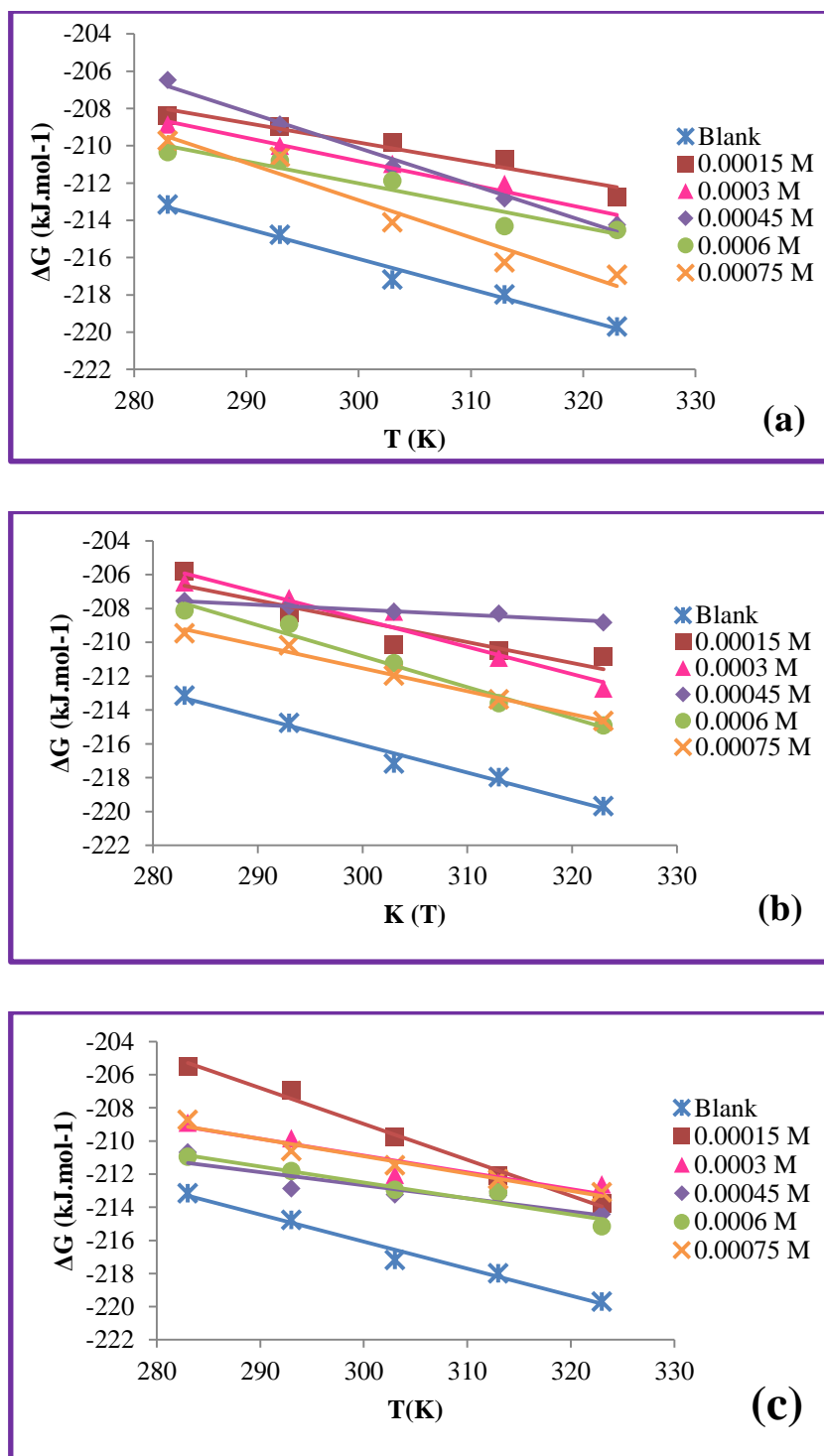


Figure 3.12. The variation of Gibbs free energies (ΔG) with temperature for the corrosion of **5052 Aluminium** in 3.5% NaCl at absence and presence different concentrations of (a) **Ampicillin** (b) **Cephalexin** (c) **Amoxicillin**.

CHAPTER THREE RESULTS AND DISCUSSION

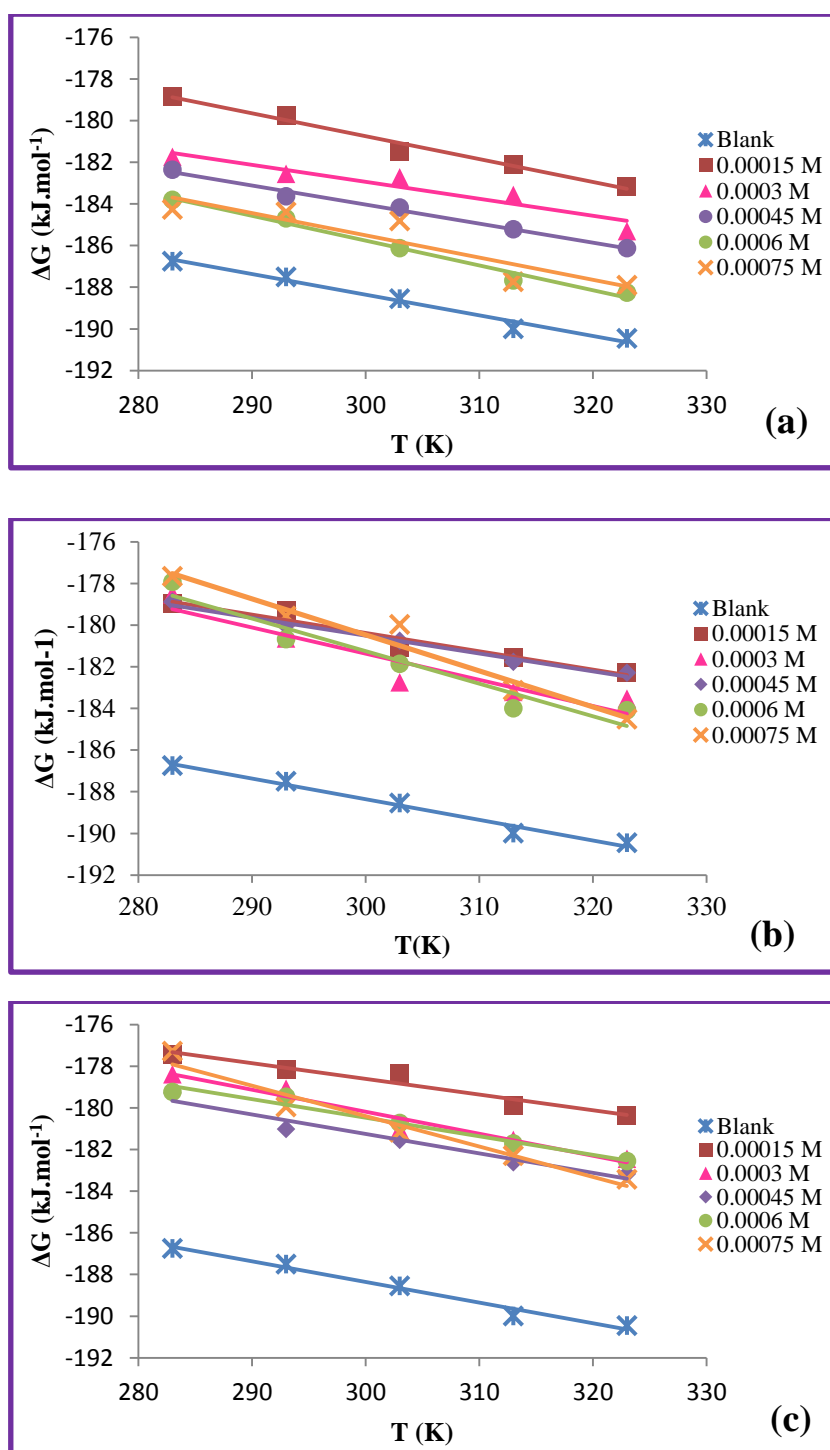


Figure 3.13. The variation of Gibbs free energies (ΔG) with temperature for the corrosion of **2024 Aluminium** in 3.5% NaCl at absence and presence different concentrations of (a) **Ampicillin** (b) **Cephalexin** (c) **Amoxicillin**.

CHAPTER THREE RESULTS AND DISCUSSION

Table 3.25. The thermodynamic functions for corrosion of **Pure Aluminium** in 3.5% NaCl at different concentration of **Ampicillin** over the temperature range 283 -323 K.

Conc. [M]	T [K]	ΔG [kJ.mol ⁻¹]	ΔH [kJ.mol ⁻¹]	ΔS [J.K ⁻¹ .mol ⁻¹]
0 (Blank)	283	-210.52	-178.98	111.44
	293	-211.62	-178.97	
	303	-213.56	-179.79	
	313	-214.02	-179.14	
	323	-214.89	-178.90	
1.5×10⁻⁴	283	-204.07	-171.22	116.07
	293	-206.38	-172.37	
	303	-207.54	-172.37	
	313	-208.03	-171.70	
	323	-209.05	-171.55	
3×10⁻⁴	283	-205.40	-160.67	158.04
	293	-207.31	-161.00	
	303	-210.09	-162.20	
	313	-210.49	-161.02	
	323	-211.71	-160.66	
4.5×10⁻⁴	283	-204.24	-171.80	114.62
	293	-205.51	-171.93	
	303	-207.22	-172.49	
	313	-208.18	-172.30	
	323	-208.64	-171.62	
6×10⁻⁴	283	-204.73	-165.25	139.52
	293	-206.03	-165.16	
	303	-206.73	-164.46	
	313	-209.10	-165.43	
	323	-210.17	-165.11	
7.5×10⁻⁴	283	-204.96	-161.14	154.86
	293	-207.97	-162.60	
	303	-210.26	-163.34	
	313	-210.78	-162.31	
	323	-211.30	-161.28	

CHAPTER THREE RESULTS AND DISCUSSION

Table 3.26. The thermodynamic functions for corrosion of **Pure Aluminium** in 3.5% NaCl at different concentration of **Cephalexin** over the temperature range 283 -323 K.

Conc. [M]	T [K]	ΔG [kJ.mol ⁻¹]	ΔH [kJ.mol ⁻¹]	ΔS [J.K ⁻¹ .mol ⁻¹]
0 (Blank)	283	-210.52	-178.98	111.44
	293	-211.62	-178.97	
	303	-213.56	-179.79	
	313	-214.02	-179.14	
	323	-214.89	-178.90	
1.5×10⁻⁴	283	-205.37	-164.49	144.44
	293	-206.73	-164.41	
	303	-209.19	-165.42	
	313	-209.83	-164.62	
	323	-211.04	-164.39	
3×10⁻⁴	283	-205.05	-161.72	153.12
	293	-207.71	-162.85	
	303	-209.10	-162.71	
	313	-210.87	-162.94	
	323	-211.13	-161.67	
4.5×10⁻⁴	283	-203.17	-171.39	112.31
	293	-206.30	-173.39	
	303	-206.47	-172.44	
	313	-206.82	-171.66	
	323	-208.52	-172.25	
6×10⁻⁴	283	-204.50	-165.34	138.36
	293	-207.13	-166.60	
	303	-207.74	-165.82	
	313	-209.45	-166.14	
	323	-210.26	-165.57	
7.5×10⁻⁴	283	-205.46	-178.26	96.10
	293	-206.18	-178.02	
	303	-207.40	-178.28	
	313	-208.15	-178.07	
	323	-209.28	-178.24	

CHAPTER THREE RESULTS AND DISCUSSION

Table 3.27. The thermodynamic functions for corrosion of **Pure Aluminium** in 3.5% NaCl at different concentration of **Amoxicillin** over the temperature range 283 -323 K.

Conc. [M]	T [K]	ΔG [kJ.mol ⁻¹]	ΔH [kJ.mol ⁻¹]	ΔS [J.K ⁻¹ .mol ⁻¹]
0 (Blank)	283	-210.52	-178.98	111.44
	293	-211.62	-178.97	
	303	-213.56	-179.79	
	313	-214.02	-179.14	
	323	-214.89	-178.90	
1.5×10⁻⁴	283	-203.43	-189.01	50.94
	293	-203.75	-188.82	
	303	-204.65	-189.21	
	313	-205.14	-189.19	
	323	-205.28	-188.83	
3×10⁻⁴	283	-204.04	-170.21	119.55
	293	-204.18	-169.16	
	303	-206.87	-170.65	
	313	-207.28	-169.86	
	323	-208.47	-169.85	
4.5×10⁻⁴	283	-204.96	-190.14	52.39
	293	-205.46	-190.11	
	303	-206.09	-190.22	
	313	-206.70	-190.30	
	323	-206.96	-190.04	
6×10⁻⁴	283	-206.32	-178.88	96.97
	293	-206.96	-178.55	
	303	-208.38	-179.00	
	313	-208.78	-178.43	
	323	-210.26	-178.94	
7.5×10⁻⁴	283	-207.13	-182.81	85.97
	293	-207.37	-182.18	
	303	-208.90	-182.85	
	313	-209.94	-183.03	
	323	-210.14	-182.38	

CHAPTER THREE RESULTS AND DISCUSSION

Table 3.28. The thermodynamic functions for corrosion of **5052 Aluminium** in 3.5% NaCl at different concentration of **Ampicillin** over the temperature range 283 -323 K.

Conc. [M]	T [K]	ΔG [kJ.mol ⁻¹]	ΔH [kJ.mol ⁻¹]	ΔS [J.K ⁻¹ .mol ⁻¹]
0 (Blank)	283	-213.155	-167.037	162.96
	293	-214.776	-167.028	
	303	-217.179	-167.801	
	313	-217.989	-166.982	
	323	-219.697	-167.060	
1.5×10⁻⁴	283	-208.408	-178.918	104.20
	293	-208.987	-178.455	
	303	-209.856	-178.282	
	313	-210.724	-178.108	
	323	-212.75	-179.092	
3×10⁻⁴	283	-208.87	-173.40	125.33
	293	-210.00	-173.28	
	303	-210.98	-173.01	
	313	-212.06	-172.83	
	323	-214.11	-173.63	
4.5×10⁻⁴	283	-206.47	-151.18	195.38
	293	-208.87	-151.62	
	303	-211.13	-151.93	
	313	-212.84	-151.68	
	323	-214.26	-151.15	
6×10⁻⁴	283	-210.35	-176.84	118.39
	293	-210.81	-176.12	
	303	-211.88	-176.01	
	313	-214.31	-177.26	
	323	-214.52	-176.28	
7.5×10⁻⁴	283	-209.74	-153.14	200.01
	293	-210.61	-152.00	
	303	-214.11	-153.51	
	313	-216.25	-153.65	
	323	-216.92	-152.31	

CHAPTER THREE RESULTS AND DISCUSSION

Table 3.29. The thermodynamic functions for corrosion of **5052 Aluminium** in 3.5% NaCl at different concentration of **Cephalexin** over the temperature range 283 -323 K.

Conc. [M]	T [K]	ΔG [kJ.mol ⁻¹]	ΔH [kJ.mol ⁻¹]	ΔS [J.K ⁻¹ .mol ⁻¹]
0 (Blank)	283	-213.155	-167.037	162.96
	293	-214.776	-167.028	
	303	-217.179	-167.801	
	313	-217.989	-166.982	
	323	-219.697	-167.060	
1.5×10⁻⁴	283	-205.80	-170.91	123.31
	293	-208.29	-172.16	
	303	-210.17	-172.81	
	313	-210.49	-171.90	
	323	-210.87	-171.04	
3×10⁻⁴	283	-206.47	-160.92	160.94
	293	-207.40	-160.24	
	303	-208.21	-159.44	
	313	-210.93	-160.55	
	323	-212.75	-160.77	
4.5×10⁻⁴	283	-207.57	-199.13	29.81
	293	-207.89	-199.15	
	303	-208.21	-199.17	
	313	-208.32	-198.99	
	323	-208.84	-199.21	
6×10⁻⁴	283	-208.12	-156.35	182.94
	293	-208.93	-155.33	
	303	-211.24	-155.82	
	313	-213.62	-156.36	
	323	-214.92	-155.83	
7.5×10⁻⁴	283	-209.48	-171.14	135.47
	293	-210.20	-170.51	
	303	-211.97	-170.92	
	313	-213.39	-170.99	
	323	-214.66	-170.91	

CHAPTER THREE RESULTS AND DISCUSSION

Table 3.30. The thermodynamic functions for corrosion of **5052 Aluminium** in 3.5% NaCl at different concentration of **Amoxicillin** over the temperature range 283 -323 K.

Conc. [M]	T [K]	ΔG [kJ.mol ⁻¹]	ΔH [kJ.mol ⁻¹]	ΔS [J.K ⁻¹ .mol ⁻¹]
0 (Blank)	283	-213.155	-167.037	162.96
	293	-214.776	-167.028	
	303	-217.179	-167.801	
	313	-217.989	-166.982	
	323	-219.697	-167.060	
1.5×10⁻⁴	283	-205.51	-144.16	216.80
	293	-206.96	-143.44	
	303	-209.77	-144.08	
	313	-212.08	-144.23	
	323	-213.79	-143.76	
3×10⁻⁴	283	-208.90	-180.23	101.31
	293	-209.86	-180.17	
	303	-212.06	-181.36	
	313	-212.52	-180.81	
	323	-212.63	-179.91	
4.5×10⁻⁴	283	-210.69	-188.33	79.02
	293	-212.87	-189.71	
	303	-213.24	-189.30	
	313	-213.30	-188.57	
	323	-214.43	-188.90	
6×10⁻⁴	283	-210.96	-183.60	96.68
	293	-211.82	-183.50	
	303	-212.95	-183.66	
	313	-213.10	-182.84	
	323	-215.15	-183.93	
7.5×10⁻⁴	283	-208.73	-179.15	104.49
	293	-210.61	-179.99	
	303	-211.48	-179.81	
	313	-212.32	-179.61	
	323	-213.10	-179.35	

CHAPTER THREE RESULTS AND DISCUSSION

Table 3.31. The thermodynamic functions for corrosion of **2024 Aluminium** in 3.5% NaCl at different concentration of **Ampicillin** over the temperature range 283 -323 K.

Conc. [M]	T [K]	ΔG [kJ.mol ⁻¹]	ΔH [kJ.mol ⁻¹]	ΔS [J.K ⁻¹ .mol ⁻¹]
0 (Blank)	283	-186.76	-158.74	98.99
	293	-187.51	-158.50	
	303	-188.55	-158.56	
	313	-190.00	-159.01	
	323	-190.46	-158.49	
1.5×10⁻⁴	283	-178.85	-147.73	109.99
	293	-179.75	-147.52	
	303	-181.49	-148.16	
	313	-182.13	-147.70	
	323	-183.17	-147.64	
3×10⁻⁴	283	-181.75	-158.73	81.34
	293	-182.56	-158.73	
	303	-182.73	-158.09	
	313	-183.57	-158.11	
	323	-185.31	-159.04	
4.5×10⁻⁴	283	-182.36	-156.55	91.18
	293	-183.63	-156.92	
	303	-184.18	-156.55	
	313	-185.22	-156.68	
	323	-186.12	-156.67	
6×10⁻⁴	283	-183.80	-150.14	118.97
	293	-184.70	-149.84	
	303	-186.12	-150.07	
	313	-187.68	-150.45	
	323	-188.26	-149.84	
7.5×10⁻⁴	283	-184.27	-154.12	106.52
	293	-184.38	-153.17	
	303	-184.82	-152.54	
	313	-187.74	-154.40	
	323	-187.91	-153.51	

CHAPTER THREE RESULTS AND DISCUSSION

Table 3.32. The thermodynamic functions for corrosion of **2024 Aluminium** in 3.5% NaCl at different concentration of **Cephalexin** over the temperature range 283 -323 K.

Conc. [M]	T [K]	ΔG [kJ.mol ⁻¹]	ΔH [kJ.mol ⁻¹]	ΔS [J.K ⁻¹ .mol ⁻¹]
0 (Blank)	283	-186.76	-158.74	98.99
	293	-187.51	-158.50	
	303	-188.55	-158.56	
	313	-190.00	-159.01	
	323	-190.46	-158.49	
1.5×10⁻⁴	283	-179.00	-154.10	87.99
	293	-179.29	-153.51	
	303	-181.08	-154.42	
	313	-181.55	-154.00	
	323	-182.27	-153.85	
3×10⁻⁴	283	-178.54	-142.90	125.91
	293	-180.65	-143.76	
	303	-182.76	-144.61	
	313	-183.23	-143.81	
	323	-183.54	-142.87	
4.5×10⁻⁴	283	-178.88	-154.64	85.68
	293	-180.04	-154.94	
	303	-180.77	-154.80	
	313	-181.78	-154.96	
	323	-182.30	-154.63	
6×10⁻⁴	283	-177.93	-133.61	156.60
	293	-180.68	-134.80	
	303	-181.87	-134.42	
	313	-184.01	-134.99	
	323	-184.09	-133.51	
7.5×10⁻⁴	283	-177.67	-128.76	172.81
	293	-179.58	-128.95	
	303	-179.98	-127.62	
	313	-183.14	-129.05	
	323	-184.53	-128.71	

CHAPTER THREE RESULTS AND DISCUSSION

Table 3.33. The thermodynamic functions for corrosion of **2024 Aluminium** in 3.5% NaCl at different concentration of **Amoxicillin** over the temperature range 283 -323 K.

Conc. [M]	T [K]	ΔG [kJ.mol ⁻¹]	ΔH [kJ.mol ⁻¹]	ΔS [J.K ⁻¹ .mol ⁻¹]
0 (Blank)	283	-186.76	-158.74	98.99
	293	-187.51	-158.50	
	303	-188.55	-158.56	
	313	-190.00	-159.01	
	323	-190.46	-158.49	
1.5×10⁻⁴	283	-177.44	-156.06	75.55
	293	-178.16	-156.02	
	303	-178.33	-155.44	
	313	-179.87	-156.22	
	323	-180.36	-155.96	
3×10⁻⁴	283	-178.39	-148.49	105.65
	293	-179.09	-148.13	
	303	-181.05	-149.04	
	313	-181.55	-148.48	
	323	-182.44	-148.32	
4.5×10⁻⁴	283	-179.29	-152.83	93.49
	293	-181.03	-153.63	
	303	-181.55	-153.22	
	313	-182.62	-153.35	
	323	-183.17	-152.97	
6×10⁻⁴	283	-179.23	-154.00	89.15
	293	-179.46	-153.34	
	303	-180.74	-153.72	
	313	-181.72	-153.82	
	323	-182.56	-153.76	
7.5×10⁻⁴	283	-177.29	-135.92	146.18
	293	-179.95	-137.13	
	303	-181.17	-136.88	
	313	-182.30	-136.55	
	323	-183.43	-136.21	

3.1.8 Adsorption Isotherm

The adsorption isotherm can be determined by assuming that inhibition effect is due mainly to the adsorption at a metal solution interface. Basic information on the adsorption of inhibitors on the metal surface can be provided by adsorption isotherm. In order to obtain the isotherm, the fractional surface coverage values (θ) as a function of inhibitor concentration must be obtained. The values of (θ) can be easily determined from the electrochemical measurements by the ratio %IE/100. So it is necessary to determine empirically which isotherm fits best to the adsorption of inhibitors on the aluminium surface. Several adsorption isotherms (viz., Frumkin, Langmuir, Temkin, Freundlich) were tested and the Langmuir adsorption isotherm was found to provide the best description of the adsorption behaviour of these inhibitors. The Langmuir isotherm is given by following equation [90]:

$$\frac{\theta}{1-\theta} = K_{ads}C \quad (3.18)$$

The rearrangement gives the following equation:

$$\frac{C}{\theta} = \frac{1}{K_{ads}} + C \quad (3.19)$$

Where C is the molar concentration of inhibitor, K_{ads} is the equilibrium constant of the adsorption process, and θ is the surface coverage. Plot C/θ versus C yields a straight line (**Figures 3.14. - 3.16**) with regression coefficient, R^2 , almost equal to 1. This suggests that AMP., CEX. and AMOX. in present study obeyed the Langmuir isotherm and there is negligible

CHAPTER THREE RESULTS AND DISCUSSION

interaction between the adsorbed molecules. Free energy of adsorption was calculated using the relation [91]:

$$K_{ads.} = \frac{1}{55.55} e^{\left(\frac{-\Delta G_{ads.}}{RT}\right)} \quad (3.20)$$

Where R is gas constant and T is the absolute temperature. The value 55.55 in the above equation is the concentration of water in solution in mol L⁻¹. The values of $K_{ads.}$ and $\Delta G_{ads.}$ were calculated at temperature range (293-323) K and are listed in **Tables 3.31.- 3.40.**

Thermodynamic parameters were obtained from Gibbs-Helmholtz equation according to this equation [92]:

$$\Delta G_{ads.} = \Delta H_{ads.} - T\Delta S_{ads.} \quad (3.21)$$

Plots of $\Delta G_{ads.}$ vs. T for adsorption of the used compounds on the surface of pure aluminium, 5052 and 2024 Al alloys in 3.5% sodium chloride solution over the temperature range from 283K to 323K are shown in **Figure 3.17.** The data gave straight lines of slope $\Delta S_{ads.}$ and in every temperature $\Delta H_{ads.}$ can be calculated.

The value of $\Delta H_{ads.}$ and $\Delta S_{ads.}$ were calculated and are listed in **Tables 3.34. - 3.36.** The negative values of $\Delta H_{ads.}$ indicates that the adsorption process is an exothermic one. Generally; in an exothermic process, physisorption is distinguished from chemisorption by considering the absolute value of $\Delta H_{ads.}$. For physisorption process, the enthalpy of adsorption is lower than 40 kJ mol⁻¹ while that for chemisorption approaches 100 kJ mol⁻¹ [93]. $\Delta H_{ads.}$ of AMP., CEX. and AMOX. Less than 40 indicate a physical adsorption of these inhibitors on surface. The adsorption of inhibitor molecules is accompanied by positive values of $\Delta S_{ads.}$.

CHAPTER THREE RESULTS AND DISCUSSION

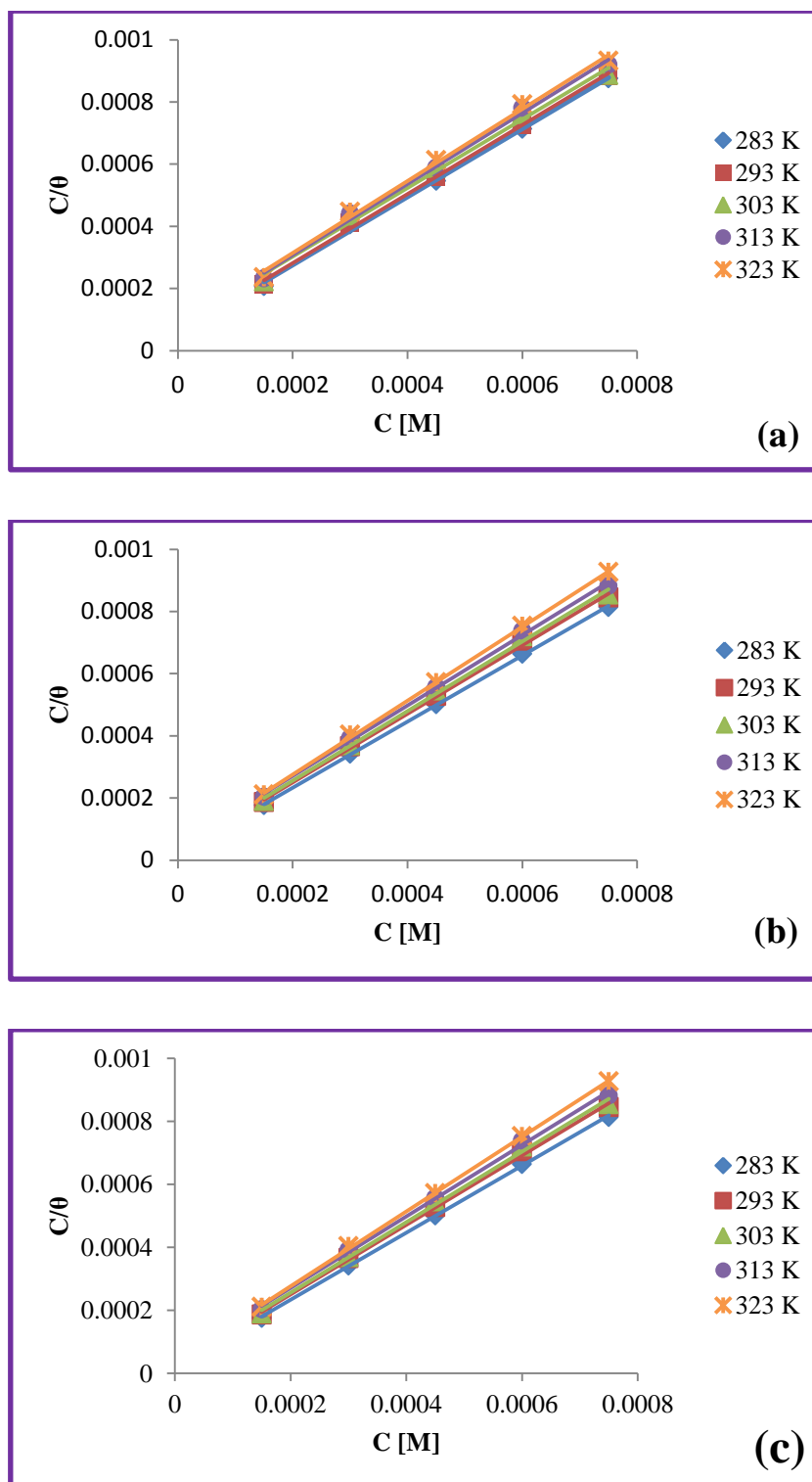


Figure 3.14. Langmuir isotherm plots for the adsorption of (a) Ampicillin (b) Cephalexin (c) Amoxicillin on Pure Aluminium in 3.5% NaCl.

CHAPTER THREE RESULTS AND DISCUSSION

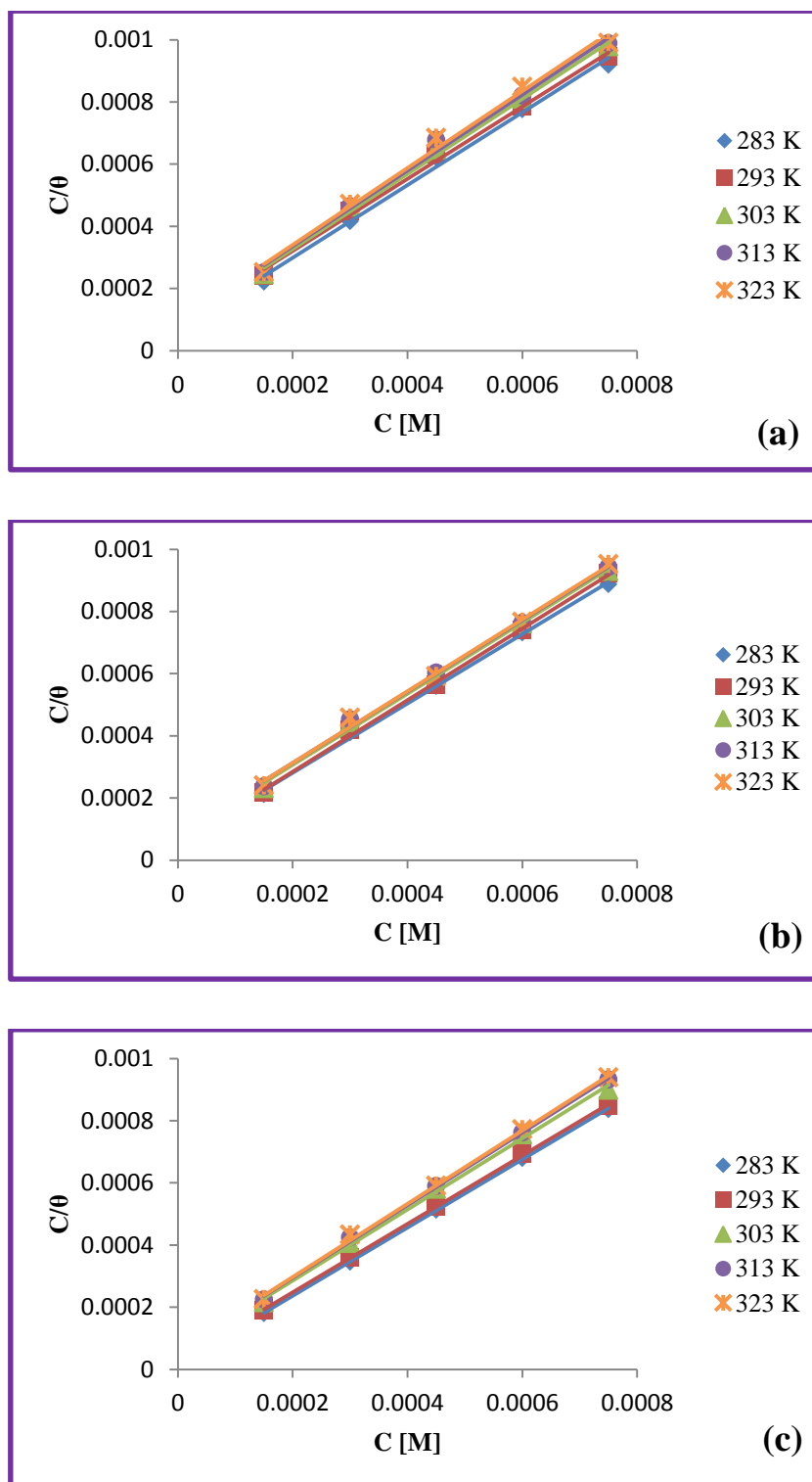


Figure 3.15. Langmuir isotherm plots for the adsorption of (a) **Ampicillin** (b) **Cephalexin** (c) **Amoxicillin** on **5052 Aluminium** in 3.5% NaCl.

CHAPTER THREE RESULTS AND DISCUSSION

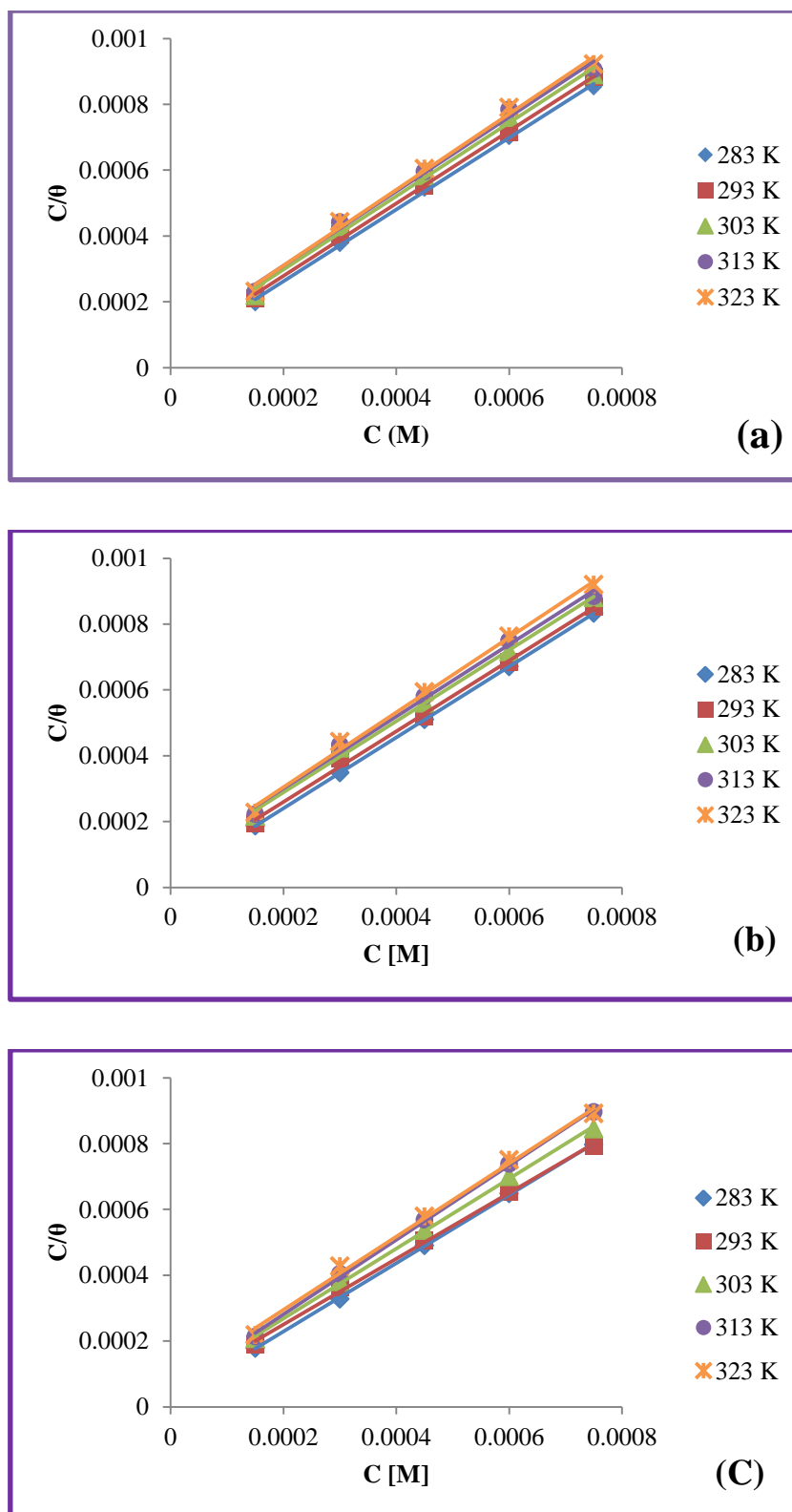


Figure 3.16. Langmuir isotherm plots for the adsorption of (a) **Ampicillin** (b) **Cephalexin** (c) **Amoxicillin** on **2024 Aluminium** in 3.5% NaCl.

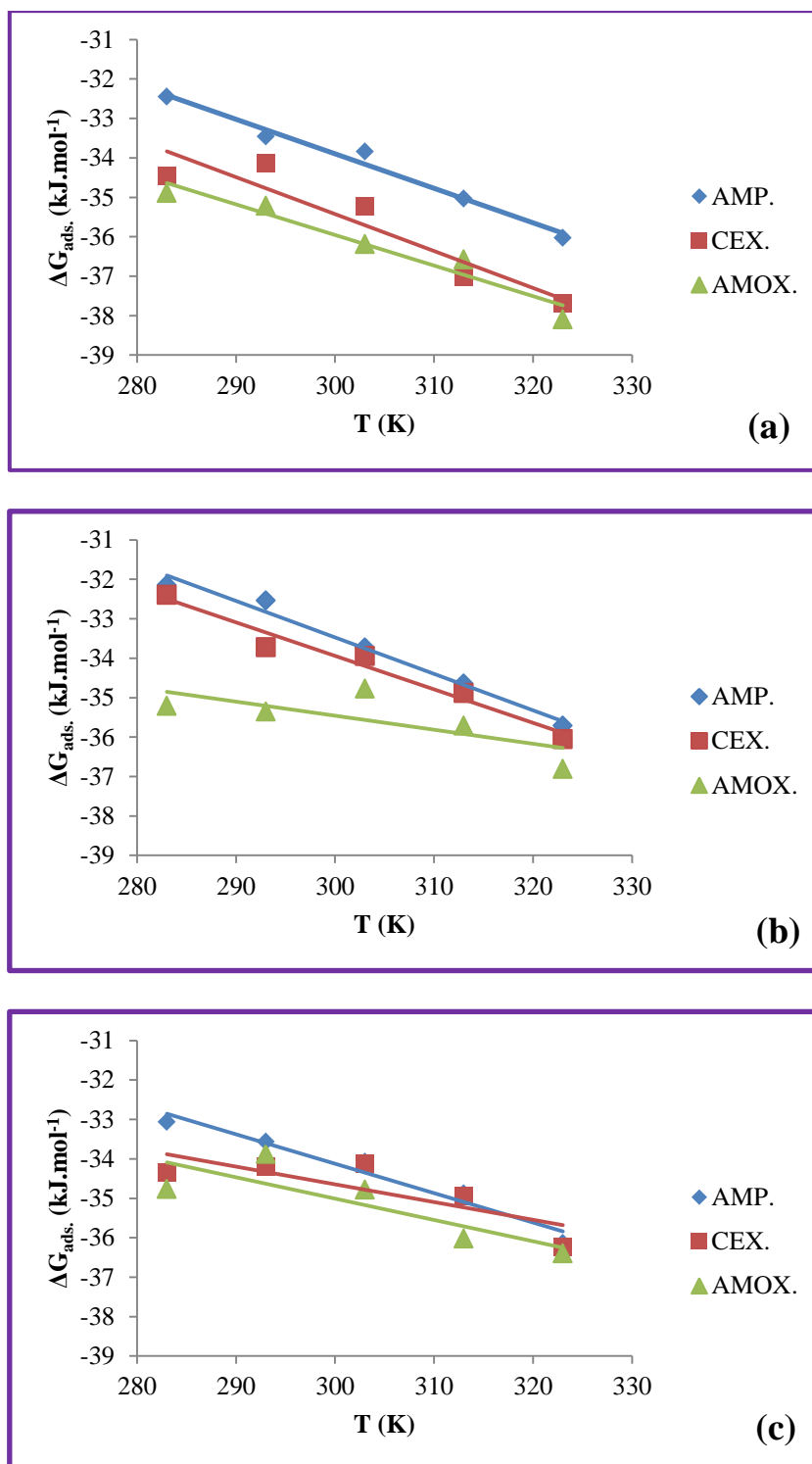


Figure 3.17. The variation of Gibbs free energies (ΔG_{ads}) with temperature for the corrosion of (a) **Pure Aluminium** (b) **5052 Aluminium** (c) **2024 Aluminium** in 3.5% NaCl at absence and presence different Ampicillin, Cephalexin, and Amoxicillin concentrations.

CHAPTER THREE RESULTS AND DISCUSSION

Table 3.34. Thermodynamic parameters for adsorption of the inhibitors on the surface of **Pure Aluminium** in 3.5% NaCl.

Conc. [M]	T [K]	K_{ads} [M^{-1}]	ΔG_{ads} [$kJ.mol^{-1}$]	ΔH_{ads} [$kJ.mol^{-1}$]	ΔS_{ads} [$J.K^{-1}.mol^{-1}$]
AMP.	283	17486.89	-32.44	-7.71	93.53
	293	16570.37	-33.46	-7.85	
	303	12225.85	-33.83	-7.35	
	313	12619.44	-35.03	-7.68	
	323	12036.75	-36.03	-7.80	
CEX.	283	41143.83	-34.46	-7.99	87.40
	293	21834.42	-34.13	-6.73	
	303	21329.91	-35.24	-6.90	
	313	27104.14	-37.02	-7.75	
	323	22344.25	-37.69	-7.48	
AMOX.	283	49411.18	-34.89	-12.90	77.70
	293	34034.33	-35.21	-12.45	
	303	31034.56	-36.18	-12.64	
	313	22835.12	-36.58	-12.26	
	323	21961.82	-38.09	-12.99	

Table 3.35. Thermodynamic parameters for adsorption of the inhibitors on the surface of **5052 Aluminium** in 3.5% NaCl.

Conc. [M]	T [K]	K_{ads} [M^{-1}]	ΔG_{ads} [$kJ.mol^{-1}$]	ΔH_{ads} [$kJ.mol^{-1}$]	ΔS_{ads} [$J.K^{-1}.mol^{-1}$]
AMP.	283	15395.33	-32.14	-6.01	92.351
	293	11335.53	-32.53	-5.47	
	303	11706.10	-33.73	-5.74	
	313	10853.38	-34.64	-5.74	
	323	10690.63	-35.71	-5.88	
CEX.	283	17086.99	-32.39	-8.38	84.83
	293	18449.75	-33.72	-8.87	
	303	12747.17	-33.94	-8.24	
	313	11913.37	-34.88	-8.33	
	323	12139.44	-36.05	-8.65	
AMOX.	283	56491.77	-35.20	-25.13	35.607
	293	35963.78	-35.35	-24.91	
	303	17733.63	-34.77	-23.98	
	313	16347.86	-35.71	-24.56	
	323	16075.15	-36.80	-25.30	

CHAPTER THREE RESULTS AND DISCUSSION

Table 3.36. Thermodynamic parameters for adsorption of the inhibitors on the surface of **2024 Aluminium** in 3.5% NaCl.

Conc. [M]	T [K]	K_{ads} [M^{-1}]	ΔG_{ads} [$kJ.mol^{-1}$]	ΔH_{ads} [$kJ.mol^{-1}$]	ΔS_{ads} [$J.K^{-1}.mol^{-1}$]
AMP.	283	22776.21	-33.07	-11.95	74.603
	293	17324.67	-33.57	-11.71	
	303	13456.35	-34.08	-11.47	
	313	11910.50	-34.80	-12.79	
	323	12547.11	-35.14	-10.79	
CEX.	283	39538.73	-34.36	-19.46	54.106
	293	22502.51	-34.20	-18.03	
	303	13724.07	-34.13	-18.39	
	313	12274.95	-34.96	-19.09	
	323	12995.56	-36.23	-18.93	
AMOX.	283	47056.83	-34.77	-21.64	33.94
	293	19690.63	-33.88	-21.04	
	303	17833.95	-34.79	-20.51	
	313	18494.86	-36.03	-20.89	
	323	13853.37	-36.40	-21.72	

The negative value of the free energy of adsorption indicate a spontaneous adsorption process, on the other hand; the high values of the adsorption constant indicate strong adsorption of these inhibitors on pure aluminium, 5052 Al and 2024 Al. Generally, the values of ΔG_{ads} . around -20 kJ mol^{-1} or less negative are consistent with electrostatic interaction (physisorption), while those -40 kJ mol^{-1} and more negative involve electron transfer to form chemical bond (chemisorptions) [94]. The calculated value of ΔG_{ads} . was around (-36 KJ mol^{-1}) which is consistent with the spontaneity of the adsorption process of inhibitors and the stability of the adsorbed layer on the surfaces. The later value is negatively less than the threshold value of -40 KJ.mol^{-1} , which is required for chemical adsorption. The value of ΔG_{ads} . obtained in this work indicates that the adsorption of inhibitors is not merely physisorption nor chemisorption. Therefore, this value of ΔG_{ads} . confirms that

CHAPTER THREE RESULTS AND DISCUSSION

the adsorption of inhibitors is not a simple physisorption but it may involve some other interactions [95]. Thus, the mechanism of corrosion inhibition of pure aluminium, 5052 and 2024 Al alloys in saline aqueous solution by AMP., CEX. and AMOX. could be explained on the basis of adsorption on the metal surface. Physisorption originates from electrostatic interactions of charged molecules with positively charged surface metal while chemisorption involves donor–acceptor interactions between π electrons of aromatic molecules and free electron pairs of heteroatoms (N, S, and O) and vacant d-orbitals of metal atoms to form coordinate type bond [88]. Therefore, the nature of interactions between the metal and inhibitors molecules are physisorption and chemisorption adsorption or mixed mode of adsorption may occur.

3.2 Theoretical calculations

Some quantum chemical parameters, which influence the electronic interactions between atoms at the surface and inhibitor such as total energy (TE), the energy of the highest occupied molecular orbital (E_{HOMO}), the energy of the lowest unoccupied molecular orbital (E_{LUMO}), the energy gap between E_{LUMO} - E_{HOMO} (ΔE_{gap}), dipole moment (μ), the fractional of electron transferred from the molecule to the surface (ΔN), and the partial charge for the individual atoms in AMP., CEX., and AMOX. Molecules. These theoretical parameters provide information about the reactive behaviour of used inhibitor molecules. The calculated results for these parameters were listed in **Tables 3.37.**, and (**3.38. - 3.40.**) plus **Figures (3.18. - 3.21.)**.

CHAPTER THREE RESULTS AND DISCUSSION

Table 3.37. The calculated quantum chemical parameters of the studied compounds.

Compound	TE (kJ/mol)	E _{HOMO} (eV)	E _{LUMO} (eV)	ΔE _{gap} (eV)	μ (Debye)	ΔN
AMP.	-40379.906	-6.0145	-2.8588	3.1557	4.2155	0.3824
CEX.	-40344.091	-5.6630	-3.2575	2.4054	8.0794	0.5114
AMOX.	-42404.288	-5.5114	-3.3546	2.1568	8.7244	0.5578

The energy of the highest occupied molecular orbital (HOMO), is measure the electron donating ability of a molecule, and explain the adsorption characteristics on the metallic surface [96]. A high value of E_{HOMO} indicate the tendency of molecule to donate electrons to appropriate acceptor molecules with low-energy (empty molecular orbital). Increasing the values of E_{HOMO} facilitate adsorption (and therefore inhibition) by influencing the transport process through the adsorbed layer [97]. It is evident from **Table 3.37.**, that the E_{HOMO} of these inhibitor compounds increased in the following order:

$$\text{AMOX.} > \text{CEX.} > \text{AMP.}$$

While, The energy of the E_{LUMO} indicates the ability of the inhibitor molecule to accept electrons from metal leading to formation of feedback bond. The lower the value of E_{LUMO}, the more probable to the molecule accept electrons. The E_{LUMO} of the three molecules under study decreased in the following order:

$$\text{AMP.} < \text{CEX.} < \text{AMOX.}$$

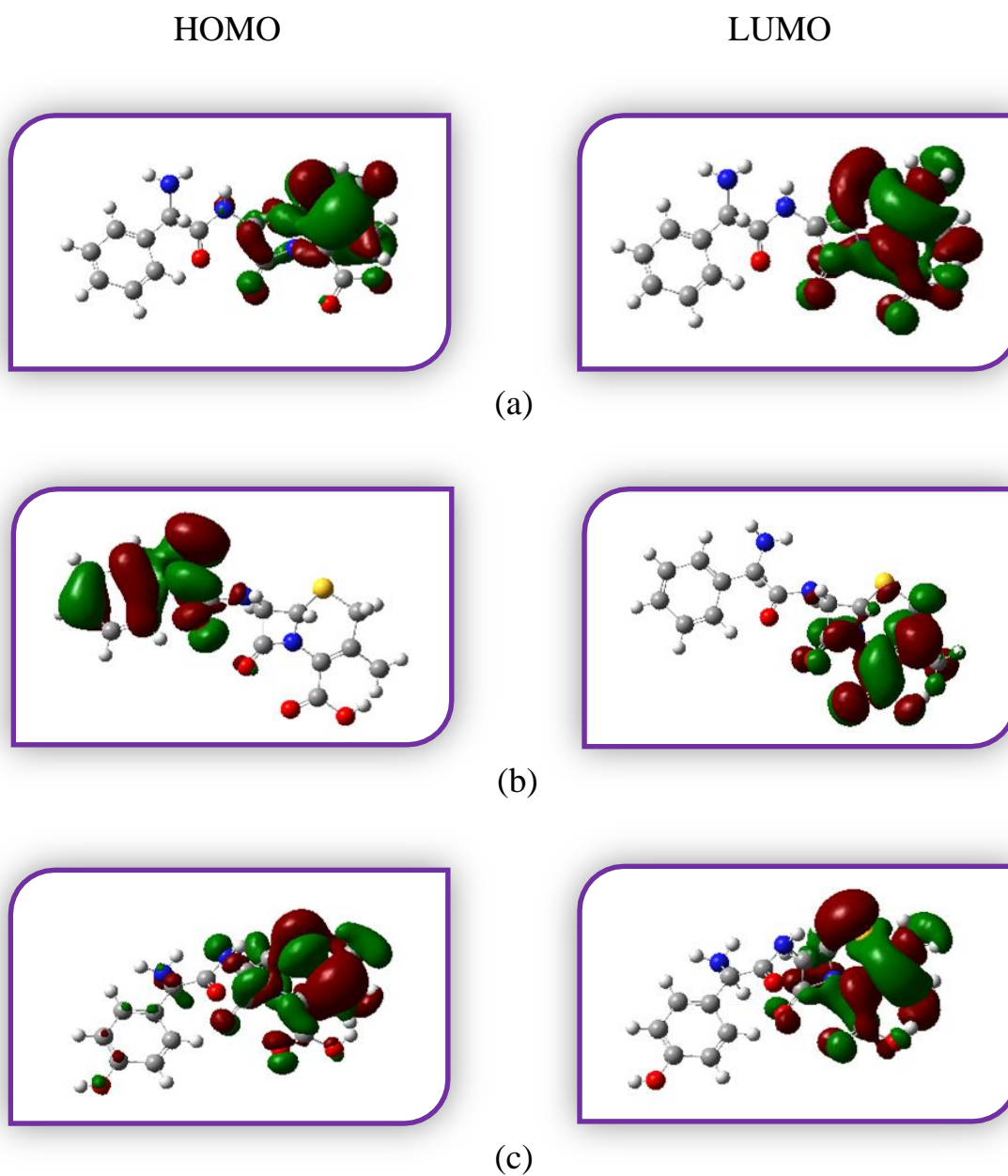


Figure 3.18. The frontier molecular orbital density distributions as calculated by DFT method for (a) Ampicillin (b) Cephalexin (c) Amoxicillin

CHAPTER THREE RESULTS AND DISCUSSION

The analysis of **Figure 3.18.** shows that the distribution of the two energies HOMO and LUMO the localized levels at the five ring for ampicillin and amoxicillin. While, for cephalexin the HOMO is located at the aromatic rings. But the LUMO located on the other side of the molecule at the six membered ring (especially at two $-\text{CH}_3$ and $-\text{COOH}$ groups).

The lower results of the energy difference ΔE_{gap} ($E_{\text{LUMO}} - E_{\text{HOMO}}$) will cause higher inhibition efficiency, because energy required to remove an electron from the last occupied orbital will be low. According to the calculated results, AMOX. has the higher inhibition efficiency than CEX. and AMP. consecutively [98].

The dipole moment (μ) is another indicator of the electronic distribution in a molecule, and is one of the properties used to discuss and rationalize the structure [99]. The higher value of (μ) for AMOX. can be attributed to the higher inhibition efficiency of this compound, compared with AMP. and CEX. (8.7244, 8.0794 and 4.2155 Debye) respectively [all of them are higher than that of the solvent H_2O ($\mu = 1.85$ Debye)]. The large value of the dipole moment probably increases the adsorption between chemical compound and metal surface [100]. Accordingly, the adsorption of AMOX. and other inhibitors molecules from the aqueous solution can be regarded as aquasi-substitution process between the inhibitor compounds in the aqueous phase [$\text{Inh.}_{(\text{aq})}$] and water molecules at the electrode surface [$\text{H}_2\text{O}_{(\text{ads})}$].

In order to calculate the fraction of electrons transferred we use equation (1.44), a theoretical value for the electronegativity of bulk aluminium was used, $\chi_{\text{Al}} \approx 3.23$ eV, and a global hardness of $\eta_{\text{Al}} \approx 0$, by assuming that for a metallic bulk $I = A$ because they are softer than the neutral metallic atoms. The data of the fractional number of electrons transferred ΔN between the surface

CHAPTER THREE RESULTS AND DISCUSSION

and the adsorbed species show inhibition effect resulted from electrons donation. According to Lukovits's study [101], if $\Delta N < 3.6$, the inhibition efficiency increases with increasing electron-donating ability.

In this study, the examined inhibitors are electron donors with varying degrees, and the aluminium surface was the acceptor. Thereby the binding compounds to the aluminium surface, resulting in inhibition adsorption layer against corrosion. The higher the values of ΔN , the higher the inhibition efficiency %IE, and hence the better the compound as inhibitor, in the following order:



The calculated Mulliken charges of the atoms for all studied molecules are presented in **Tables 3.38. - 3.40.** It can be readily observed that N, O and phenyl carbon atoms are negatively charged, so it can be adsorbed on the metal surface, through the donor - acceptor type interaction [102]. The result indicates that all the nitrogen atoms present a considerable excess negative charge, and also around carbon atoms of the aromatic rings. Similar indication can be made for the oxygen atoms. Therefore, we conclude that AMP., CEX. and AMOX. molecules can be adsorbed on the aluminium surface using these active centers (N and O) leading to corrosion inhibition.

CHAPTER THREE RESULTS AND DISCUSSION

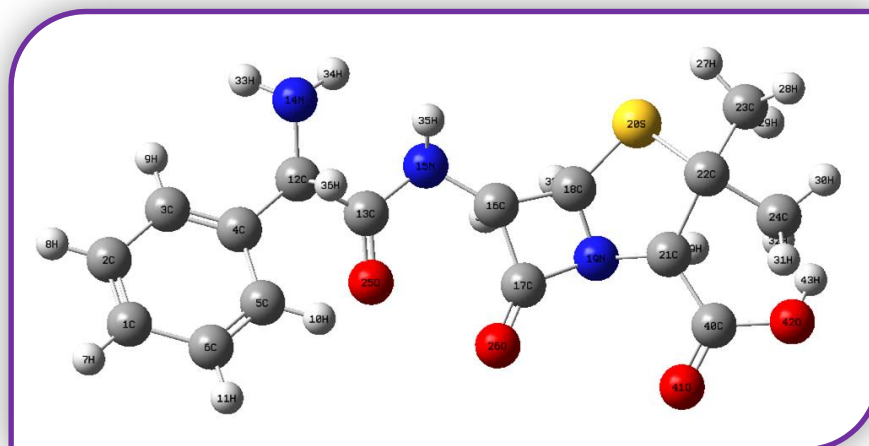


Figure 3.19. The structure of ampicillin.

Table 3.38. Mulliken atomic charges results of **Ampicillin** molecule.

Atomic number	Atomic symbol	Atomic charge	Atomic number	Atomic symbol	Atomic charge
1	C	-0.115992	23	C	-0.546174
2	C	-0.124753	24	C	-0.787662
3	C	-0.178608	25	O	-0.417618
4	C	0.123754	26	O	-0.346775
5	C	-0.086832	27	H	0.216268
6	C	-0.141251	28	H	0.189117
7	H	0.124909	29	H	0.187911
8	H	0.124390	30	H	0.200919
9	H	0.111052	31	H	0.331888
10	H	0.163763	32	H	0.136890
11	H	0.133037	33	H	0.295023
12	C	-0.203686	34	H	0.275434
13	C	0.456977	35	H	0.308424
14	N	-0.683024	36	H	0.288570
15	N	-0.614178	37	H	0.292161
16	C	-0.087882	38	H	0.273744
17	C	0.459042	39	H	0.247124
18	C	-0.371257	40	C	0.484491
19	N	-0.450078	41	O	-0.353757
20	S	0.439111	42	O	-0.491465
21	C	-0.095695	43	H	0.389081
22	C	-0.156389			

CHAPTER THREE RESULTS AND DISCUSSION

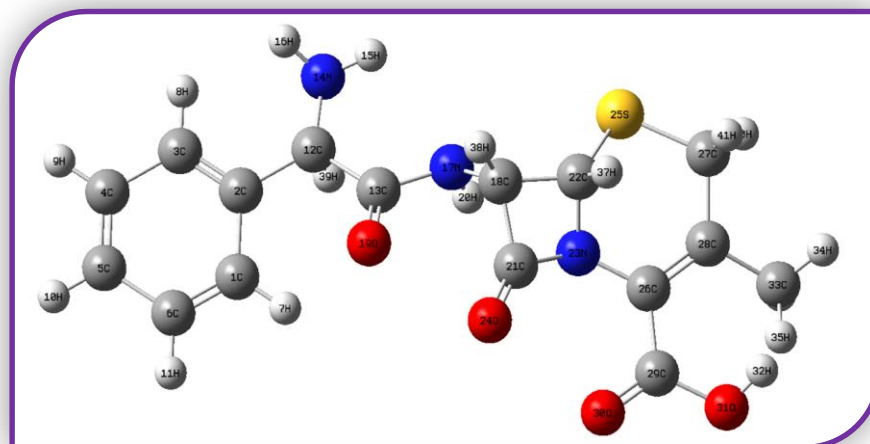


Figure 3.20. The structure of cephalixin.

Table 3.39. Mulliken atomic charges results of **Cephalexin** molecule.

Atomic number	Atomic symbol	Atomic charge	Atomic number	Atomic symbol	Atomic charge
1	C	-0.096661	22	C	-0.335764
2	C	0.108114	23	N	-0.506933
3	C	-0.191617	24	O	-0.352565
4	C	-0.123021	25	S	0.385254
5	C	-0.118855	26	C	0.222711
6	C	-0.137522	27	C	-0.574655
7	H	0.161137	28	C	0.060145
8	H	0.114293	29	C	0.492198
9	H	0.122872	30	O	-0.360292
10	H	0.121714	31	O	-0.525351
11	H	0.129706	32	H	0.365501
12	C	-0.138781	33	C	-0.437698
13	C	0.366278	34	H	0.156293
14	N	-0.682111	35	H	0.064335
15	H	0.300721	36	H	0.202102
16	H	0.283853	37	H	0.206468
17	N	-0.547033	38	H	0.190814
18	C	-0.033501	39	H	0.274286
19	O	-0.388112	40	H	0.199099
20	H	0.330969	41	H	0.206124
21	C	0.485487			

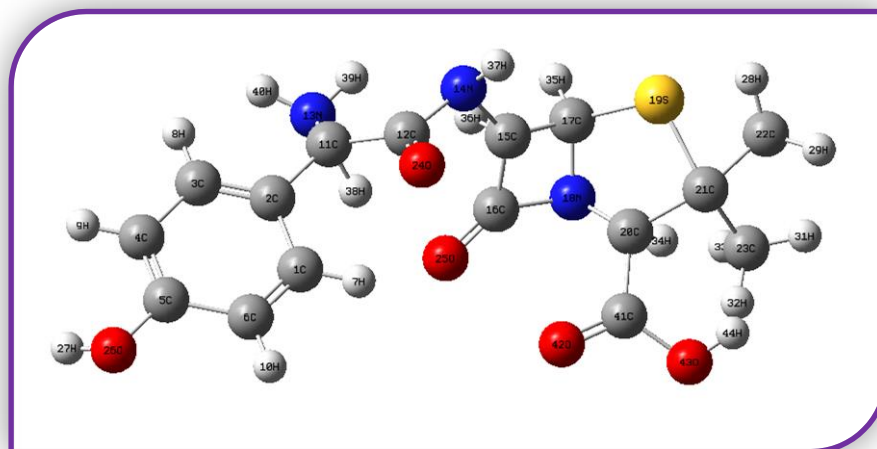


Figure 3.21. The structure of amoxicillin

Table 3.40. Mulliken atomic charges results of Amoxicillin molecule.

Atomic number	Atomic symbol	Atomic charge	Atomic number	Atomic symbol	Atomic charge
1	C	-0.083428	23	C	-0.527603
2	C	0.124326	24	O	-0.401066
3	C	-0.175235	25	O	-0.367347
4	C	-0.171778	26	O	-0.630833
5	C	0.274090	27	H	0.367992
6	C	-0.121629	28	H	0.222354
7	H	0.169304	29	H	0.182703
8	H	0.113545	30	H	0.200867
9	H	0.114894	31	H	0.166396
10	H	0.144308	32	H	0.098343
11	C	-0.187691	33	H	0.218151
12	C	0.368337	34	H	0.266021
13	N	-0.688479	35	H	0.230997
14	N	-0.607430	36	H	0.262769
15	C	-0.016530	37	H	0.329180
16	C	0.447951	38	H	0.320163
17	C	-0.402277	39	H	0.292711
18	N	-0.383695	40	H	0.288263
19	S	0.469138	41	C	0.545027
20	C	-0.221916	42	O	-0.355891
21	C	-0.220673	43	O	-0.464948
22	C	-0.540176	44	H	0.350796

CHAPTER THREE RESULTS AND DISCUSSION

3.3 Scanning electron microscopy

Scanning electron microscopy of the pure aluminium samples after potentiostatic examination is presented in **Figure 3.22**. The SEM study shows that the inhibited alloy surface is found smoother than the uninhibited surface. **Figure 3.22. (c)** illustrates that there was much less damage on the aluminium surface in the presence of $7.5 \times 10^{-4} \text{M}$ of AMP., Accordingly, it concluded that the adsorption film was able to efficiently retard the corrosion of the pure aluminium.

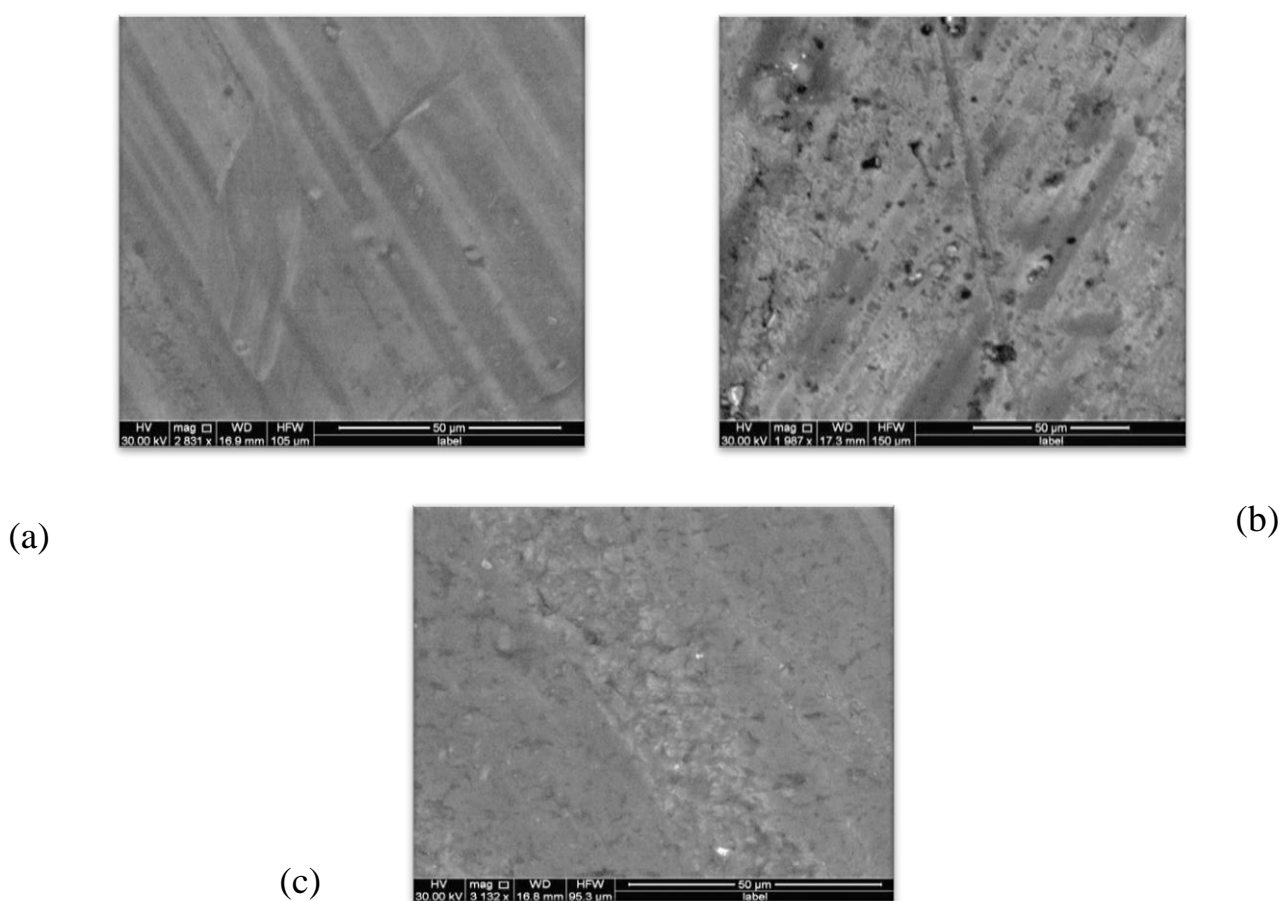





Figure 3.22. Scanning electron micrographs of (a) Polished **Aluminium** specimen, (b) In 3.5% NaCl, (c) in the presence of $7.5 \times 10^{-4} \text{M}$ **Ampicillin**.



CHAPTER FOUR
CONCLUSIONS
AND
FURTHER
SUGGESTIONS

4.1 Conclusions

The corrosion behaviour of pure aluminium and of two of its alloys has been investigated in the saline medium over temperatures ranging from 283 to 323K. Certain conclusions can be derived from the results and discussion are summarized in the following listed points:

- 1) At constant temperature the corrosion resistance of pure aluminium and its alloys in the sodium chloride solution may be summarized in terms of increasing corrosion current density according to the following sequence:

Pure Al > 5052 alloy > 2024 alloy

- 2) In the presence of inhibitors (ampicillin, cephalexin and amoxicillin) corrosion rate decreased, and the higher inhibition efficiency achieved by amoxicillin, respectively cephalexin, and ampicillin.

AMOX. > CEX. > AMP.

- 3) The inhibition efficiency increases with increasing the concentration of inhibitors. This means that inhibitors act as an adsorption inhibitor for the corrosion of pure aluminium and its alloys under study in 3.5% NaCl solution.
- 4) The inhibition efficiency of AMP, CEX. and AMOX. decrease with increase the temperature. This mean these inhibitors are physical adsorbed on the surface.
- 5) It is clear that 7.5×10^{-4} M of AMP, CEX. and AMOX. lead to the lowest corrosion and penetration rate at 283K.

- 6) According to corrosion potential AMP, CEX. and AMOX. act as mixed type inhibitors in 3.5% NaCl.
- 7) The kinetic data reveal that the activation energies which were relatively higher than that obtained in the absence of the inhibitors. Thus, the presences of inhibitors shift the corrosion to surface site because E_a is higher than the normal energy of activation in the absence of AMP, CEX. and AMOX..
- 8) The kinetic data show that the adsorption of AMP, CEX. and AMOX. on the surface is physical adsorption type.
- 9) The thermodynamic data demonstrate that values of ΔG were negative in the absence and presence of the inhibitors. The negative values of ΔG indicate that the process is feasible and spontaneous in nature.
- 10) The thermodynamic results reflect that the dissolution of pure aluminium, 5052 aluminium and 2024 aluminium in 3.5% NaCl is an exothermic process.
- 11) The values of ΔS were generally positive due to the negativity of ΔG , the positive values mean that the adsorption processes accompanied by an increase in entropy for the adsorption of inhibitor onto the surface, this suggest that metal ions replace some water molecules from solution previously adsorbed on the surface of the adsorbent. These displaced molecules gain more translation entropy than that lost by the adsorbate ions, which allowing the prevalence of randomness in the system.
- 12) Adsorption data lead that, the adsorption processes for all inhibitors obey Langmuir isotherm type.

- 13) The relationship between the experimental efficiency of inhibition of AMP, CEX. and AMOX. and the E_{HOMO} , E_{LUMO} , ΔE_{gap} ($E_{\text{LUMO}} - E_{\text{HOMO}}$) plus ΔN which calculated by DFT method are in conformity with each other. While the AMOX. acts as the best inhibitor than CEX. and AMP. respectively.
- 14) Quantum chemical calculation revealed that the adsorption of AMP, CEX. and AMOX. on surface may be concentrated around the nitrogen and oxygen atoms as active centers.

4.2 *Suggestions for Further Research*

It is worthwhile to forward several suggestions for the extension of the present work in the future:

- 1) The present work has concentrated only on the effect of NaCl on corrosion for pure aluminium and two of its alloys. In order to draw more general conclusions on corrosion and protection of aluminium, it is necessary to study another media like basic, acidic media.
- 2) There is possibility for increasing the protection efficiencies by using other inhibitors; organic or inorganic compounds in saline, acidic or basic media.
- 3) Study the effect of environmental pollution, and industrial product on the corrosion of alloys.
- 4) There is possibility to used natural plants as corrosion inhibitors for alloys.

- 5) There is possibility to make theoretical study for the different organic and inorganic compounds structure before used, which can be suggested there protection mechanism.



REFERENCES



References

- [1] V. S. Sastri, E. Ghali and M. Elboudjaini, “Corrosion Prevention and Protection Practical Solutions”, 1st. ed., John Wiley and Sons, (2007).
- [2] V. Cicek and B. Al-Numan, “Corrosion Chemistry”, 1st. ed., Scrivener Publishing, (2011).
- [3] V. Cicek, “Cathodic Protection Industrial Solutions for Protecting Against Corrosion”, 1st. ed., Scrivener Publishing, (2013).
- [4] M. Schütze, “Corrosion and Environmental Degradation”, R. W. Cahn, P. Haasen and E. J. Kramer (Ed.), 1st. ed., Wiley-VCH, (2000).
- [5] “Green Corrosion Chemistry and Engineering_ Opportunities and Challenges”, S. K. Sharma (Ed.), 1st. ed., Wiley-VCH Verlag and Co. KGaA, Germany, (2011).
- [6] M. G. Fontana, “Corrosion Engineering”, 3rd. ed., McGraw–Hill book Company, New York, (1986).
- [7] [HSC Online - Corrosion: Public enemy](#)
- [8] C. Wagner and Traud, “Concerning the evaluation of corrosion reactions by superposition of electrochemical partial reactions concerning the potential formation on mixed electrodes”, Z. Electrochem., 44, pp.391, (1938).
- [9] E. McCafferty, “Introduction to Corrosion Science”, Springer Science and Business Media, (2010).

REFERENCES

- [10] L.L. Shrier, R.A. Jarman and G.T. Burstein, “Corrosion Control”, Vol.2, 3rd ed., Butterworth-Heinemann, Oxford, BO, (1994).
- [11] M. Stern and A. L. Grary, “Electrochemical Polarization: I. A Theoretical Analysis of the Shape of Polarization Curves”, J. Electrochem Soc.,104, 56-63, (1957).
- [12] Y. Ahmed, “Protection of Aluminum Alloy (AA7075) from Corrosion by Sol-Gel Technique”, Ph.D. Thesis, Faculty of Science, chemnitz university of technology, (2012).
- [13] “Metal Handbook”, J. R. Davis (Ed.), 2nd. ed., ASM International, (1998).
- [14] C. Vargel, M. Jacques, and M. P. Schmidt, “Corrosion of Aluminium”, 1st. ed., Elsevier, (2004).
- [15] L. Paussa, “Thin ZrO₂-Based SOL-GEL Films For The Protection Of Aluminum Alloys: Barrier, Adhesion And Inhibition Abilities”, Ph.D. Thesis, Department Chemical Processes Engineering, University of Padova, (2011).
- [16] “Corrosion of Aluminum and Aluminum Alloys”, J. R. Davis (Ed.), 1st. ed. ASM International, (1999).
- [17] M. Pourbaix, “Atlas of electrochemical equilibrium in aqueous solutions, National Association of Corrosion Engineers”, Houston, TX, (1974).

REFERENCES

- [18] L. L. Shreir, G. T. Burstein, R. A. Jarman, “Corrosion: Metal - Environment reactions”, Vol.1, 3rd. ed., Butterworth-Heinemann, Oxford, BO, (1994).
- [19] K. M. Abu Al-Naja, “Acidic Corrosion of Aluminium and Iron Metals and its Inhibition Using Some Mono and Bisazo Dyes Derived from Dihydroxynaphthalene” , M.Sc. Thesis, Chemistry Department, Umm Al-Qura University, Kingdom of Saudi Arabia, (2009).
- [20] “Springer Handbook of Materials Measurement Methods”, H. Czichos, T. Saito, L. Smith (Ed.), 1st. ed., Springer Science & Business Media, (2006).
- [21] “Corrosion Mechanisms in Theory and Practice”, P. Marcus (Ed.), 2nd. ed., P. Marcus and J. Oudar, (2002).
- [22] “Introduction to the Fundamentals of Corrosion, Corrosion: Fundamentals, Testing, and Protection”, S. D. Cramer, B. S. Covino, Jr (Ed.), Vol 13A, ASM Handbook, ASM International, (2003).
- [23] R. W. Revie, H. H. Uhlig, “Corrosion and Corrosion Control” 4th. ed., John Wiley and Sons,(2008).
- [24] “Uhlig's Corrosion Handbook”, R. W. Revie (Ed.), 2nd. ed., John Wiley and Sons, Canada, (2000).
- [25] S. A. Bradford , “Corrosion Control”, 1st. ed., Van Nostrand Reinhold, (1993)
- [26] S. A. Bradford, “Corrosion Control”, 2nd. ed., CASTI Pub., (2001).

REFERENCES

- [27] D. Jones, “Principles and Prevention of Corrosion”, 2nd. ed., Prentice Hall, Inc., NJ, (1996).
- [28] “Corrosion mechanisms in theory and practice”, P. Marcus (Ed.), 3rd. ed., CRC Press, (2011).
- [29] E. Ghali, “Corrosion Resistance of Aluminum and Magnesium Alloys: Understanding, Performance, and Testing”, John Wiley and Sons, (2010).
- [30] B. Einar, “Corrosion and protection—Engineering materials and Processes”, Springer-Verlag London Limited, Vol.1, (2004).
- [31] A. Groysman, “Corrosion for Everybody”, Springer Science & Business Media, (2010).
- [32] “ASM Hand Book”, T.L. Yau ,R. C. Sutherlin , A. W. Chang (Ed.), ASM International Handbook Committee, vol. 13 B. ,(2005).
- [33] “Corrosion: Understanding the Basics”, J. R. Davis (Ed.), ASM International, (2000).
- [34] P. A. Schweitzer, “Corrosion of Linings & Coatings: Cathodic and Inhibitor Protection and Corrosion Monitoring”, 2nd. ed., (2006).
- [35] P. R. Roberge, “Handbook of Corrosion Engineering”, McGraw-Hill Companies, New York, (2000).
- [36] “Developments in Corrosion Protection”, M. Aliofkhazraei (Ed.), InTech, (2014).

- [37] D. Landolt, “Corrosion and Surface Chemistry of Metals”, 1st. ed., EPFL Press, (2007).
- [38] P. A. Schweitzer, “Fundamentals of Corrosion: Mechanisms, Causes, and Preventative Methods”, CRC Press, (2009).
- [39] A. Singh, A. Kumar Singh and M. A. Quraishi, “Dapsone: A Novel Corrosion Inhibitor for Mild Steel in Acid Media”, *Open Electrochem J*, 2, 43-51, (2010).
- [40] V. S. Sastri, “Green Corrosion Inhibitors”, John Wiley and Sons, (2011).
- [41] G. Gece, “Drugs: A review of promising novel corrosion inhibitors”, *Corrosion Science*, 53, 3873–3898, (2011).
- [42] A.A. Siaka, N.O. Eddy, S.O. Idris, A. Muhammad, C. M. Elinge, and F.A. Atiku, FTIR Spectroscopic Information on the Corrosion Inhibition Potentials of Ampicillin in HCl Solution, *Innovations in Science and Engineering*, 2, 41-48, (2012).
- [43] E. E. Ebenso, T. Arslan, F. Kandemirli, I. Love, C. Oğretir, M. Saracoglu, S. A. Umoren, “Theoretical Studies of Some Sulphonamides as Corrosion Inhibitors for Mild Steel in Acidic Medium”, *Int. J. Quantum Chem*, 110, 2614–2636,(2010).
- [44] E.E. Ebenso, N.O. Eddy, A.O. Odiongenyi, “Corrosion Inhibition and Adsorption Properties of Methocarbamol on Mild Steel in Acidic Medium”, *Portugaliae Electrochimica Acta*, 27, 13–22, (2009).

- [45] N. O. Eddy and E. E. Ebenso, "Corrosion Inhibition and Adsorption Characteristics of Tarivid on Mild Steel in H_2SO_4 ", *E-JChem.*, 7, S442-S448,(2010).
- [46] A. S. Raja, S. Rajendran, J. Sathiyabama, T.S. muthumegala, A.krishnaveni, N.P alaniswamy, P. Prabhakar, Corrosion inhibition by arginine – Zn^{2+} system, *Zaštita materijala*, 52, 101-108, (2011).
- [47] S.A. Odoemelam, N.O. Eddy, Sparfloxacin and norfloxacin as corrosion inhibitors for mild steel: Kinetics, thermodynamics and adsorption consideration, *J. Mater Sci*, 4, 1-5,(2008).
- [48] M. Abdallah, Rhodanine azosulpha drugs as corrosion inhibitors for corrosion of 304 stainless steel in hydrochloric acid solution, *Corros Sci.*, 44, 717-728,(2002).
- [49] W.T. Sing, C.L. Lee, S.L. Yeo, S.P. Lim, M.M. Sim, Arylalkylidene rhodanine with bulky and hydrophobic functional group as selective HCV NS3 protease inhibitor, *Bioorg Med Chem Lett*, 11, 91-94, (2001).
- [50] A. El-Dissouky, A.A. El-Bindary, A.Z. El-Soubati, A.S. Hilali, "Structural and models of dioxouranium(VI) with rhodanine azodyes-V", *Spectrochim Acta A*, 57, 1163-1170, (2001).
- [51] G. Gece, "The use of quantum chemical methods in corrosion inhibitor studies", *Corros. Sci.*, 50, 2981–2992, (2008).
- [52] D. C. Young,. "Computational Chemistry: A Practical Guide for Applying Techniques to Real-World Problems", John Wiley & Sons, Inc,(2001).

- [53] N. O. Eddy, E. E. Ebenso and U. J. Ibok, “Adsorption, synergistic inhibitive effect and quantum chemical studies of ampicillin (AMP) and halides for the corrosion of mild steel in H₂SO₄”, *J Appl Electrochem.*, 40, 445-456, (2010).
- [54] D. B. Hmamou, R. Salghi, H. Zarrok, A. Zarrouk, B. Hammouti, M. El Hezzat and M. Bouachrine, “Temperature Effects on the Corrosion Inhibition of Carbon Steel in Acidic Solutions by Alizarin Red”, *Advances in Materials and Corrosion*, 2, 36-42, (2012).
- [55] H. Gerengia, H. Goksua, P. Slepiskib, “The Inhibition Effect of Mad Honey on Corrosion of 2007-Type Aluminium Alloy in 3.5% NaCl Solution”, *Materials Research*, 17, 255-264, (2014).
- [56] P. A. Popoola, S. Omotayo, C. A. Loto, O. M. Popoola, “Inhibitive Action of Ferrous Gluconate on Aluminum Alloy in Saline Environment”, *Advances in Materials Science and Engineering*, 8 pages, (2013).
- [57] S. Chen, Tapas Kar, “Theoretical Investigation of Inhibition Efficiencies of Some Schiff Bases as Corrosion Inhibitors of Aluminum”, *Int. J. Electrochem. Sci.*, 7, 6265 – 6275, (2012).
- [58] A. Singh, Y. Lin, W. Liu, J. Pan, C. Ren, D. Zeng, S. Yu, “Berberine as an Effective Corrosion Inhibitor for 7075 Aluminium Alloy in 3.5% NaCl Solution”, *Int. J. Electrochem. Sci.*, 9, 5164 – 5176, (2014).
- [59] E. M. Sherif, “Corrosion and Corrosion Inhibition of Aluminum in Arabian Gulf Seawater and Sodium Chloride Solutions by 3-Amino-5-

- Mercapto-1,2,4-Triazole”, *Int. J. Electrochem. Sci.*, 6, 1479 – 1492, (2011).
- [60] H. Shi, E. H. Han, F. Liu, “Corrosion protection of aluminium alloy 2024-T3 in 0.05 M NaCl by cerium cinnamate”, *Corrosion Science*, 53, 2374–2384, (2011).
- [61] E.M. Sherif, Su-Moon Park, “Effects of 1,4-naphthoquinone on aluminum corrosion in 0.50 M sodium chloride solutions”, *Electrochimica Acta*, 51,1313–1321, (2006)
- [62] N. Perez., “*Electrochemistry and Corrosion Science*”, 1st. ed. Kluwer Academic Publishers Boston , (2004).
- [63] “*Uhlig's Corrosion Handbook*”, R. W. Revie (Ed.), 3rd. ed., John Wiley and Sons, 2011.
- [64] [Calomel electrode @ Chemistry Diction](#)
- [65] J. C. Scully, “*The fundamentals of corrosion*”, 3rd. ed., pergamon press, Oxford, New York, (1990).
- [66] H. H. Uhlig, *Corrosion and Corrosion control*, 2nd. ed., McGraw - Hill book Company, New York, (1987).
- [67] M. T. Frisch, G. W. Trucks and H. B. Schlegel, *Gaussian 09*, Gaussian, Pittsburgh, Pa, USA, (2009).
- [68] “*Modern Electrochemical Methods in Nano, Surface and Corrosion Science*”, M. Aliofkhazraei (Ed.), InTech, (2014).
- [69] J. O. Bockris, A. K. Reddy, “*Modern Electrochemistry*”, Vol.2, 2nd. ed., Plenum Publishers, New York, Boston, London, Moscow, (1970).

- [70] A. Singh, E. E. Ebenso and M. A. Quraishi, “Theoretical and Electrochemical Studies of Metformin as Corrosion Inhibitor for Mild Steel in Hydrochloric Acid Solution”, *Int. J. Electrochem. Sci.*, 7, 4766 – 4779, (2012).
- [71] A. A. Sabirneeza, S. Subhashini and R. Rajalakshmi, “Water soluble conducting polymer composite of polyvinyl alcohol and leucine: An effective acid corrosion inhibitor for mild steel”, *Mater. Corros.*, 64, 74-82, (2013).
- [72] A. Eddib, M. Hamdani, “Electrochemical Studies of Ampicillin as Corrosion Inhibitor for Stainless Steel in Hydrochloric Acid Solution”, *Mor. J. Chem.*, 2, 165-174, (2014).
- [73] A. Etor., “Electrochemical Measurement of Crevice Corrosion of Type AISI 304 Stainless Steel”, MSc. Thesis, University of Saskatchewan, Canada,(2009).
- [74] F. Mansfeld, “metal Corrosion” , 8th. ed., *Intr.Comgr. Dechema*, Germany, (1981).
- [75] H. Shih, “Corrosion Resistance”, 1st. ed. , *InTech*, (2012).
- [76] B. A. Abd-El-Nabey, A. M. Abdel-Gaber, G. Y. Elewady, M. M. El. Sadeek and H. Abd-El-Rhman, ”Inhibitive Action of Benzaldehyde Thiosemicarbazones on the Corrosion of Mild Steel in 3 M H₃PO₄” , *Int. J. Electrochem. Sci.*, 7, 11718 – 11733, (2012).
- [77] H. H .Uhlig, “Corrosion and Corrosion Control”, 1st. ed., *Wiley*, New York, (1971).

- [78] J. M. Saleh , Y. K. Al-Hayderi, “Inhibition Effect of Ethanethiol, Dimethyl sulfide, and Dimethyl disulfide on the Corrosion of Stainless Steel (405) in Sulfuric Acid”, Bull. Chem. Soc., Jpn, 62, 1237-1245, (1989).
- [79] A. Zarrouk¹, I. Warad², B. Hammouti, Kinetic Parameters of Activation , Int. J. Electrochem. Sci., 5, 1516 – 1526, (2010).
- [80] N O. Eddy, E.E. Ebenso, U.J. Ibok, “Adsorption and Quantum Chemical Studies of the Inhibitive Properties of Tetracycline for the Corrosion of Mild Steel in 0.1 H₂SO₄” , The Journal of the Argentine Chemical Society, 97, 178-194, (2009).
- [81] B. Hammouti, A. Zarrouk, S.S. Al-Deyab And I. Warad, “Temperature Effect, Activation Energies and Thermodynamics of Adsorption of ethyl 2-(4-(2-ethoxy-2-oxoethyl)-2-p- Tolyloquinoloxalin-1 (4H)-yl) Acetate on Cu in HNO₃”, Orient. J. Chem., 27, 23-31, (2011).
- [82] L. Herrag, B. Hammouti, S. Elkadiri, A. Aouniti, C. Jama, H. Vezin, F. Bentiss, “Adsorption properties and inhibition of mild steel corrosion in hydrochloric solution by some newly synthesized diamine derivatives: Experimental and theoretical investigations”, Corros. Sci., 52, 3042–3051, (2010).
- [83] A. Popova, E. Sokolova, S. Raicheva, M. Christov, “AC and DC study of the temperature effect on mild steel corrosion in acid media in the presence of benzimidazole derivatives”, Corros. Sci., 45, 33-58, (2003).

- [84] M. M. Solomon, S.A. Umoren, I.I. Udoso, A.P. Udoh, "Inhibitive and adsorption behaviour of carboxymethyl cellulose on mild steel corrosion in sulphuric acid solution" *Corros. Sci.*, 52, 1317-1325, (2010) .
- [85] S. A. Umoren, M.M. Solomon, I.I. Udoso, A.P. Udoh, "Synergistic and antagonistic effects between halide ions and carboxymethyl cellulose for the corrosion inhibition of mild steel in sulphuric acid solution", *Cellulose*, 17, 635-648, (2010).
- [86] N. M. Guan, I. Xueming, I. Fei, "Synergistic inhibition between o-phenanthroline and chloride ion on cold rolled steel corrosion in phosphoric acid", *Mater. Chem. Phys.*, 86, 59-68, (2004).
- [87] I. El Ouali, B. Hammouti, A. Aouniti, Y. Ramli, M. Azougagh, E. M. Essassi, M. Bouachrine, "Thermodynamic characterisation of steel corrosion in HCl in the presence of 2-phenylthieno (3, 2-b) quinoxaline" *J. Mater. Envir. Sci.*, 1, 1-8, (2010).
- [88] L. L. Shrier, R.A. Jarman, "Corrosion Metal/Environment Reactions, Vol. 1, 3rd. ed., Butterworth-Heinemann, Oxford, Boston, (1994).
- [89] N. K. Nemer, "Investigation, Evaluation and Treatment of Corrosion in Crude Oil Tanks", Ph.D. Thesis, chemistry department, college of science for women, University of Baghdad, Iraq, (2013).
- [90] S. Bilgic, N. Caliskan, "The effect of N-(1-toluidine) salicylaldehyde on the corrosion of austenitic chromium–nickel steel", *Appl. Surf. Sci.*, , 152, 107–114, (1999).
- [91] E. Khamis, "The effect of temperature on the acidic dissolution of steel in the presence of inhibitors", *Corrosion*, 46, 476–484, (1990) .

- [92] K.J. Laidler, “Chemical Kinetics”, Tata McGraw-Hill Pub.Co. New Delhi, (1979).
- [93] A. M. Badiea, K. N. Mohana, “Effect of temperature and fluid velocity on corrosion mechanism of low carbon steel in presence of 2-hydrazino-4,7-dimethylbenzothiazole in industrial water medium” *Corros. Sci.*, 51, 2231-2241, (2009).
- [94] Singh A. K. and Quraishi M. A., “Inhibitive effect of diethylcarbamazine on the corrosion of mild steel in hydrochloric acid” *Corros. Sci.*, 52, 1529-1535, (2010).
- [95] Zarrok H., Zarrouk A., Hammouti B., Salghi R., Jama C., Bentiss F., “Corrosion control of carbon steel in phosphoric acid by purpald – Weight loss, electrochemical and XPS studies” , *Corros. Sci.*, 64, 243-252, (2012).
- [96] S. John, K. M. Ali and A. Joseph, “Electrochemical, surface analytical and quantum chemical studies on Schiff bases of 4-amino-4H-1, 2, 4-triazole-3,5-dimethanol (ATD) in corrosion protection of aluminium in 1N HNO₃”, *Bull. Mater. Sci.*, 34, 1245–1256, (2011).
- [97] I. B. Obot, N. O. Obi-Egbedi, “Theoretical study of benzimidazole and its derivatives and their potential activity as corrosion inhibitors”, *Corros. Sci.*, 52, 657–660, (2010).
- [98] A. Popova, M. Christov, and T. Deligeorgiev, “Influence of the Molecular Structure on the Inhibitor Properties of Benzimidazole Derivatives on Mild Steel Corrosion in 1 M Hydrochloric Acid”, *Corrosion*, 59, 756-764, (2003).

- [99] M. Şahin, G. Gece, F. Karcı, S. Bilgiç, “Experimental and theoretical study of the effect of some heterocyclic compounds on the corrosion of low carbon steel in 3.5% NaCl medium”, *J Appl Electrochem*, 38, 809–815, (2008).
- [100] K. Ramji, D.R. Cairns, S. Rajeswari, “Synergistic inhibition effect of 2-mercaptobenzothiazole and Tween-80 on the corrosion of brass in NaCl solution”, *Appl. Surf. Sci.*, 254, 4483–4493, (2008).
- [101] I. Lukovits, E. Kalman, F. Zucchi, “Corrosion Inhibitors—Correlation between Electronic Structure and Efficiency”, *Corrosion*, 57, 3-9, (2001).
- [102] G Bereket, , E Hür, C Öğretir, “Quantum chemical studies on some imidazole derivatives as corrosion inhibitors for iron in acidic medium”, 578, 79–88, (2002).



APPENDIX



Appendix 1. Electromotive Force Series for Metals

Electrode reaction	Standard potential at 25 °C (77 °F), V vs. SHE
$\text{Au}^{3+} + 3e^{-} \rightarrow \text{Au}$	1.50
$\text{Pd}^{2+} + 2e^{-} \rightarrow \text{Pd}$	0.987
$\text{Hg}^{2+} + 2e^{-} \rightarrow \text{Hg}$	0.854
$\text{Ag}^{+} + e^{-} \rightarrow \text{Ag}$	0.800
$\text{Hg}_2^{2+} + 2e^{-} \rightarrow 2\text{Hg}$	0.789
$\text{Cu}^{+} + e^{-} \rightarrow \text{Cu}$	0.521
$\text{Cu}^{2+} + 2e^{-} \rightarrow \text{Cu}$	0.337
$2\text{H}^{+} + 2e^{-} \rightarrow \text{H}_2$	(Reference) 0.000
$\text{Pb}^{2+} + 2e^{-} \rightarrow \text{Pb}$	-0.126
$\text{Sn}^{2+} + 2e^{-} \rightarrow \text{Sn}$	-0.136
$\text{Ni}^{2+} + 2e^{-} \rightarrow \text{Ni}$	-0.250
$\text{Co}^{2+} + 2e^{-} \rightarrow \text{Ni}$	-0.277
$\text{Tl}^{+} + e^{-} \rightarrow \text{Tl}$	-0.336
$\text{In}^{3+} + 3e^{-} \rightarrow \text{In}$	-0.342
$\text{Cd}^{2+} + 2e^{-} \rightarrow \text{Cd}$	-0.403
$\text{Fe}^{2+} + 2e^{-} \rightarrow \text{Fe}$	-0.440
$\text{Ga}^{3+} + 3e^{-} \rightarrow \text{Ga}$	-0.53
$\text{Cr}^{3+} + 3e^{-} \rightarrow \text{Cr}$	-0.74
$\text{Cr}^{2+} + 2e^{-} \rightarrow \text{Cr}$	-0.91
$\text{Zn}^{2+} + 2e^{-} \rightarrow \text{Zn}$	-0.763
$\text{Mn}^{2+} + 2e^{-} \rightarrow \text{Mn}$	-1.18
$\text{Zr}^{4+} + 4e^{-} \rightarrow \text{Zr}$	-1.53
$\text{Ti}^{2+} + 2e^{-} \rightarrow \text{Ti}$	-1.63
$\text{Al}^{3+} + 3e^{-} \rightarrow \text{Al}$	-1.66
$\text{Hf}^{4+} + 4e^{-} \rightarrow \text{Hf}$	-1.70
$\text{U}^{3+} + 3e^{-} \rightarrow \text{U}$	-1.80
$\text{Be}^{2+} + 2e^{-} \rightarrow \text{Be}$	-1.85
$\text{Mg}^{2+} + 2e^{-} \rightarrow \text{Mg}$	-2.37
$\text{Na}^{+} + e^{-} \rightarrow \text{Na}$	-2.71
$\text{Ca}^{2+} + 2e^{-} \rightarrow \text{Ca}$	-2.87
$\text{K}^{+} + e^{-} \rightarrow \text{K}$	-2.93
$\text{Li}^{+} + e^{-} \rightarrow \text{Li}$	-3.05

SHE, standard hydrogen electrode

(B3LYP) وباستخدام برنامج كاوسين للربط بين التأثير التثبيطي والتركيبي الجزيئي للمثبطات المستخدمة، وقد تطابقت الحسابات النظرية مع النتائج العملية.

وقد تم إنجاز دراسة لسطح الألمنيوم النقي باستخدام المجهر الإلكتروني الماسح وأظهرت الصور إن سطح الألمنيوم النقي كان أكثر نعومة بوجود $7,5 \times 10^{-4}$ مولاري من الامبسلين ، وهذا بسبب تكون حاجز واقى من خلال طبقة الامتزاز.

الملخص :-

يتضمن موضوع هذه الرسالة دراسة سلوك تآكل الألمنيوم النقي فضلا عن اثنين من سبائكه في محلول ٣,٥٪ كلوريد الصوديوم على مدى من درجات الحرارة تتراوح من ٢٨٣ إلى ٣٢٣ كلفن بغياب ووجود الأمبيسلين، السيفالكسين، والأموكسيسيلين كمثبطات للتآكل. وأظهرت الدراسة الكهروكيميائية النتائج التالية:

١. تزداد كثافة تيار التآكل بزيادة درجة الحرارة بالمدى الحراري من (٢٨٣-٣٢٣) كلفن.
٢. زيادة كفاءة التثبيط مع زيادة تركيز المثبطات (الأمبيسلين، السيفالكسين، والأموكسيسيلين) وهذا يعني أن هذه المثبطات تعمل بمثابة مثبطات الأمتزاز على السطح لتآكل الألمنيوم النقي واثنان من سبائكه (٥٠٥٢, ٢٠٢٤) في ٣,٥٪ كلوريد الصوديوم.
٣. وجد ان كفاءة تثبيط الأمبيسلين، السيفالكسين، والأموكسيسيلين تتناقص مع زيادة درجات الحرارة من ٢٨٣ إلى ٣٢٣ كلفن
٤. وفقا لقيم جهد التآكل تبين إن كل من الأمبيسلين، السيفالكسين، والأموكسيسيلين تسلك سلوك التثبيط المختلط حيث إن جهد التآكل لم يتغير تقريبا في محلول كلوريد الصوديوم.
٥. تم حساب الدوال الترموديناميكية والتي تشمل طاقة كبس الحرة (ΔG) تغير الأنتالبي والانتروبي ($\Delta H, \Delta S$) لعملية التآكل عند تراكيز مختلفة من المثبطات وعند درجات حرارية مختلفة. أشارت هذه القيم إن عملية التآكل تلقائية وباعثه للحرارة.
٦. يعتمد السلوك العام للدراسة الحركية على معادلة أرينيوس، وأوضحت البيانات المستحصلة بأن أمتزاز المثبطات على السطح هو امتزاز فيزيائي.
٧. قيم الدوال الترموديناميكية لعملية الأمتزاز تم الحصول عليها من أيزوثيرمات لانكماير، وكانت قيم ΔG و ΔH سالبه وهذا يشير إلى إن عميلة الامتزاز حصلت بشكل تلقائي وباعث للحرارة.

تتضمن هذه الرسالة أيضا الحسابات النظرية لبعض القيم الكمية لجزيئات الأمبيسلين، السيفالكسين، والأموكسيسيلين باستخدام طريقة نظرية دوال الكثافة (DFT) لعناصر قاعدة (6-311G) وبأسلوب

بِسْمِ اللَّهِ الرَّحْمَنِ الرَّحِيمِ

﴿ يُؤْتِي الْحِكْمَةَ مَنْ يَشَاءُ وَمَنْ يُؤْتَ الْحِكْمَةَ

فَقَدْ أُوتِيَ خَيْرًا كَثِيرًا وَمَا يَذَّكَّرُ إِلَّا أُولُو

الْأَلْبَابِ ﴿٦٦﴾ ﴿

صدق الله العظيم

(سورة البقرة / الآية ٢٦٩)



جمهورية العراق
وزارة التعليم العالي
والبحرث العلمي
جامعة النهريين
كلية العلوم
قسم الكيمياء

دراسة عمليه ونظريه لفعالية بعض العقاقير كمثبطات لتآكل معدن الألمنيوم وبعض سبائكه في المحلول الملحي

رسالة

مقدمه إلى كلية العلوم / جامعة النهريين
كجزء من متطلبات نيل درجة الماجستير في علوم الكيمياء

من قبل

سمر ثامر حميد

بكالوريوس ٢٠١٢

إشراف

الأستاذ المساعد الدكتور
تغريد علي سلمان

الأستاذ المساعد الدكتور
شذى فاضل السعيدي

نيسان
م٢٠١٥

جمادى الآخرة
ه١٤٣٦